

Examining Cell Movements in the Neurulating Chick Embryo

By

Abby Li

A thesis

presented to the University of Waterloo

in fulfillment of the

thesis requirement for the degree of

Master of Science

in

Biology

Waterloo, Ontario, Canada, 2007

© Abby Li 2007

Author's Declaration

I hereby declare that I am the sole author of this thesis. This is a true copy of the thesis, including any required revisions, as accepted by my examiners.

I understand that my thesis may be made electronically available to the public.

Abstract

The avian embryo is a popular animal model because it is widely available (Antin *et al.*, 2004), it is easily manipulated, and it can provide important insights into normal and abnormal embryo development (Kulesa, 2004). While *in vivo* and *in vitro* cultures of chick embryos are common, *in ovo* cultures are rarer, and none have been designed where the egg did not have to be resealed afterwards. The present study aimed to develop a set-up in which the egg would be windowed without resealing the egg so that the embryo would remain accessible for experimental manipulation. As well, this study aimed to track cell movement during neurulation by microinjecting points of dye along the embryo. Two prototypes were developed based on the concept that temperature and moisture controlled air passing over the windowed egg would serve as a blanket. When these prototypes were unable to keep the embryo alive, a protocol developed by Kulesa and Fraser (2004) was adapted for the study. This protocol involved the construction of a Teflon window which was placed in the windowed egg and sealed with beeswax. Initial microinjection tests with Fast Green FCF showed that the dye dissipated quickly after injection, most likely because of the hydrophilicity of the dye. Therefore, a list of non-fluorescent, hydrophobic dyes were chosen and tested for suitability to cell tracking. Time restrictions prevented the actual cell tracking experiments from taking place, but it was found that Oil Red O fulfilled the criteria. As Oil Red O is usually used to identify lipids in static experiments, it remains to be seen whether it would function as a vital dye. Future experiments include expanding the set-up for use with a confocal microscope for a 4-D rendering of cell movement, and taking advantage of the symmetrical nature of

neurulation in the chick embryo to examine perturbations to the normal progress of development, via drugs such as valproic acid.

Acknowledgments

First and foremost, I would like to thank Dr. Brodland, for giving me the opportunity to study with him these past two years. His patience and support were invaluable. I would also like to thank my committee members, Dr. Duncker and Dr. Ward, for their guidance, especially when I was feeling concerned about the progress of my work. Thanks also go to Goretti Portela from ISA North America for providing the chick embryos.

There are many people who have been integral parts of my project: Caleb Horst, for building the camera system, and for always having a solution to my problems; Jim Veldhuis, for coding all of the programs I used; Denis Viens, for doing all the grunt work on Ol' Misty, and for all the drives to Cambridge; and Jen, for teaching me how to work with chicks in the first place. Others in the Biomechanics lab have also made my time here better: Fatima Kakal, for being my sounding board, my moral support, my biology buddy and my best friend; Richard Benko, for always letting me rant out my frustrations; Paul Groh, for being my go-to jokes guy; Xiaoguang Chan, Simon Tsui, Tony Leung, Justina Yang and Graham Cranston, for always being there, either for work or just to hang out. You guys make up much of the good memories I have from the past two years.

I had a lot of support from outside the lab as well. To my parents, thank you for being so supportive, not minding when work would keep me from visiting home for weeks at a time. Thank you also to my little sister, Barbara, not only for her access to the McMaster library catalogue, but also for being enthusiastic and interested in my project, even at times when my own enthusiasm and interest waned. And to my friends, thank you for putting up with my inability to talk of anything else but work and the lab.

Last, but definitely not least, I'd like to thank Alex, for being my unfailing rock of sanity. I'll never understand how he put up with me bringing my frustrations home, if and when I actually came home, but I'm very glad he did.

Table of Contents

Author's Declaration.....	ii
Abstract.....	iii
Acknowledgments.....	v
Table of Contents.....	vii
List of Tables.....	x
List of Figures.....	xi
List of Terms and Abbreviations.....	xiii
1. Introduction.....	1
1.1. Spina bifida and neural tube defects.....	1
1.2. Animal Studies.....	5
1.3. Neurulation in the chick embryo.....	8
1.4. Present Study.....	12
2. Visualizing the Embryo.....	13
2.1. Introduction.....	13
2.2. Considerations.....	14
2.3. Basic Chick Embryo Techniques.....	15
2.4. Prototype 1: Air Blanket.....	16
2.4.1. Methods and Materials.....	16
2.4.2. Results and Discussion.....	20
2.5. Prototype 2: Convection.....	24
2.5.1. Methods and Materials.....	24
2.5.2. Results and Discussion.....	26

2.6. Current Prototype: Transparent Window.....	33
2.6.1. Methods and Materials.....	34
2.6.2. Results and Discussion	36
2.7. Conclusion	38
3. Tracking Cell Movements.....	39
3.1. Introduction.....	39
3.1.1. History of Cell Tracking	39
3.1.2. Microinjection.....	41
3.2. Methods and Materials.....	43
3.2.1. Approximating Microinjection Volume	43
3.2.2. Choosing a Dye.....	44
3.2.3. Cell Tracking	44
3.3. Results and Discussion	44
3.3.1. Testing Other Dyes	45
3.3.1. Approximating Microinjection Volume	47
3.3.3. Cell Tracking	48
3.4. Conclusions.....	50
4. Conclusions and Future Directions.....	52
4.1. Conclusions.....	52
4.2. Future Directions	53
4.2.1. Future experiments regarding cell movement.....	53
4.2.2. Future experiments regarding visualization.....	54
Appendix I	62

Appendix II.....	65
Appendix III.....	66
Appendix IV.....	72
Appendix V.....	73
Appendix VI.....	82

List of Tables

Table 1: Flow times of the original Prototype 1 components, to determine efficacy of the air flow through the apparatus	22
Table 2: Testing flow rates of different air stones to improve air flow in Prototype 1	23
Table 3: Estimating Volume Expelled from Micropipette per Injection, with $p_i = 900$ psi and $p_c = 300$ psi	48
Table 4: Temperature and relative humidity test of Prototype 2. Lid closed, vent closed. Raw data.....	66
Table 5: Temperature and relative humidity tests for Prototype 2. Lid closed, vent open. Raw data.....	67
Table 6: Temperature and relative humidity tests of Prototype 2. Lid closed, vent half-open. Raw data.....	68
Table 7: Temperature and relative humidity tests for Prototype 2. Lid open 1 cm, vent closed. Raw data.	69
Table 8: Temperature and relative humidity for Prototype 3. Raw data.....	71

List of Figures

Figure 1.1: Three forms of spina bifida	2
Figure 1.2: Primary and secondary neurulation.....	9
Figure 1.3: Neurulation in the chick embryo compared to other organisms.....	9
Figure 1.4: Schematic representation of cell shapes in the chick neuroepithelium during neurulation	10
Figure 1.5: Illustration of changes in neuroepithelial cell shape change during the cell cycle.	11
Figure 2.1: Prototype 1, an open system in which the egg sits without being resealed or placed in a chamber	19
Figure 2.2: The camera system used in Prototypes 1 and 2.....	20
Figure 2.3: Representative images of 1-day old chick embryos using Prototype 1.....	21
Figure 2.4: Prototype 2, a semi-closed system in which air is forced to go over the windowed egg	25
Figure 2.5: Temperature and relative humidity measurements of Prototype 2 when the lid and the ventilation panel are completely closed	27
Figure 2.6: Temperature and relative humidity measurements of Prototype 2 when the lid is closed and the ventilation panel is completely open.....	28
Figure 2.7: Temperature and relative humidity measurements of Prototype 2 when the lid is closed and the ventilation panel is half-opened	28
Figure 2.8: Temperature and relative humidity measurements of Prototype 2 when the lid is partially open and the ventilation panel is closed	29
Figure 2.9: Teflon windows adapted from Kulesa and Fraser (2004) for prototype 3	34
Figure 2.10: Prototype 3, designed to visualize a chick embryo within a closed environmental chamber.....	35

Figure 2.11: Following the protocol set out by Kulesa and Fraser (2004) resulted in condensation forming on the inside of the Teflon windows..... 36

Figure 2.12: Temperature and relative humidity measurements of Prototype 3..... 37

Figure 2.13: A successful run showing a 1-day old embryo undergoing neurulation in Prototype 3 38

Figure 3.1: A chick embryo with a microinjected grid of Fast Green FCF compared at two time points, showing dissipation of the dye over time..... 45

Figure 3.2: Comparing Oil Red O, Janus Green B and Neutral Red microinjected into a 3-day old chick embryo to determine which would be able to remain visible for the longest amount of time..... 47

Figure 3.3: A sample microinjection done with Neutral Red shows that precise microinjection is difficult when the micromanipulator is driven by hand, and that Neutral Red dissipates too quickly to be suitable as a tracking dye 50

List of Terms and Abbreviations

Air stone: A porous stone which is used to release tiny bubbles of air from an air pump; normally used to diffuse oxygen into a fish tank.

DLHP: Dorso-lateral hinge points

HH: Hamburger-Hamilton stage

In ovo: Experiment takes place within the egg. Often used interchangeably with *in vivo* when talking about chicken embryos.

In vitro: Experiment takes place outside the organism. In terms of chick embryos, this means any experiment where the embryo is removed and cultured outside the egg.

In vivo: Experiment takes place within the organism. Often used interchangeably with *in ovo* when talking about chicken embryos.

MHP: Median hinge point

Microinjection: The use of a fine needle to inject a substance into a cell, or a group of cells, through pressurized air.

P_i: Injection pressure of the microinjector, which is only applied during the injection process.

P_c: Compensation pressure, which ensures that no medium flows into the needle. This pressure is applied at all times

Psi: Pounds per square inch, a unit of measurement for pressure.

Relative humidity: the ratio of the partial pressure of the water vapour in the mixture to the saturation vapour pressure of water at the temperature of the mixture

T_i: Injection time, the period during which the injection pressure is maintained.

Windowing: The removal of a portion of the egg shell for the purposes of exposing the contents of the egg, specifically the embryo.

1. Introduction

1.1. Spina bifida and neural tube defects

Neural tube defects (NTDs) are a group of disorders result from abnormal tissue movements during neurulation, where the spinal cord and the brain are formed. These NTDs can vary in location, as well as in severity. Anencephaly is caused by a defect in the cranial region, and results in the skull and brain being incompletely formed, a defect that is incompatible with life (Detrait *et al.*, 2005). Spina bifida is a defect in the spinal region of the neural tube, and can have varied results, based on the location and severity of the effect. The majority of infants born with spina bifida now survive, but usually only through extensive surgery and subsequent medical care (Botto *et al.*, 1999). The most severe, and most common, form of spina bifida is myelomeningocele (Figure 1.1a). With this disorder, the spinal cord and dura mater protrude from an opening in the tube of the spine and grows into a sac on the back (Northrup & Volcik, 2000). Because the nerves are no longer being protected by the spine, people with myelomeningocele often have loss of sensation and paralysis in the regions below the defect (IFSBH, 2007). Other possible effects include mental retardation, orthopaedic disabilities (Walsh & Adzick, 2003), and problems with the bowels and the bladder, resulting in symptoms such as fecal incontinence (Vande Velde *et al.*, 2007). Meningocele is similar to myelomeningocele, but rarer and milder (Figure 1.1b). The sac is still present, but only contains the meninges and cerebral spinal fluid. The spinal cord is still protected so the nerves are not as damaged and there is often little disability. Since both myelomeningocele and meningocele involve sacs on the spinal region of the back, they are often classified together as *spina bifida cystica* (IFSBH, 2007). The mildest form of spina bifida is its

closed form, or *spina bifida occulta*, involved a slight defect in one of the vertebrae (Figure 1.1c). Other than a small dimple or mole on the back above the defect, there are usually no other visible signs of spina bifida occulta. Unfortunately, even in these cases, complications can occur. Because there is still a defect in the vertebrae, the spinal cord may snag; and with growth, tension in the spine may begin to affect bladder control and mobility (IFSBH, 2007). But most often, in studies of spina bifida, spina bifida occulta is excluded because its relation to spina bifida cystica is unclear (Botto *et al.*, 1999).

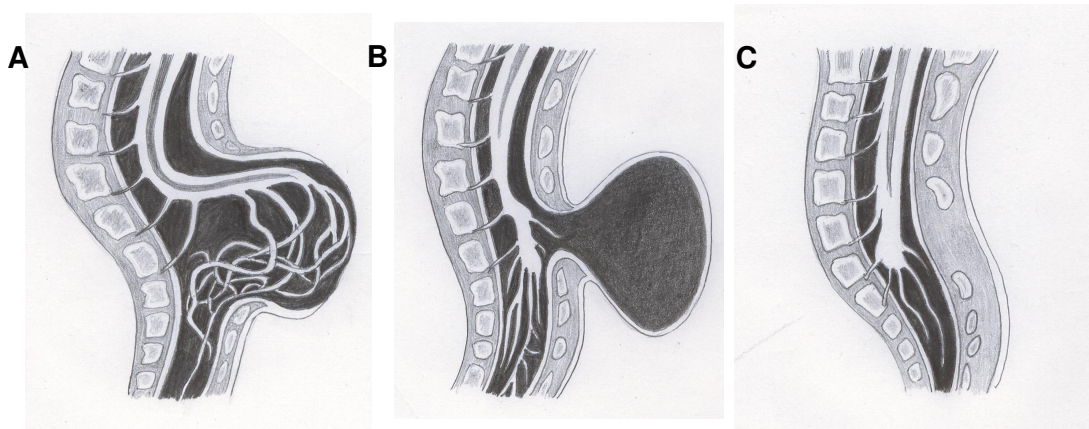


Figure 1.1: Three forms of spina bifida. A) Myelomeningocele. The spinal cord and nerves grow into a cyst-like sac protruding from the back. B) Meningocele. The cyst-like sac remains, but only contains the meninges and cerebrospinal fluid. The spinal cord and nerves remain within the protective covering of the spine. C) Spina bifida occulta. “Closed” form of spina bifida with little outward sign of a defect. The spinal cord and nerves grow almost normally.

Of the NTDs, spina bifida is the more prevalent form, occurring in 3 of every 10,000 births, though the incidence rate varies with geography and race (Acuna *et al.*, 1999). It was been estimated that of the 2500 infants born with NTDs in the United States each year, 1500 of those have spina bifida (CDC, 1992a). Worldwide, spina bifida and NTDs appear in approximately 300,000 births (Botto *et al.*, 1999). The advent of technologies such as screening ultrasounds, amniocentesis and fetal MRI have allowed for earlier and more accurate detection of NTDs (Sutton, 2007). With early detection, surgery may be performed on the baby either before birth (prenatal surgery) or after birth

(postnatal surgery). Currently, in the United States, surgery for myelomeningocele is offered through the Management of Myelomeningocele Study (MOMS), a 5-year randomized clinical trial which began in 2003, which compares the two approaches (Sutton, 2007).

The epidemiology of spina bifida, and of NTDs in general, has been a widely studied topic. Accurate numbers for the prevalence of NTDs has been historically hard to determine. Much of the data comes from documentation of live and still births. But because NTDs occur early in development, many fetuses/embryos undergo spontaneous abortion (Frey & Hauser, 2003). Prevalence data is further muddled by the advent of prenatal diagnoses, with more and more women carrying fetuses with NTDs choosing to undergo therapeutic abortion (Frey & Hauser, 2003). Still, prevalence estimates show that there had been a decline in the rate of NTDs over time. For example, a report by the CDC (1992a) showed that rates of spina bifida have declined from 5.9 to 3.2 cases per 10,000 births in the period from 1984-1990. Such decreases can be attributed to the discovery that the intake of 4.0mg of folic acid per day was capable of decreasing the risk of NTDs in pregnant women (CDC, 1992b). However, despite the advent of preventative therapies such as folic acid, the underlying causes of spina bifida and NTDs in general have still not been completely understood. In fact, causes are determined in fewer than 10% of newborns with NTDs (Holmes *et al.*, 1976). However, it is obvious that they are complex, multifactorial disorders, where both environmental and genetic factors can play a role.

Many environmental influences have been put forth as possible factors in the etiology of spina bifida, but few have been confirmed. For example, some studies have

noted that the risk of NTDs increases with maternal age, while others found no correlation. Similarly, conflicting studies have also been published about the effect of low socioeconomic status, as well as parental occupations (Northrup & Volcik, 2000). Some external factors that have shown a consistent correlation with increased risk of NTDs and spina bifida include febrile illnesses in the first trimester, as well as heat exposure, for example, use of a hot tub or sauna (Frey & Hauser, 2003). Maternal obesity has been fairly well established as having a definite correlation with increased risk of NTD-affected pregnancies (Waller *et al.*, 2007). In fact, one study showed that mothers who are obese show increased risk of having a child with spina bifida compared to mothers who were not obese, by a ratio of 3.5 (Watkins *et al.*, 2003). Compared to the odds ratio of 1.8 for NTDs in general, the result implies that spina bifida may be more susceptible to maternal obesity (Northrup & Volcik, 2000). Maternal diabetes has also been shown to be associated with an increased risk of NTDs in offspring, though not as consistently. The risk has been estimated to be between 2% to 8% (Northrup & Volcik, 2000). It is thought that both maternal obesity and maternal diabetes support the idea that glucose metabolism may be important in the formation of NTDs. This, coupled with the fact that intake of folates has been shown to decrease the risk of NTDs, have led scientists to believe that there is also a genetic component to the disorder.

Because spina bifida is a disease that affects the embryo, genetic or inherited factors have been widely studied. Research has shown that mothers who have previously had NTD-affected pregnancies were more likely to have a subsequent pregnancy be affected by NTDs, with a recurrence rate of approximately 4.0% (Farley, 2006). As well, folate-related genes have been analyzed, because of their ability to reduce the risk of

NTDs. And while the mechanism underlying the association of folates and NTDs is not yet fully established, it is known that folate participates in metabolic pathways that may affect embryogenesis. The disruption of folate metabolism has also been shown to increase homocysteine levels, which have been shown to interfere with neurulation (Afman *et al.*, 2003). Genes that control neurulation have also been widely studied, as their disruption would inevitably cause NTDs. Much of the information on candidate genes have come from animal studies (e.g. George & McLone, 1995).

1.2. Animal Studies

When studying spina bifida, animal models are often used because testing on human embryos is not only unethical, but it would also require too much time, as the gestation period of a human is much longer than that of most model organisms. There are two key ideas to consider when choosing an animal model to study NTDs: 1) there must be a resemblance to how the disease presents itself in humans, so results obtained have some applicable relevance; and 2) the experimental analysis must be relatively simple, so the experiment can be reproduced. One of the first models of myelomeningocele was developed in late-gestation primates (Sutton, 2007). Other researchers have developed a model of spina bifida in sheep that mimic the most common anatomical defects seen in humans (Meuli *et al.*, 1995). But these models are rarely used, because of the complexity of the organisms. Two common animal models used for to study NTDs are the mouse and the chick, as neurulation in both is similar to humans (George & McLone, 1995). The mouse model has the advantage of having a more completely understood genome, and certain strains have naturally occurring NTDs

(Campbell *et al.*, 1986). For example, the curly tail mouse naturally develops a lumbrosacral myelomeningocele, is phenotypically identical to nonsyndromic NTDs in humans, and is used as a model of caudal neural tube closure (Detrait *et al.*, 2005). The mouse has mainly been used to conduct studies for candidate genes in normal and abnormal neurulation, with as many as 190 mutants described thus far (Kibar *et al.*, 2007). The chick model, on the other hand, has a simpler experimental set-up, and can be bred in large quantities at a relatively low cost (Antin *et al.*, 2004). The chick embryo is also preferable over other model organisms such as amphibians and fish because it undergoes true growth during morphogenesis, where the embryo and its organs increase in size, similar to the manner in which the human embryo develops. The present study focuses on the chick model.

One additional difference of the chick model from the mouse model is that as spontaneous mutants rarely occur, a molecular biology approach, rather than a genetic one, is needed. There have been cases of spina bifida occurring naturally, but it is usually present with other deformities, such as triophthalmia (three eyes) or deformed beaks, indicating a more general defect (Wojnarowicz & Olkowski, 2007). These cases are rare, and most studies need to induce spina bifida in the chick embryo in order to study it. Lopez de Torre and colleagues (1990) induced NTDs in chick embryos by removing a portion of the albumen at the end of the first day of incubation. It was found that after re-incubation, approximately 12% of the embryos had developed NTDs, with the majority having myelomeningocele. Unfortunately, this procedure also resulted in a fairly high mortality rate, with more than half (55%) of embryos dying. Other studies have used more specific methods of inducing defects in chick embryos. Spontaneous mutants are

rare in chicks, so many researchers use anti-sense oligonucleotides to target specific gene products. By blocking the creation of proteins from RNA, anti-sense oligonucleotides are ideal for generating loss-of-function mutants (George and McLone, 1995). This technique has been used in determining what genes are involved in the process of neurulation, and what causes NTDs.

Another method that has often been used to induce spina bifida is windowing, a standard technique in examining chick embryos *in ovo* (Mann and Persaurd, 1979; Fisher and Schoenwolf, 1983; Fineman *et al.*, 1986). It has been shown that approximately 46% of embryos that have been windowed display a range of defects, mainly dysraphic and non-dysraphic NTDs (Fineman *et al.*, 1986). The rate of occurrence of these defects seems to be related to the stage at which the embryo is windowed. It seems the earlier the windowing occurs, the greater chance of developing an NTD (Fisher and Schoenwolf, 1983). This effect can be minimized by partially filling the windowed eggs with albumen or saline, or by turning the eggs 180° before reincubation. Doing both will virtually eliminate all windowing effects (Fisher and Schoenwolf, 1983). It has been proposed that windowing-induced NTDs are caused by the prolonged mechanical stress involved with the process (Fineman & Schoenwolf, 1987).

With the ability to induce spina bifida, and its similarities to developmental anomalies in the human, the chick embryo provides a good model for the study of normal and abnormal neurulation.

1.3. Neurulation in the chick embryo

The chick embryo is often used as a model organism in the study of neural tube defects that occur in humans, as the two processes occur in a similar fashion.

Neurulation in the avian embryo is the process by which the flat epiblast becomes a cylindrical neural tube, which will eventually form the brain and the spinal cord. This process can be divided into two broad steps (Figure 1.2 and Figure 1.3): primary neurulation, when the neural plate forms and bends to form the cranial levels of the neural tube (Schoenwolf, 1991); and secondary neurulation, during which the medullary cord, derived from a mass of cells called the tail bud, cavitates to form the caudal portion of the neural tube (Yang *et al.*, 2006). The majority of neurulation research has focused on primary neurulation in a wide variety of organisms (Schoenwolf and Delongo, 1980), so much is known about this subject. From a clinical perspective, primary neurulation is more significant for humans, as abnormal development in this phase results in neural tube defects (Schoenwolf and Smith, 2000). The distinction of the two broad steps in neurulation is a bit of an oversimplification, as the closing of the neural tube has been suggested to occur in many steps (Van Straaten *et al.*, 1996), a phenomenon that has also been suggested in human embryos (Van Allen *et al.*, 1993).

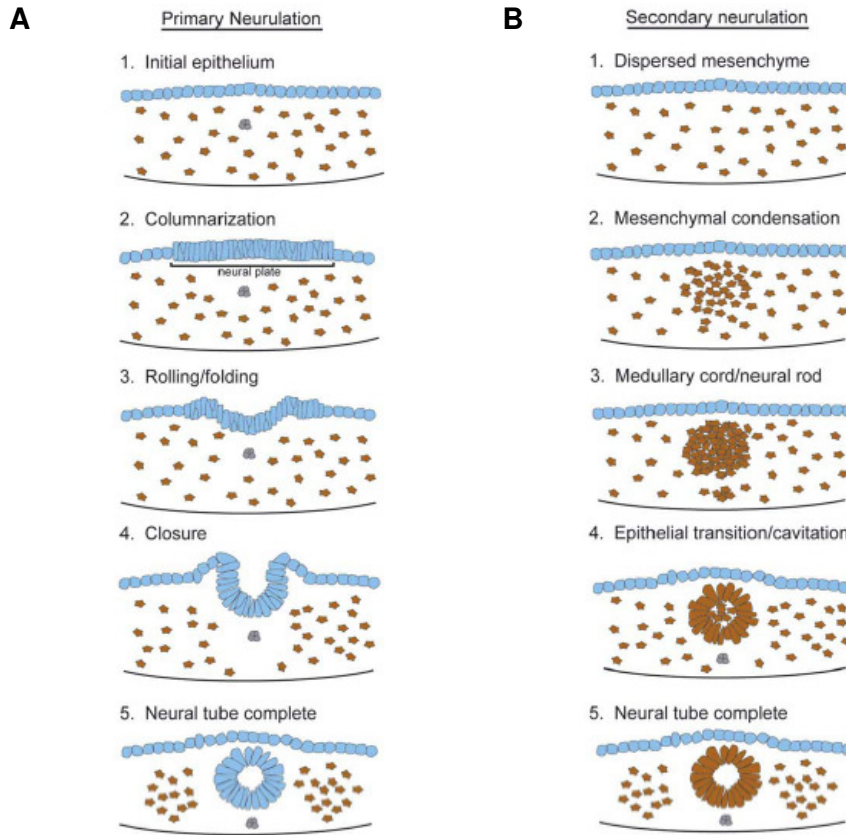


Figure 1.2: Primary and secondary neurulation. A) Primary neurulation occurs in the anterior portion of the organism. Epithelial cells become columnar, then roll or fold to become the neural tube. B) Secondary neurulation occurs in the posterior or tail region of the organism. Mesenchymal cells condense to form a rod, which then cavitates to form the neural tube. (From Lowery & Sive, 2004)

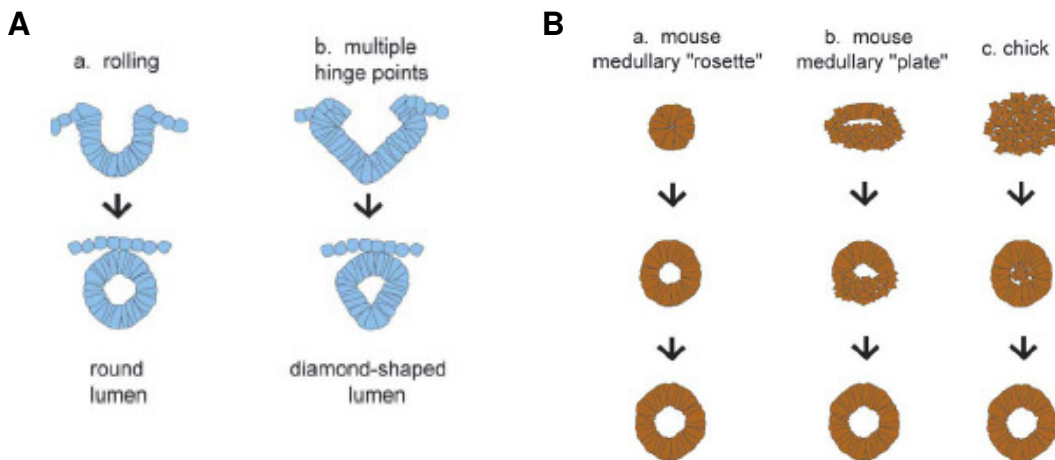


Figure 1.3: Neurulation in the chick embryo compared to other organisms. A) Primary neurulation in chicks involve the formation of the medial hinge point and two dorsolateral hinge points, which results in a diamond shaped lumen (b). This is compared to the round lumen formed during primary neurulation in the mouse and *Xenopus* embryos. B) Secondary neurulation in chicks consists of a separation of the mesenchymal cells: those in the centre remain mesenchymal, while the cells at the edge become epithelial. Cavitation then creates the lumen. (From Lowery & Sive, 2004)

During neurulation, the thickness of the neural plate depends on the height of individual cells. Cells are irregularly shaped, but can be categorized into four groups (Figure 1.4): spindle-shaped cells, which are bulbous around the middle, with tapered processes at the base and apex; wedge-shaped cells, which have a bulbous base and a tapered apex; inverted wedge-shaped cells, which have a bulbous apex and a tapered base; and globular cells, which are spherical cells found at the apex of the neural plate during mitosis, with nuclei residing in the widest part of the cell (Schoenwolf and Smith, 1990).

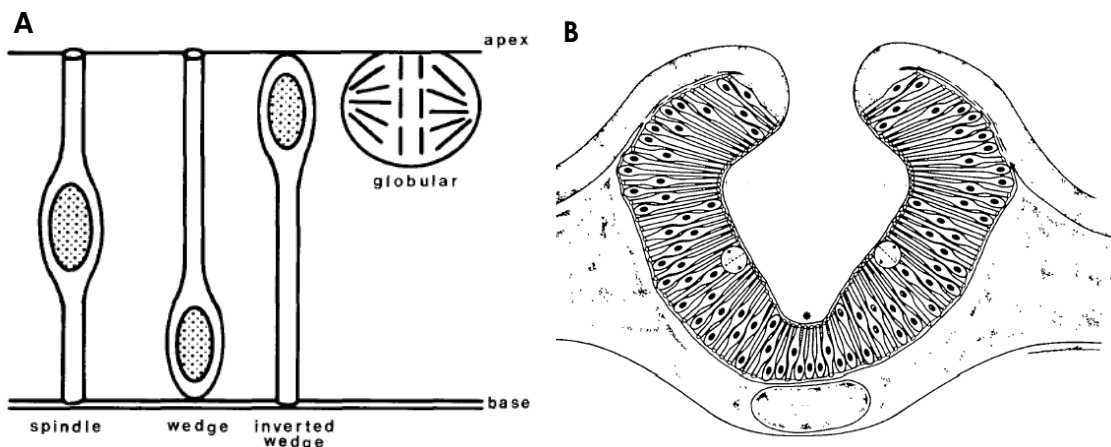


Figure 1.4: Schematic representation of cell shapes in the chick neuroepithelium during neurulation. A) The four basic categories of cell shapes. Cells with basal nuclei are called wedge-shaped; those with apical nuclei are inverted wedge-shaped; those with nuclei in the middle are called spindle-shaped. Globular cells occur during M-phase only (from Smith & Schoenwolf, 1988) B) A transverse cross-section of the chick neuroepithelium, depicting how the four cell shapes would look during bending of the neural plate. The asterisk represents the medial hinge point. (from Schoenwolf & Smith, 1990)

Research has shown that individual cells can change between these different cell shapes, and it may be the changing of cell shapes that causes the basal expansion that is seen during neurulation (Schoenwolf and Franks, 1984). It has also been shown that the nuclei of cells in the medial hinge point (MHP) tend to be at the apex of the cells during M phase, move more centrally during the G_1/S phase transition, then to the base of the cell

during the S phase and most of G₂ phase, and finally back towards the center during the lattermost part of the G₂ phase (Figure 1.5; Smith and Schoenwolf, 1988).

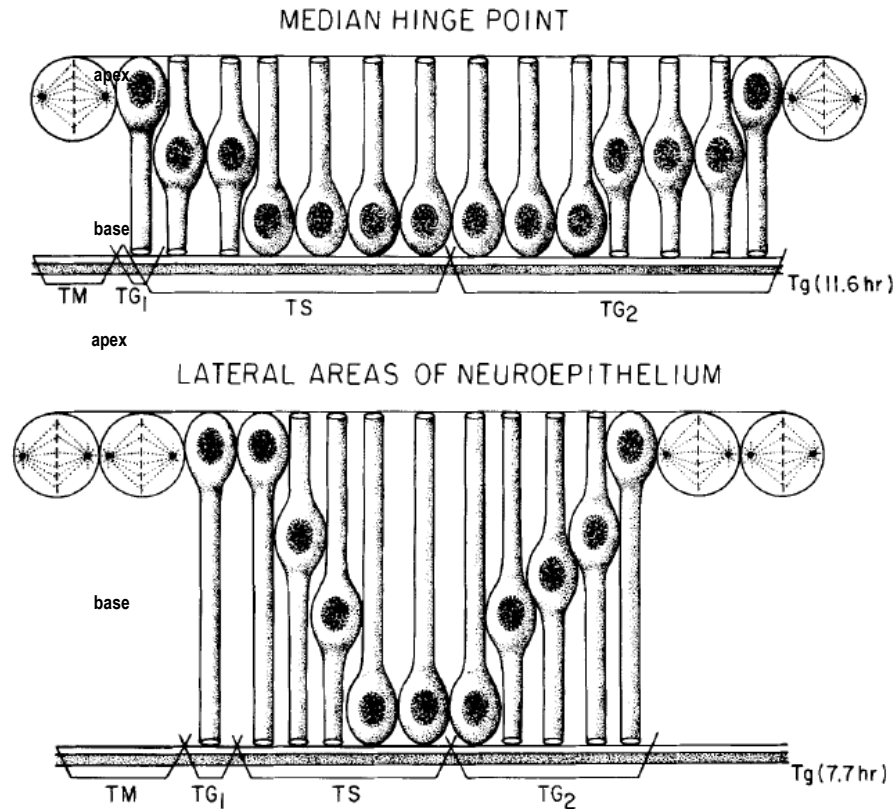


Figure 1.5: Illustration of changes in neuroepithelial cell shape change during the cell cycle. Note that the transition between S-phase and G₂-phase occurs mostly basally, while M-phase and G₁-phase occur mostly at the apex. It has been suggested that the changing of cell shapes is the driving force for the bending of the neural plate. (from Smith and Schoenwolf, 1988)

Given that the nucleus is found in the widest portion of the cell, this means that during the cell cycle, the cell changes from inverted wedge-shaped to spindle-shaped to wedge-shaped and back again. Combined with the fact that MHP cells tend to have a longer cell cycle, though the time spent in M phase is considerably shorter than cells in the lateral areas of the neuroepithelium (Smith and Schoenwolf, 1988), it could be concluded that it is the increased proportion of wedge-shaped cells cause the bending of the neural plate. Other factors that may be involved in cell shape changes include microtubules which may be involved in the elongation of neuroepithelial cells and apical

microfilament bands, which may play a role in cell wedging in the DHLP (Schoenwolf and Smith, 1990).

1.4. Present Study

The present study had two objectives: 1) create a method where the embryo can develop *in ovo*, but is still available for manipulations and visualization during its development and 2) examine the movement of cells in the early chick embryo during neurulation using that method. It was hypothesized that the set-up developed will allow the embryo to develop at a normal rate, comparable to other published data, and similar to the stages of development set out by Hamburger and Hamilton (see Appendix I). It is the hope that by developing this new method of visualizing the embryo, we can learn more about the cell movements that are crucial to neurulation. This thesis will be divided into two main chapters, one for each of the objectives listed above. The fourth chapter will bring the two steps together, and suggest some future directions for the work.

2. Visualizing the Embryo

2.1. Introduction

The chick embryo is a classic model organism for studying development. Because of this, researchers have explored many ways of culturing the chick embryo, both in (*in ovo or in vivo*) and outside (*in vitro*) of its natural environment, so that it can be manipulated for experiments. One of the first researchers to successfully culture the early chick embryo *in vitro* was Waddington (1932). He developed the plasma clot method, in which a watch glass was placed in a Petri dish, kept moist by cotton wool soaked in hot water. Then, in the watch glass, a mixture of blood plasma from an adult fowl and “embryo extract” was allowed to form a clot. Finally, the blastoderm is placed on top of the clot (Waddington, 1932). While this approach allowed the embryos to develop for 2 to 3 days, the ectoderm tended to form cysts in the outer regions, and development occurred at a slower rate (Waddington, 1932). As well, the set up was complex and difficult, requiring sterile conditions, and did not allow the embryo to expand as it would in the egg (Stern & Bachvarova, 1997). Other researchers attempted to improve on this technique (see Packard *et al.*, 2000, for examples), but little advancement was made until Denis New developed his technique in 1955. New’s method differed from the previous ones in that his set up attempted to emulate the relationship between the blastoderm and the vitelline membrane within the egg (Stern & Bachvarova, 1997). The blastoderm is explanted and stretched over a glass ring sitting in a watch glass. Albumen is injected below the blastoderm, and acts as a nutrient supply (New, 1966). Because albumen has bacteriostatic properties, it offers a vast advantage over Waddington’s set up, in that experiments no longer needed to be conducted under

strict sterile conditions (Stern & Bachvarova, 1997). Other studies have attempted variations on New's technique (see Stern & Bachvarova, 1997, for overview), but the New technique is still the most often used.

In vivo, or *in ovo*, cultures of chick embryos mostly involve a window being cut in the shell of the egg, exposing the internal contents. The egg usually undergoes experimental manipulation, and is then resealed and reincubated, to be examined at a later time. Few studies have developed methods of visualizing embryonic developing *in ovo*. Kulesa and Fraser (2000) have developed a method for *in ovo* time-lapse confocal imaging of the migration of chick neural crest cells, involving a Teflon window being sealed into the egg once it had been windowed. The present study aimed to develop a method where the egg did not need to be resealed in order to facilitate visualization of neurulation to be possible.

2.2. Considerations

When designing an incubator apparatus, three main considerations need to be kept in mind: temperature, relative humidity, and accessibility. Poor hatching results, implying poor survival rates, are usually the result of improperly controlled temperature or relative humidity.

Temperature is generally considered to be the most critical aspect of incubating an egg. The young chick embryo is not very flexible with respect to deviations in the temperature of its surroundings (Meijerhof, 2002). The optimal temperature for the incubation of chicken eggs is 37.8°C. Changes in temperature above or below the optimum will slow down development (Lourens, 2002). Ideal storage conditions of chicken eggs have been shown to be at approximately 12°C and 74% relative humidity.

The relative humidity at which an embryo is grown also needs to be controlled, though not as strictly as temperature. Under ideal conditions, the normal development of the chicken embryo involves a 16-18% loss of their initial mass through water vapour, though embryos have been shown to survive losses of up to 25% (Snyder & Birchard, 1992). Relative humidity thus needs to be controlled. It is suggested that the relative humidity be kept at 58-60% until three days before hatching. If the relative humidity is too high, the evaporation necessary for normal development is hampered. If the relative humidity is too low, excessive evaporation occurs, and the embryo runs the risk of sticking to the shell.

Accessibility is the final consideration. While other studies have developed methods to visualize the embryo, none have developed a set up in which the embryo could still be manipulated during development. This was one of the purposes of the present study.

2.3. Basic Chick Embryo Techniques

Chick embryos (White Leghorn) were obtained from ISA North America (Cambridge, Ontario). They were stored at 12°C, and then incubated at 37.8°C until Hamburger-Hamilton stage 6-7, approximately 23 hours (see Appendix I). Incubation was done in the OVA-Easy 380 Cabinet Incubator (Brinsea, Titusville, Florida; product # OE380). Relative humidity in the incubator was controlled using the Digital Incubator Humidity Management Module (Brinsea, product # H22). Chicks were windowed according to Selleck (1996). The egg was then laid on its side and swabbed with 70% ethanol. Approximately 5 mL of albumen was removed from the blunt end of the egg with a 18G1.5-gauge hypodermic needle. The area to be removed was marked out on the

side of the shell with pencil, and tape was applied to that area, which was then cut out with small scissors. The albumen was replaced and a few drops of chick Ringer's solution (7.2g NaCl, 0.23g CaCl₂·H₂O, 0.37g KCl, dH₂O to 1L) was placed on top of the embryo. A 1:29 dilution of India ink (Pelikan Fount India Ink, Hannover, Germany) was injected beneath the blastoderm using a 25G5/8-gauge hypodermic needle to enhance contrast between the embryo and the background. The embryo was then ready for experimental manipulation.

2.4. Prototype 1: Air Blanket

The design of Prototype 1 is shown in Figure 2.1. The theory behind Prototype 1 was that air of a specific temperature and relative humidity would be streamed over the windowed egg. The warm air would act as a blanket, creating a local air pocket that would push out the surrounding air, keeping the embryo at temperature and relative humidity.

2.4.1. Methods and Materials

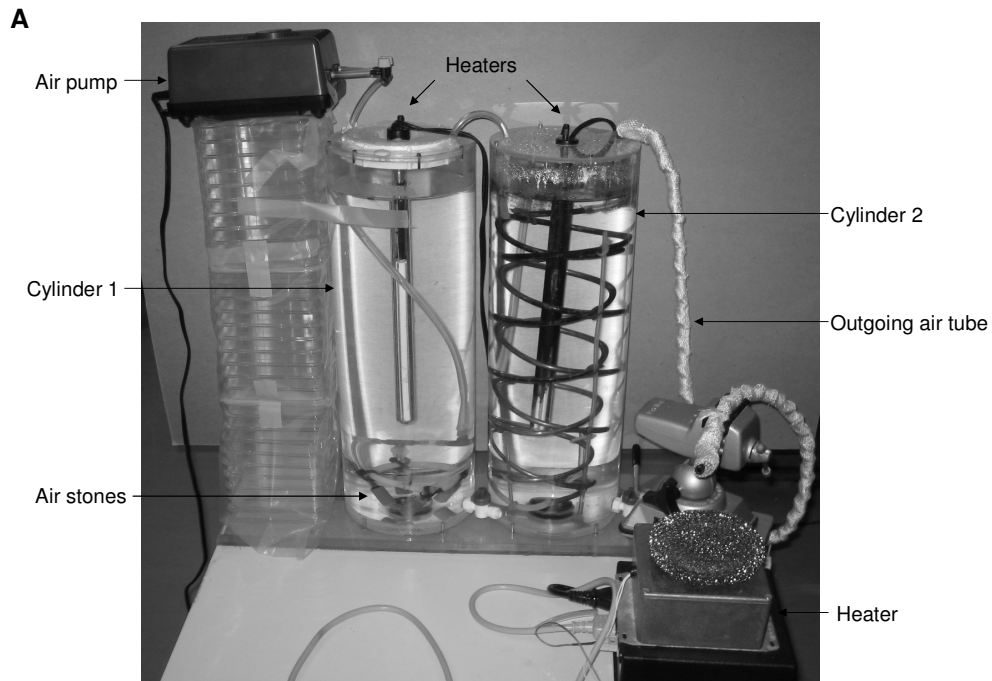
The main component of this prototype is the Air Temperature and Moisture Control unit which was designed to produce air at a specific relative humidity and temperature. Figure 2.1B depicts a diagram of the prototype. An aquarium air pump pumps room-temperature air into cylinder 1, which contains distilled water heated to a specific temperature. As the air bubbles through air stones and rises through cylinder 1, the air is raised to the same temperature as the water and 100% relative humidity. Because cylinder 1 sealed airtight, the bubbling air was forced through a second hole in the top of the cylinder into cylinder 2. The second cylinder is kept at a higher

temperature, which increases the temperature of the air as it travels through the copper tubing, and lowers the relative humidity to the desired level. The temperatures of the two cylinders were controlled by submersible aquarium heaters. The final tube is wrapped in a heated wire to keep the relative humidity and temperature of the air constant. The outgoing air is placed so that the air is blowing across the open window of the egg.

Both cylinders 1 and 2 are 45.72cm (18") high, made of acrylic tubing that has a 16.51cm (6.5") outer diameter (OD) and is 0.635cm (0.25") thick. The caps and bases are made from an acrylic plate of 0.635cm (0.25") thickness. The entire set-up is mounted on a 1.27cm (0.5") thick acrylic sheet on four rubber feet to isolate it from surrounding vibrations. The aquarium pump (Petcetera AP700, Richmond, British Columbia) is designed to produce a volumetric flow of 1.8 liters per minute with a pressure of 4 psi. The pump is connected to cylinder 1 by a piece of Tygon tubing, with an inner diameter (ID) of 0.3175cm (1/8") and an outer diameter (OD) of 0.635cm (1/4"). This tubing continues down to the bottom of cylinder 2, where it connects to 4 cylindrical air stones (Petcetera). Tubing of the same dimensions was used to connect cylinders 1 and 2. The copper tubing inside cylinder 2 is made of two pieces of copper tubing (ID = 0.3175cm = 1/8", OD = 0.635cm = 1/4"), coiled into helices, and connected at the bottom by a piece of Tygon tubing, so that the entire structure resembles a double helix. The outgoing tube was originally made from Tygon tubing, but was replaced with a thicker tubing made of rubber (OD = 0.79375cm = 5/16", ID = 0.3175cm = 1/8"). The heated wire surrounding the tubing was controlled manually.

Initially, the Air Temperature and Moisture Control unit was also designed to keep the entire egg and embryo at the optimal temperature. Unfortunately, the

temperature could not be kept consistent enough for the development of an embryo (i.e. less than 0.5°C deviation). Therefore, an extra heating mechanism was added. A metal box was constructed, and an adhesive Kapton foil heater (Cole Parmer, EW-36060-40, Montreal, Quebec) was placed on the underside of the top. The egg was nestled in a copper scourer, which should distribute the heat more evenly throughout the egg than if the heating mechanism was simply placed underneath. The camera was placed above the specimen.



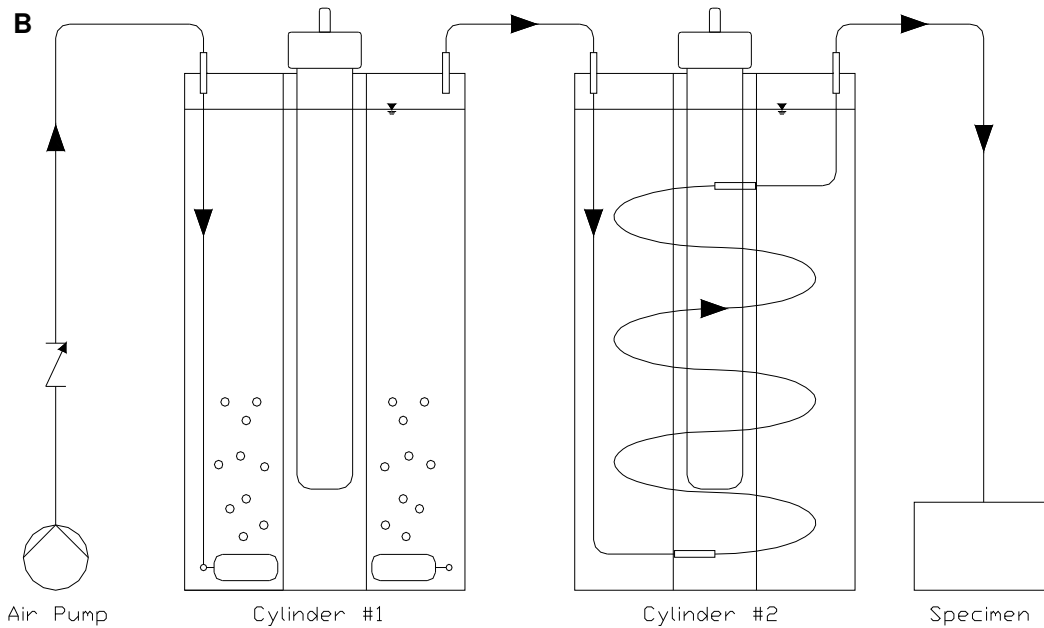


Figure 2.1: Prototype 1, an open system in which the egg sits without being resealed or placed in a chamber. A) The device was built to regulate the temperature and relative humidity of the specimen. Air is provided by the aquarium air pump, and is heated in cylinder 1. At the top of cylinder 1, the air should have reached 100% relative humidity. In cylinder 2, the temperature is adjusted so that the desired relative humidity is reached. The outgoing air tube is heated to keep the air at relative humidity. B) A schematic representation of the layout of the machine.

The camera system is shown in Figure 2.2. The camera is a Retiga 1300 Cooled Monochromatic camera (QImaging, RET-1300-M-12-C, Surrey, British Columbia), connected to a Optem Zoom 100 lens system via a 2x dovetail tube (Qioptiq Imaging, 33-12-20-000, Fairport, New York). The entire system is mounted on a stand so that when zoomed all the way out, the bottom of the lens is 23 cm away from the base. Lighting was generated by a Fostec DCR (product #8360-2) optics light source and directed to the specimen using a ring light.

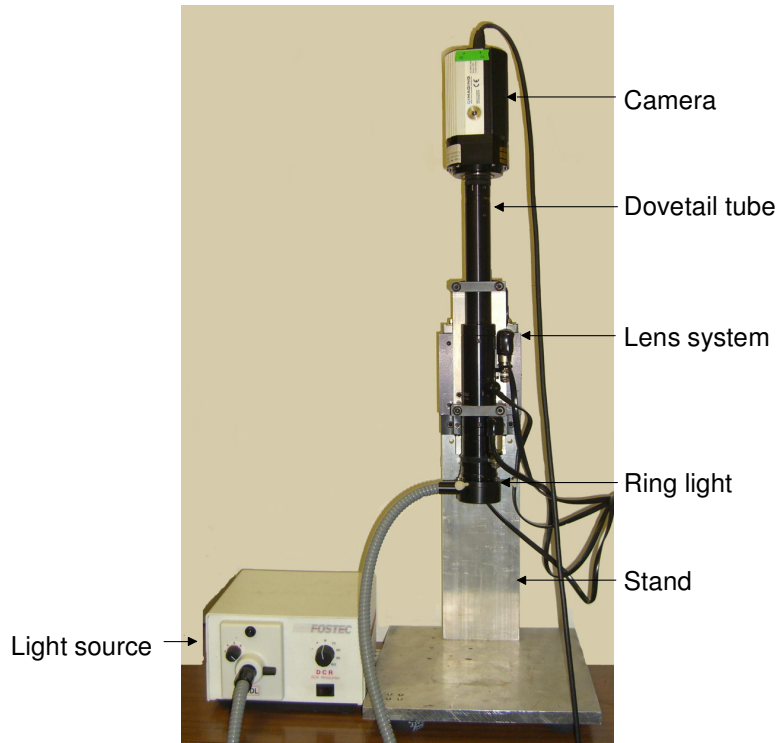


Figure 2.2: The camera system used in Prototypes 1 and 2. The camera is a Retiga 1300 cooled monochromatic camera, which is attached to an Optem Zoom 100 lens system via a 2x dovetail tube. The system is attached to a metal stand, where, at its highest point, the lens is approximately 23 cm away from the base. The light source is a ring light connected to a Fostec fiber optics light source. This camera system is also used in Prototype 3, though the ring light and Fostec light source were replaced with a Volpi Intralux 6000 with a trifurcated gooseneck light attachment.

2.4.2. Results and Discussion

The Air Temperature and Humidity Control unit was designed to output air at 37.8°C and 58-60% relative humidity. While this goal was achieved, the unit was unable to create an environment in which the embryo could develop. Initially, the outgoing air tube was not heated. It was found that the air dropped in temperature and began to condense in the tube, resulting on water dripping onto the embryo. The original Tygon tubing was replaced with rubber tubing with a thicker wall, in an attempt to keep the temperature constant as the air traveled to the specimen. When the condensation continued, the heating wire was then added to keep the air at temperature and relative

humidity until it reached the egg. This addition was still not enough to allow the embryo to develop. The embryo was still drying out within an hour of windowing (Figure 2.3). Further testing revealed that the force of the air coming from the output tube was not strong enough to flow over the entire window (approximately 2 cm x 2 cm square). The reported flow rate of the air pump was 1.8 liters per minute at 4 psi. As well, testing showed that the temperature of the air dropped to room temperature approximately 1.5 cm from the end of the output tube.

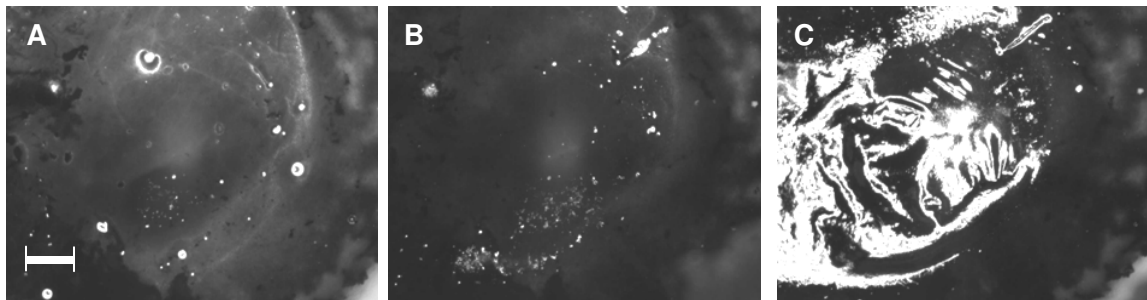


Figure 2.3: Representative images of 1-day old chick embryos using Prototype 1. A) At $t = 0$. B) At $t = 60$ minutes, the embryo is still visible though there are signs of drying out at the edges (arrow). C) At $t = 75$ minutes, the embryo has dried out and a crust has formed. The scale bar represents $100\ \mu\text{m}$, and the zoom was constant throughout the test.

To increase the amount of air being pumped from the unit, a simple test was used to determine the rate of air flowing through the unit. A bag approximately 2L in volume was attached to the output tube, and the time it took to fill up the bag was determined. Initial flow times (i.e. time required for air flowing through to fill the bag) can be seen in Table 1.

Table 1: Flow times of the original Prototype 1 components, to determine efficacy of the air flow through the apparatus. This was done because airflow coming from the output tube did not match the flow rate of 1.8L/min stated on the air pump. Each component was tested once.

Component	Flow Time* (min)
Air pump through 10 cm of tubing	1.0
Cylinder 1	2.0
Cylinder 2	1.5
Entire system	5.0

* Flow time refers to the amount of time taken to fill a small 2L plastic bag.

Each component of the unit was tested and adjusted to improve air flow. For cylinder 1, four different types of air stones were tested to determine which would allow the most air to diffuse into the set-up: 4 cylindrical air stones, which were 1.27cm (0.5”) wide and 2.54cm (1”) long (Petccetera); a round air disk, 10.16cm (4”) in diameter (Top Fin Round Airstones, Petsmart # 2752196); another round air disk, 10.16cm (4”) in diameter (Petccera); and an air bar, 10.16cm (4”) in length (Petccetera). To test these air stones, a 500 mL beaker was placed upside down in a tub of water so that the beaker was completely filled with water (i.e. no air bubbles). The air stones were then connected to the air pump and placed in cylinder 1. Rather than connecting to cylinder 2, a length of Tygon tubing was connected to the output nozzle of cylinder 1. The other end of this tube was placed into the tub, so that air would flow into the upside-down beaker. Each set of air stones was tested once. Table 2 shows the results of this testing.

Table 2: Testing flow rates of different air stones to improve air flow in Prototype 1. A 500mL beaker was placed upside down in a tub of water, so that no air bubbles are in the beaker. Each type of air stone was connected to the air pump and placed in cylinder 1. A tube was connected to the output nozzle of cylinder 1, with the other end under the beaker. Each type of air stone was tested once.

Type of Air Stone	Flow Time* (s)	Flow rate (L/min)
4 cylindrical air stones	10 s	3 L/min
Air disk (Top Fin)	21 s	1.5 L/min
Air disk (Petcetera)	13 s	2.3 L/min
Air bar	13 s	2.3 L/min

* Flow time refers to the time taken to fill a 500 mL beaker with air.

Other changes were made in an attempt to increase airflow throughout the system. A larger air pump (Tetra Whisper Air Pump, Petsmart #2783029) was purchased. The Tygon tubing was replaced with tubing of greater diameter (from 0.3175cm [1/8"] to 0.47625cm [3/16"] ID) throughout the entire setup. Copper tubing with a greater diameter (ID = 0.635cm [1/4"], OD = 0.9525cm [3/8"]) was purchased, but the greater diameter made the fashioning of the double helix shape impossible without producing kinks in the tubing, so the diameter of the copper tubing was kept the same (ID = 0.3175 [1/8"], OD = 0.635cm [1/4"]). The improved version showed a substantial increase in the amount of airflow, in that one could feel a greater amount of air coming form the output tube. The window cut in the egg was also made narrower (from approximately a 2 cm x 2 cm square to approximately a 1.5 cm x 1.5 cm square) so that the air would have less area to cover. To compensate for the fact that hot air rises, the output tube was aimed at a downward angle to the specimen.

Unfortunately, even with these changes, we were unable to maintain the conditions needed for an embryo to develop (see Appendix IV). As no temperature or

relative humidity measurements were taken, success or failure of the prototype depended on whether the embryo was able to develop, or whether it dried out. As well, with the addition of the heater, and the control module for the heated wire on the output tube, the sheer size of the entire set-up made it unfeasible as a final design.

2.5. Prototype 2: Convection

The set up of prototype 2 is depicted in Figure 2.4. This prototype makes use of the concept that hot air rises in order to provide gentle circulation.

2.5.1. Methods and Materials

The major change from the previous prototype was that the Air Temperature and Moisture Control unit was removed. In its place, the egg was now placed within a plastic container with a domed lid. Water is placed in the bottom of the container (diameter = 10.5 cm, height = 6.5 cm), with the idea that as the warm air rises, the domed lid forces it to flow over the open window in the egg, acting much like the blanket concept from the previous prototype. The air then exits through the hole at the top (1.6 cm wide), which is also where the camera views the egg. Initially, the egg was nestled in a copper scourer, similar to the previous prototype. As discussed in the next section, the scourer was then replaced with a metal flange sitting on an acrylic pedestal. The heater from Prototype 1, a metal box with a Kapton foil heater, was re-used. This was connected to a temperature control module. The temperature control module is run on a feedback mechanism, which is diagrammed in Figure 2.3B. A Type K thermocouple (Chromel/Alumel) is placed into the container, at approximately the level of the egg. The thermocouple then relays the temperature back to the module (CAL Controls 9400 Autotune Temperature Controller),

which will then adjust the heat output from the heater. This ensures that the temperature of the air, and not the water, is at optimal temperature.

A



B

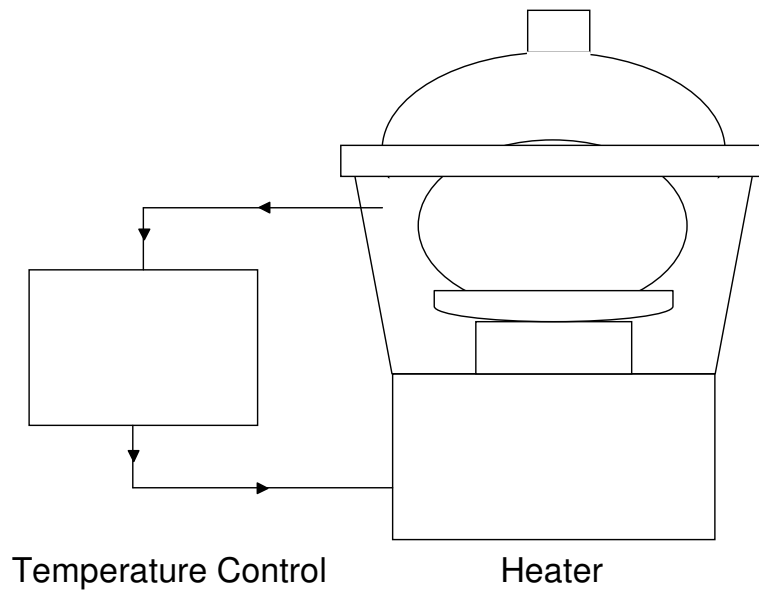


Figure 2.4: Prototype 2, a semi-closed system in which air is forced to go over the windowed egg. A) Prototype 2 was designed with the idea that hot air rises. The Air Temperature and Moisture Control unit has been replaced by a semi-closed system. Water sits in the bottom of the container, and is heated from below by the heater. The heated air rises around the egg, acting as a blanket, then out through the domed lid. B) A schematic representation of the layout of Prototype 2.

The consistency of the temperature and relative humidity was tested by operating the prototype for 3 – 6 hours. Initially, 75 mL of distilled water was placed in the container and its level was marked. As the water evaporated, more distilled water was added to keep the water at that level. Temperature was measured using the thermocouple and temperature control module, and relative humidity was measured using the Digital Humidity Management Module (Brinsea #H22). The humidity sensor was placed in the metal flange so that the sensor was approximately the same level as the top of an egg sitting in the set-up. Four configurations were tested: 1) Both the lid and the ventilation panel were closed; 2) The lid was closed and the ventilation panel was completely open; 3) The lid was closed and the ventilation panel was half-open; 4) The lid was partially open and the ventilation panel was closed. Measurements were taken every 5 minutes.

2.5.2. Results and Discussion

The initial design of prototype 2 involved the egg being nestled in a copper scourer, with the idea that copper is an excellent heat conductor, and would be able to surround the egg, keeping the entire egg at the same temperature. Unfortunately, it was found that not only was the copper scourer unable to keep the egg at temperature, it also prevented the heated air from rising, which ran counter to the concept upon which the prototype was designed. Therefore, the scourer was replaced with a metal flange sitting on an acrylic ring. The metal flange was chosen because it was approximately the correct shape to hold an egg on its side.

Another adjustment made to the initial design was the addition of a sliding panel on the side to act as a vent. In the initial design, the opening at the top of the domed lid

acted as both a viewing window and as a source for fresh air. Ventilation can play a role in the proper incubation of an egg, as embryos can suffocate if placed in an air-tight environment, but too much ventilation removes humidity.

For all four configurations of Prototype 2, relative humidity measurements were shown to be far above the 58-60% RH suggested by previous literature (See Appendix III for raw data). Figure 2.5 - Figure 2.8 show the temperature and relative humidity measurements for the four configurations.

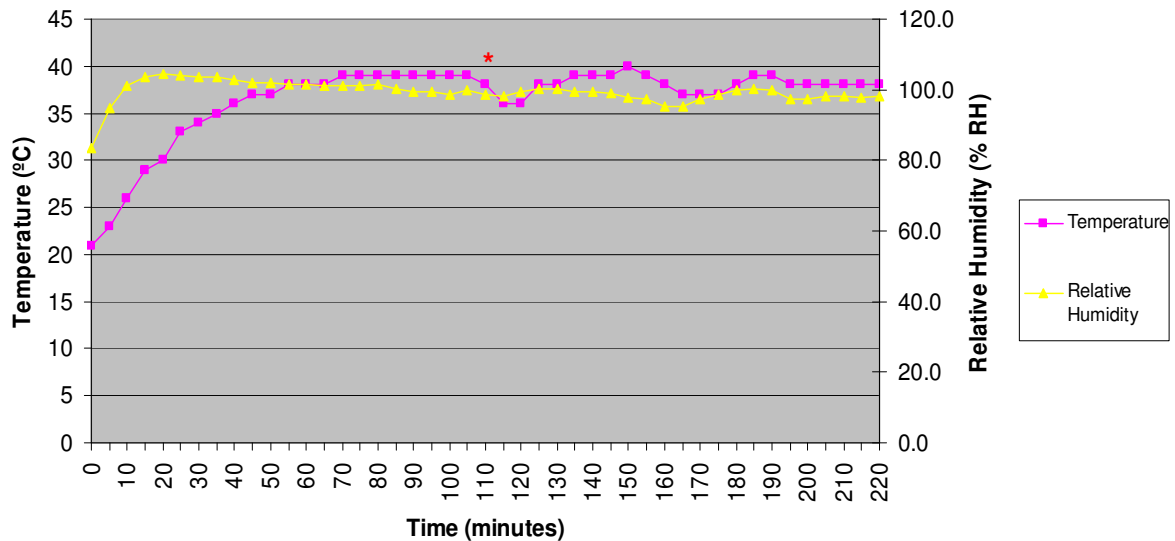


Figure 2.5: Temperature and relative humidity measurements of Prototype 2 when the lid and the ventilation panel are completely closed. The test was run for 220 minutes, with measurements taken every 5 minutes. Time (in minutes) is measured on the X axis. Temperature (in °C) is shown on the left Y-axis, and relative humidity (% RH) is shown on the right Y-axis. Temperature measurements are represented by the pink squares, relative humidity by the yellow triangles. The red asterisk indicates when the container was refilled with distilled water. The average temperature was 36.5°C, with a standard deviation of 4.2°C. The average relative humidity was 99.4%, with a standard deviation of 3.3%.

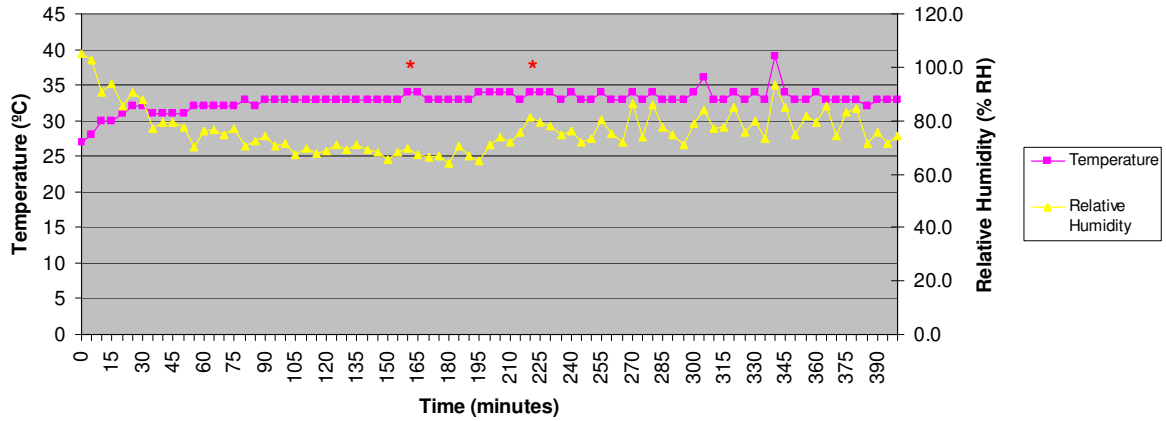


Figure 2.6: Temperature and relative humidity measurements of Prototype 2 when the lid is closed and the ventilation panel is completely open. The test was run for 400 minutes, with measurements taken every 5 minutes. Time (in minutes) is measured on the X axis. Temperature (in °C) is shown on the left Y-axis, and relative humidity (% RH) is shown on the right Y-axis. Temperature measurements are represented by the pink squares, relative humidity by the yellow triangles. The red asterisk indicates when the container was refilled with distilled water. The average temperature was 32.9°C, with a standard deviation of 1.5°C. The average relative humidity was 76.3%, with a standard deviation of 8.1%.

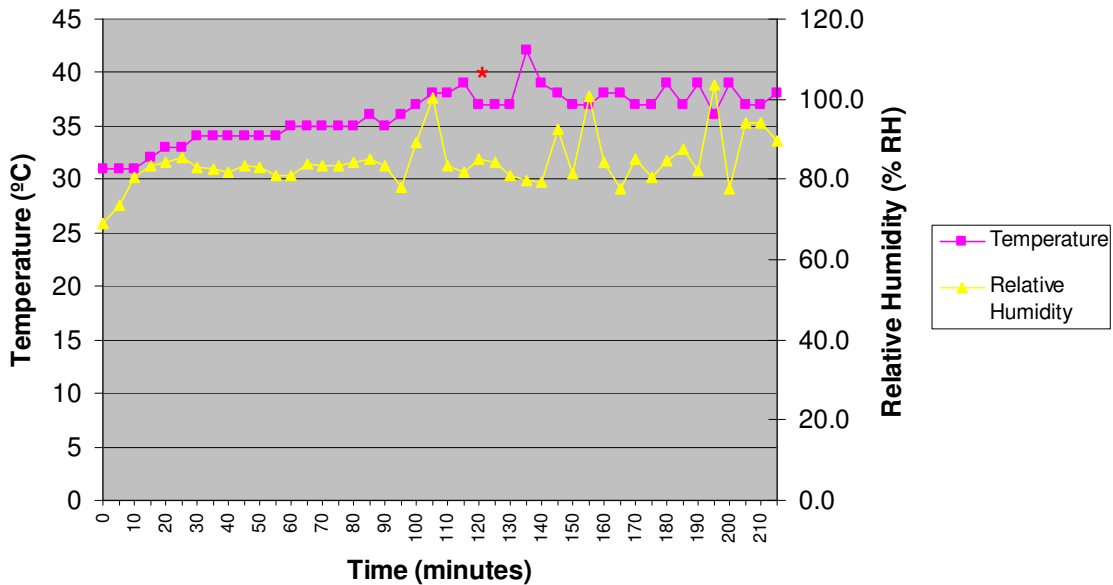


Figure 2.7: Temperature and relative humidity measurements of Prototype 2 when the lid is closed and the ventilation panel is half-opened. The test was run for 215 minutes, with measurements taken every 5 minutes. Time (in minutes) is measured on the X axis. Temperature (in °C) is shown on the left Y-axis, and relative humidity (% RH) is shown on the right Y-axis. Temperature measurements are represented by the pink squares, relative humidity by the yellow triangles. The red asterisk indicates when the container was refilled with distilled water. The average temperature was 36.0°C, with a standard deviation of 2.4°C. The average relative humidity was 84.4%, with a standard deviation of 6.5%.

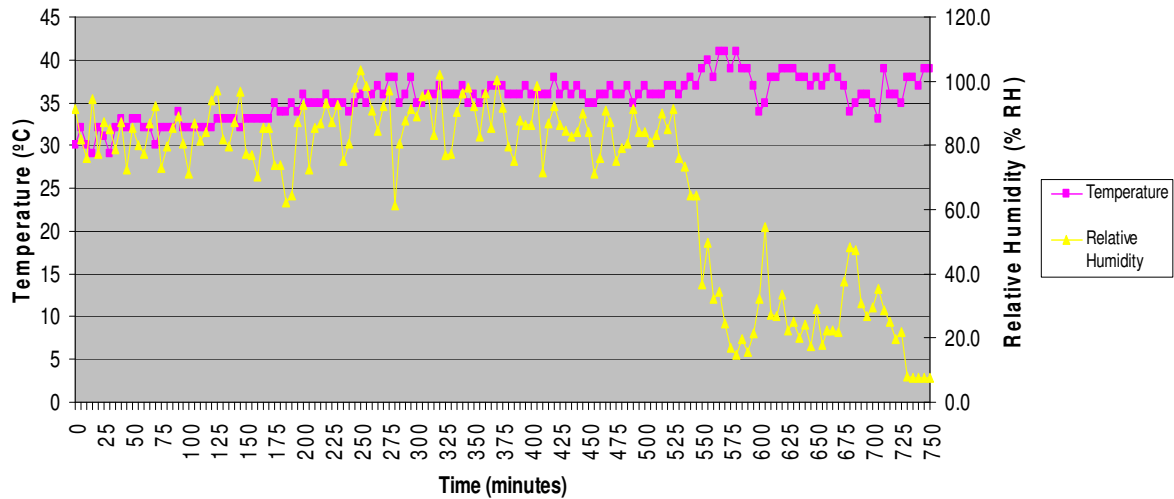


Figure 2.8: Temperature and relative humidity measurements of Prototype 2 when the lid is partially open and the ventilation panel is closed. The test was run for 750 minutes, with measurements taken every 5 minutes. Time (in minutes) is measured on the X axis. Temperature (in °C) is shown on the left Y-axis, and relative humidity (% RH) is shown on the right Y-axis. Temperature measurements are represented by the pink squares, relative humidity by the yellow triangles. The container was not refilled with distilled water during this test. One can see that after 545 minutes, the water has evaporated from the container and the relative humidity drops. The average temperature was 35.5°C, with a standard deviation of 2.4°C. The average relative humidity was 68.5%, with a standard deviation of 27.9%.

From these figures, it can be seen that while temperature could be kept fairly consistent, relative humidity was most of the time above the 58-60% range required for normal development in the embryo. Temperature and relative humidity were most consistent when both the lid and the ventilation panel were closed (Figure 2.5). The average temperature was 36.5°C, with a standard deviation of 4.2°C. The average relative humidity was 99.4%, with a standard deviation of 1.7%. While the standard deviation in temperature seems large, especially since chick embryos can only withstand temperature variations of approximately 1°C, it is important to note that in a standard test, the egg would not be placed in the apparatus until it reaches 37°C. Therefore, if one discounts the time points before the apparatus reaches 37°C (before $t = 45$ minutes), the average temperature is 38.2°C, with a standard deviation of 0.9°C. As well, one should note that

there is a slight dip in the temperature at $t = 110$ minutes, when the water in the container had to be refilled.

When the ventilation panel is completely open (Figure 2.6), the average temperature was 32.9°C , with a standard variation of 1.5°C . The average relative humidity was 76.3% , with a standard variation of 8.1% . Again, the container was refilled at $t = 165$ minutes and $t = 210$ minutes. While the relative humidity was lower, and closer to the desired range of $58\text{-}60\%$, the apparatus never reaches the temperature required for an embryo to develop normally.

When the ventilation panel was partially open, the average temperature was 36.0°C , with a standard deviation of 2.4°C . The average relative humidity was 84.4% , with a standard deviation of 6.5% . The container was refilled after approximately 120 minutes. There are a few spikes in relative humidity during this test, which could be attributed to condensation accumulating on the sensor, or dripping condensation from the lid of the apparatus. Though the temperature was kept close to the required temperature for chick embryo growth, the variation is still too great to ensure that the embryo grows normally.

It was thought that perhaps the large variations in relative humidity inside the prototype when the ventilation panel was open might be due to the panel being on the side of the container, so that the warm air was not necessarily rising and circulating over the sensor, but simply flowing out the vent. Therefore, one more test was done with the ventilation panel closed, but the lid open approximately 1cm (Figure 2.8). In this situation, theoretically, the warm air would still rise, and still create that localized air pocket over the embryo before escaping out the top. It was found that temperature took

almost 6 times as long to reach 37°C ($t = 265$ minutes). The average temperature was found to be 35.5°C, with a standard deviation of 2.4°C. The average relative humidity was 68.5%, with a standard deviation of 27.9%. This large standard variation is mostly due to the fact that the test was run overnight, and all the water from the container had evaporated by approximately $t = 545$ minutes, which is indicated by the large drop in relative humidity. If one only considers the time points before this drop, the variation is no longer so large (average = 85.1%, standard deviation = 8.5%). The variation is still quite large, which is most likely due to the very large opening. The design of Prototype 2 assumed that the dome shape of the lid is what forces the rising warm air to pass over the embryo. If the lid were open, then the dome shape is no longer centered, varying amounts of air would pass over the embryo, and thus the sensor would show fluctuations in the relative humidity.

Because of the fluctuations in the temperature for all the configurations except when both the lid and the ventilation panel were closed, the first configuration was used for all tests with the embryo. No tests with embryos were conducted with the other configurations.

One important thing to note regarding the relative humidity measurements is that the equation for the calculation of relative humidity is dependent on temperature. Relative humidity is defined as the ratio of the partial pressure of the water vapour in the mixture to the saturation vapour pressure of water at the temperature of the mixture (Bohren & Albrecht, 1998, p. 186). As temperature increases, saturation vapour pressure increases non-linearly, thus relative humidity changes as well (Bohren & Albrecht, 1998, pp. 192-194). Therefore, for the present purposes of determining the stability of

temperature and relative humidity in the apparatus, relative humidity measurements taken before the temperature stabilizes need to be taken with a grain of salt, and most likely should not be included in calculations.

At several points during the tests, the relative humidity exceeds 100%. While, intuitively, this seems wrong, as conventional thinking sees air as a sponge with pores that can hold onto a finite amount of water vapour molecules, it has been shown that there are conditions under which the air could become supersaturated (Bohren & Albrecht, 1998, p. 182), usually where there is nothing upon which the vapour can condense. Further testing is required to determine whether this is the case here.

It was found that prototype 2 was able to keep a three-day old embryo alive for approximately 3 hours when placed in the first configuration (lid completely closed, ventilation panel closed). This was determined by examining the amount of time the heart of the embryo could be seen beating. While this was an improvement from prototype 1, it was still not suitable for the purposes of the present experiment. The process of neurulation, under ideal conditions, takes at least 6 hours (Stern & Holland, 1993). Therefore, the eventual prototype needs to be able to keep an embryo alive for at least that long. When the prototype was tested with a 1-day old embryo, growth was difficult to see, most often because the embryo was indiscernible from the background, even after the India ink solution was injected (see Appendix V). Lighting was also an issue, as the ring light originally used tended to reflect off the liquid surface of the embryo, resulting in a spot of glare in the middle of the picture, usually obscuring a part of the embryo. This problem was resolved by replacing the original ring light with a

three-way optic fiber light source, which allowed for multidirectional lighting to reduce the glare.

Other modifications were made in an attempt to address some of the issues of the prototype. Despite the fact that relative humidity was higher than the level recommended for the development of embryos (Figure 2.5), the embryo was still drying out, which indicates that having a semi-closed chamber was not enough to act as a virtual seal on the windowed egg, regardless of the relative humidity inside the chamber. Therefore, a cover for the window was considered, using, for example, a cover slip. Unfortunately, the amount of moisture caused condensation on the slide, obscuring the window. Since condensation occurs when the heated moist air is cooled, a heated lid was also considered. The heating wire from the previous prototype was wrapped around the domed lid of the container. As this was still unable to keep the viewing window clear for viewing, it was decided to focus on developing a set-up that allowed the embryo to grow while being visualized. The emphasis on accessibility was lessened, as microinjection of tracking points could be done before resealing.

2.6. Prototype 3: Transparent Window

The present prototype follows the protocol described by Kulesa and Fraser (2004). This technique has been used to investigate neural crest cell migration patterning under various conditions (Kulesa & Fraser, 2000; Kulesa *et al.*, 2000). The technique involves the assembly of a teflon window which is sealed in the windowed egg with beeswax. This allows the egg to grow within a sealed environment, much like an undisturbed egg, while allowing researchers to visualize the embryo as it develops.

2.6.1. Methods and Materials

The Teflon window was assembled using high-sensitivity, oxygen-permeable Teflon membrane (VWR, Cat. #52457-596), and an acrylic ring (OD = 2.5 cm, ID = 1.9 cm). White beeswax was warmed in a double-boiler set-up using a heating block. The acrylic ring was dipped in the beeswax, and then placed on a sheet of the Teflon membrane. An o-ring (OD = 3 cm, ID = 2.4 cm) was placed above the acrylic ring and pressed down. This traps the membrane, and pulls it taut, creating a flat window. Once the wax has solidified, the o-ring was removed, and excess Teflon was cut away. The resulting windows can be seen in Figure 2.9.

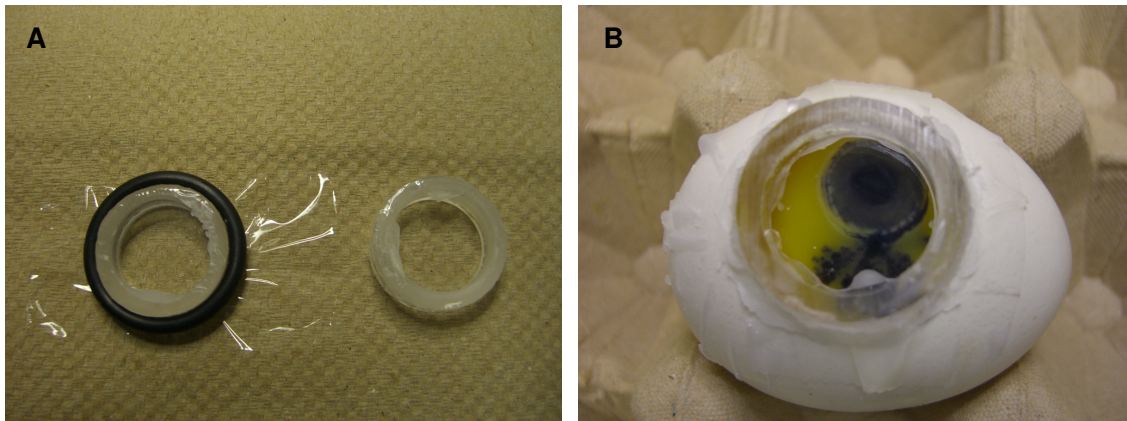


Figure 2.9: Teflon windows adapted from Kulesa and Fraser (2004) for prototype 3. A) Teflon windows for Prototype 3. The windows are made by stretching a sheet of high-sensitivity, oxygen-permeable Teflon membrane over an acrylic ring. B) The window is placed in the egg, making a fluid interface with the embryo, and sealed with beeswax.

The egg was then opened using a slightly modified version of the standard protocol (see Section 2.3). Rather than simply cutting a 2 cm square of shell, the outer diameter of the acrylic ring was traced on the shell, and that was cut away. The window was placed in the hole, so that the Teflon touched the surface, forming a fluid interface,

and was sealed with more beeswax. Care was taken so that the window was sitting level, as angles on the window may reflect light and cause a glare spot.

The set-up is similar to Prototype 2, and can be seen in Figure 2.10. The windowed egg sits inside a container on top of the heater, which is connected to the temperature control module. The domed lid was removed, and replaced with a chamber built out of cardboard, and covered with thermal insulation (Reflectix, R-value = 4.0). A hole was cut out of the chamber at the top, to allow room for the camera and lights.

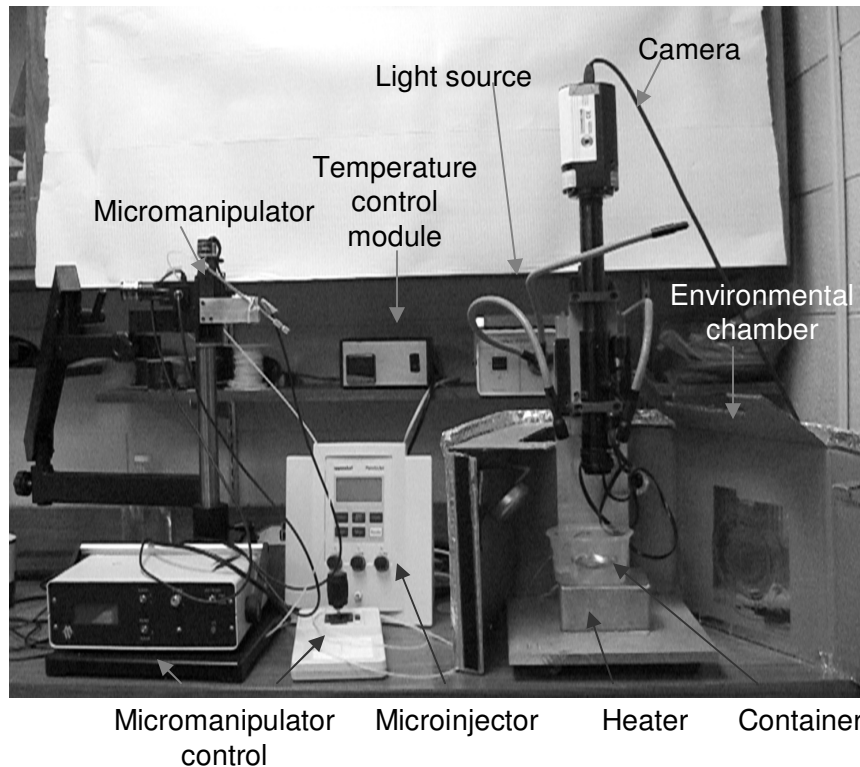


Figure 2.10: Prototype 3, designed to visualize a chick embryo within a closed environmental chamber. The egg sits within the container, which sits on the heater. The heater is controlled by the temperature control module, which functions according to a feedback mechanism. The container and heater are surrounded by an environmental chamber made from cardboard, and covered with thermal insulation. The light source is a three-way fiber optics light box. The microinjector is connected to the micromanipulator, which is controlled by a joystick that has x, y and z control capabilities.

Relative humidity was tested in a manner similar to that done for Prototype 2 (see section 2.5.1).

2.6.2. Results and Discussion

A few modifications needed to be made from the original protocol (Kulesa & Fraser, 2004). The protocol initially required the window to be placed in the egg with the Teflon window on top and the acrylic ring below. It was found that with that method, an air bubble would always be trapped below the surface, disturbing the fluid interface, and causing condensation on the inside of the window (Figure 2.6). Therefore, the window was placed so that the Teflon faced inwards, with the acrylic ring facing the outside. Doing this eliminated the air bubble, and allowed the clear visualization of the embryo during its development (Figure 2.11A).

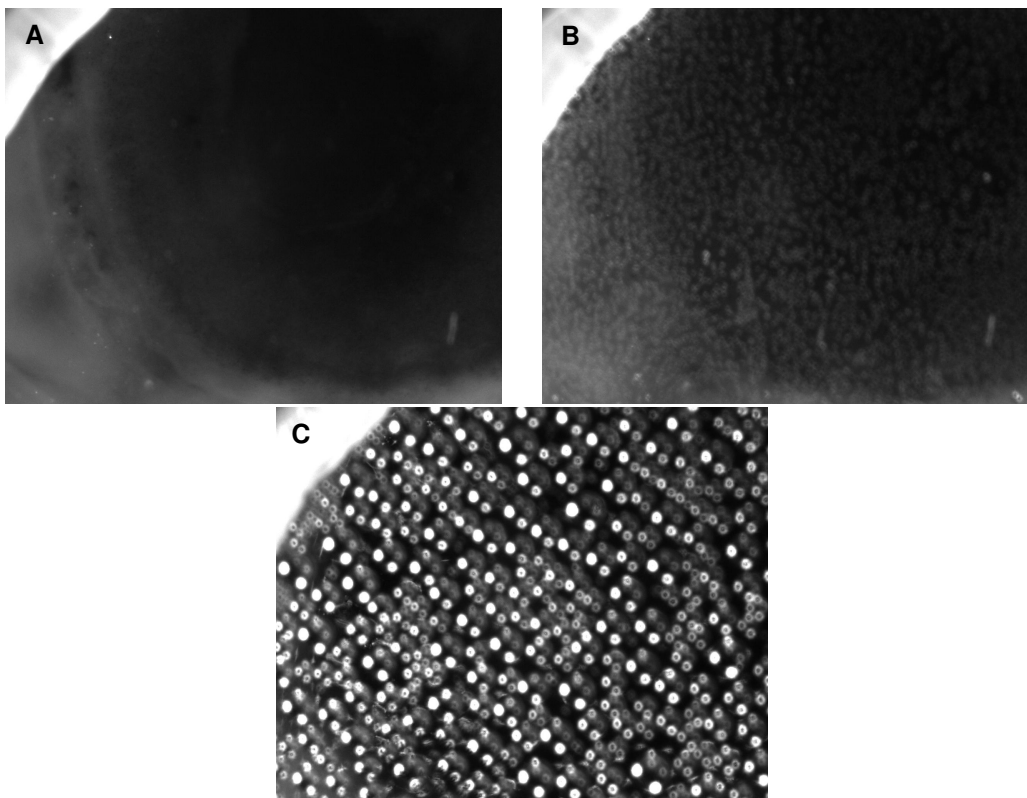


Figure 2.11: Following the protocol set out by Kulesa and Fraser (2004) resulted in condensation forming on the inside of the Teflon windows. As the window was placed with the acrylic ring down, and the Teflon membrane on top, an air bubble often became trapped, which caused condensation to form. A) at $t = 0$, the window is clear, and the embryo can be seen below. B) At $t = 60$ minutes, condensation has begun to form, and the embryo is beginning to be obscured. C) At $t = 360$ minutes (6 hours), the embryo is completely obscure from view by the condensation. A solution was found by simply reversing the window, so that the Teflon membrane touched the surface of the embryo first.

The relative humidity test did not turn out as expected (Figure 2.12). Prototype 3 was shown to be able to keep the temperature almost exactly at the temperature required for normal chick embryo growth (average = 37.9°C, standard deviation = 1.2°C), but the relative humidity was far below the recommended range (average = 17.2%, standard deviation = 2.5%). One possible explanation is that the humidity sensor was placed outside of the container, so the test may not be replicating the conditions of the egg exactly. Theoretically, since the environmental chamber is essentially a closed system, the relative humidity should be approximately the same throughout.

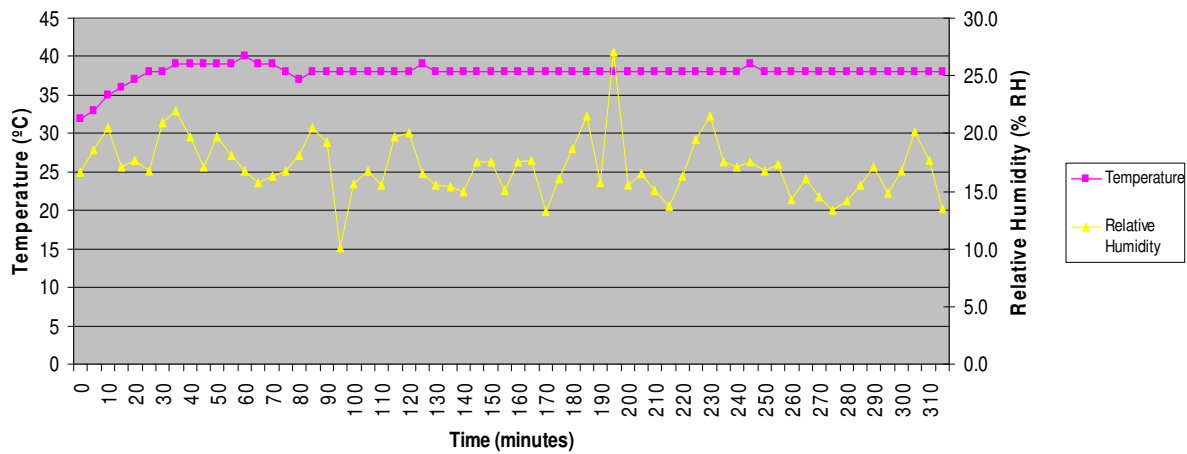


Figure 2.12: Temperature and relative humidity measurements of Prototype 3. The test was run for 315 minutes, with measurements taken every 5 minutes. Time (in minutes) is measured on the X axis. Temperature (in °C) is shown on the left Y-axis, and relative humidity (% RH) is shown on the right Y-axis. Temperature measurements are represented by the pink squares, relative humidity by the yellow triangles. The average temperature was 37.9°C, with a standard deviation of 1.2°C. The average relative humidity was 17.2%, with a standard deviation of 2.5%.

Tests showed that an embryo placed in this set-up was able to undergo neurulation, but at a decreased rate, taking approximately 24 hours for the neural folds to meet (Figure 2.13; see Appendix VI for more). This is likely due to the fact that relative humidity is lower than recommended.

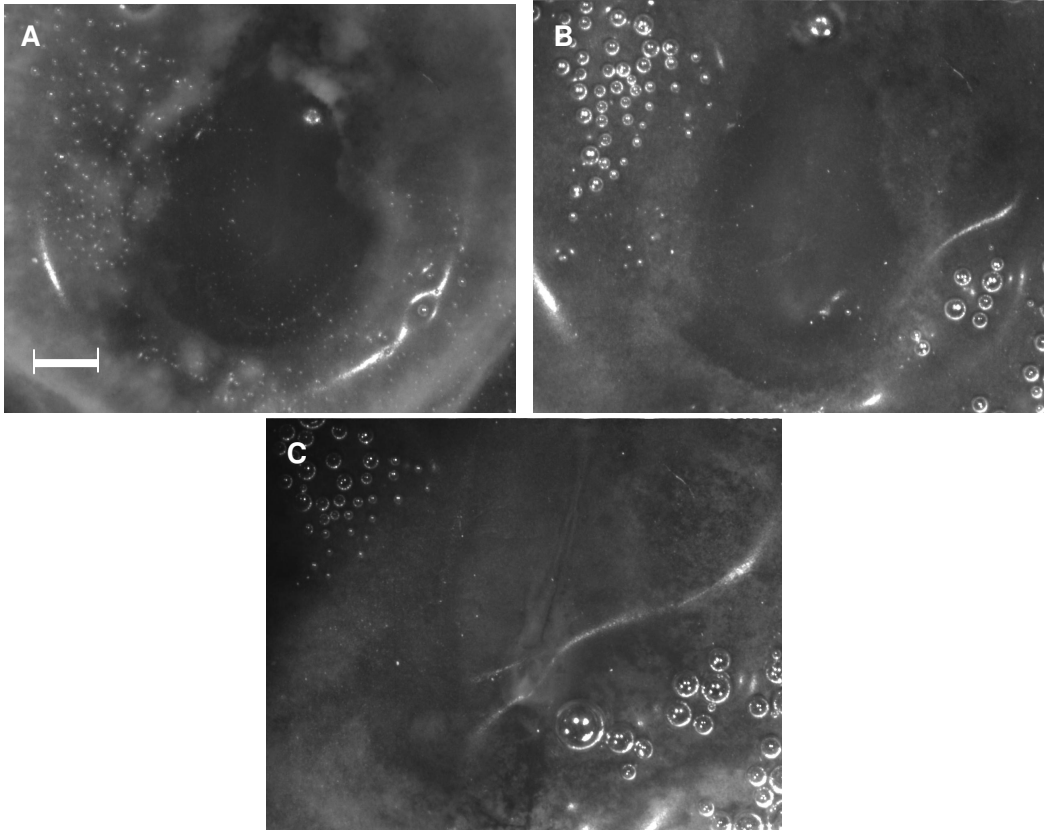


Figure 2.13: A successful run showing a 1-day old embryo undergoing neurulation in Prototype 3. A) At $t = 0$, the embryo is at approximately HH stage 6. B) At $t = 360$ minutes, the time in which neurulation is supposed to occur, according to Hamilton and Hamburger. The neural folds have not met at this time. C) At $t = 24$ hours, the neural folds meet. The scale bar represents $100 \mu\text{m}$, and applies to all the pictures.

2.7. Conclusion

A method for incubating chick embryos was found, but it required that a window cover the embryo, thus restricting the manipulations that could be carried out.

3. Tracking Cell Movements

3.1. Introduction

The second aim of the present study was to track small groups of cells in the early chick embryo as it undergoes neurulation. In order to accomplish this aim, a dye had to be chosen for microinjecting into the embryo.

3.1.1. History of Cell Tracking

Movement of cells is central to the process of neurulation, and thus an understanding of these movements is key to a complete understand of neurulation. Researchers have developed many ways to follow cells and their descendents throughout development. Initial experiments examined early cleavages in invertebrates such as tunicates and axolotls (Stern & Fraser, 2001). These organisms were used as they had differentiated pigmentation in their cells, thus making tracking much simpler. For organisms that do not have cells with different pigmentation, tracking cells depends on a researcher's ability to identify a particular cell or group of cells and their descendents. One technique often used is the application of vital dyes, the word "vital" indicating that the dye can be used for living cells (Stern & Fraser, 2001). This method was developed by Vogt in 1929 (Stern & Fraser, 2001), who applied chips of blue agar to the surface of amphibian embryos. The chips would stain a small group of cells, which would remain with the descendents regardless of where they moved. The main flaw with this approach was that the dye was water-soluble, which meant that results could not discount the possibility that the dye was transferred from cells to adjacent cells, rather than being passed on from mother to daughter cells.

Trinkhaus & Gross (1961) developed a method to address the major flaw of the previous method, using radioactively-labeled compounds. It was found that hydrogen- and tritium-tagged thymidine residues localized to the nucleus of the cell. As the thymidine is incorporated into new DNA as the cells divide, it is unlikely that the radioactivity would pass between adjacent cells (Kulesa, 2004). The drawback of this system is that the radioactivity becomes diluted as the cells divide, as the radioactivity is divided amongst the descendant cells.

The advent of carbocyanine dyes (DiI, DiO, etc.), which were fluorescent, lipid-soluble vital dyes. They were a vast improvement over previous dyes as they were incorporated nearly irreversibly into the plasma membrane, and were passed through many more generations than previously possible (Kulesa, 2004). These dyes have been used to track neural crest cells (Serbedzija *et al.*, 1989) as well as neuronal axon tracers (Honig & Hume, 1986). Microinjection techniques were developed to label cells, from individual cells to groups of one hundred or greater. Of course, ideally, a single cell would be labeled, and its descendants tracked, but this is technically challenging, especially when the cell of interest is small.

More recently, researchers have used GFP (green fluorescent protein), a genetically encoded fluorescent marker, as means of tracking cells (Chalfie *et al.*, 1994). GFP and its variants have the advantage of being bright, non-toxic and resistant to photobleaching. Other molecular techniques, such as alkaline phosphatase or β -galactosidase, also genetically encoded via retroviral vectors, but infection is random, thus cells cannot be chosen.

As each method of cell tracking has its advantages and disadvantages, the choice of the best method depends on the requirements of the particular question being addressed. The restrictions of the present study thus dictated which labeling method, and dye in particular, was chosen. For example, while GFP would seem to be the best method, folding of GFP at temperatures above 25°C is inefficient, leading to large amounts of insoluble protein (Scholz *et al.*, 2000). As well, since the set-up is not equipped to handle fluorescence, it does not make sense to choose fluorescent dyes, such as DiI or DiO. Finally, as the cells need to be tracked for the entire duration of neurulation, the dye should be hydrophilic, ensuring that it remains within the cell.

3.1.2. Microinjection

Microinjection is the process by which a small drop of liquid is expelled from a microcapillary through the application of pressurized air over a defined period of time. Using fine microcapillaries (with diameters of less than 1µm at the tip) a wide variety of substances can be injected directly into cells (Celis, 1984). This technique was initially developed by Graessman (1970), who used air pressure and a glass microcapillary to suck up a nucleus from a tumour cell and inject it into a mouse embryonic cell. He showed that the injected nucleus was able to take over the normal cellular functions of the mouse embryonic cell as autoradiography showed that it was able to undergo nuclear division, implying that microinjection has applications in living cells. The main advantage of microinjection over other techniques to introduce substances into a cell is that there are few to no restrictions as to what type of cell can be injected, as well as what substance is injected (Celis, 1984). The only limitations of the substance and where it can be injected are defined by the dimensions of the tip. Researchers have developed methods in which

miniscule volumes, down to nanoliters (van Dongen, 1984) and picoliters (McCaman *et al.*, 1977; Ansorge, 1982), can be injected using variations on the pressurized system. The volume injected depends on several factors: the injection pressure, injection time, viscosity and density of the substance being injected, and the inner diameter of the tip. Volumes can be measured in several ways. The microdrop technique (McCaman *et al.*, 1977; van Dongen, 1984) involves immersing the micropipette tip in mineral oil, then measuring the diameter of the ejected water droplets. This technique determines volumes greater than 100 picoliters with high reproducibility (standard deviation of 8%), but the standard deviation rises to 30% for volumes smaller than 100 picoliters (van Dongen, 1984). Another common method is measurement of fluorescence or radioactivity injected into a cell (Minaschek *et al.*, 1989). Using this technique, it has been found that even when a single microcapillary is used, the injected volume varies from cell to cell (Minaschek *et al.*, 1989)

Microinjection has been used extensively in avian embryonic research. DNA can be microinjected into zygotes using an *in vitro* culture of the chick. While this technique can develop transgenic chickens that contain and can pass on the plasmid DNA (Sang, 2004), it is labour-intensive and has a low efficiency rate. It has been suggested that approximately 1% of microinjected ova result in transgenic embryos, and only 10% of those grow to sexual maturity (Sang, 1994). Another common use for microinjection in chick embryo studies is the injection of dyes into small groups of cells for tracking purposes (Kulesa, 2004). This technique has been used extensively in the study of neural crest cells (e.g. Ruffins *et al.*, 1998; Kulesa & Fraser, 2000; Teddy *et al.*, 2005), where dyes, usually fluorescent ones, are injected into the neural lumen and are taken up by the

neural crest cells. The neural crest cells then migrate, and carry the dye with them so the research is able to follow the path. With the advent of dyes that can target specific components of a cell (GFP) and dyes that can be bound almost irreversibly to the plasma membrane, microinjection is a powerful tool that can be used to explore cell movements in the chick embryo.

3.2. Methods and Materials

Eggs were windowed as previously stated (see section 2.3). Microinjection was done with an Eppendorf FemtoJet (catalogue # 920010504), and Femtotips II, with an inner diameter of 0.5 μm and an outer diameter of 0.7 μm (catalogue # 930000043). A three-axis micromanipulator, the MCL-3 (Märzhäuser Wetzlar GmbH Co., #00-79-220-0835), was connected to control the injections (Figure 2.10 for diagram of the set-up). The eggs were then sealed as previously stated.

3.2.1. Approximating Microinjection Volume

It was determined that the simplest and most reproducible way to determine the volume per injection was to determine how many injections a specific volume contained, at a given pressure and for a given duration. To estimate the amount of liquid expelled in each injection, 2 μL of a very dilute solution of Fast Green FCF (0.1% w/v) was loaded into a FemtoTip II. The tip was then attached to the microcapillary holder of the FemtoJet. Injection pressure (p_i) was set at 900 psi and compensation pressure was set at 300 psi. Injection time was varied from 0.1s to 1.0s. The number of injections required to completely empty the tip was counted. Each injection time was tested 3 times and the average and standard deviation were calculated.

3.2.2. Choosing a Dye

The initial tests were done with 10% (w/v) solution of Fast Green FCF (CI 42053, $C_{37}H_{34}N_2Na_2O_{10}S_3$). Later tests used 0.5% (w/v) solutions of Neutral Red (CI 50040, $C_{15}H_{17}ClN_4$), Oil Red O (CI 26125, $C_{26}H_{24}N_4O$) and Janus Green B (CI 13025, $C_{30}H_{31}N_6Cl$). The methods for the tests were similar. A small amount of each dye is injected into the embryo ($p_i = 150$, $p_c = 50$, $t_i = 0.5s$). The embryo is then allowed to develop in the set-up at temperature and relative humidity, and pictures were taken every 5 minutes.

3.2.3. Cell Tracking

Taking advantage of the chick embryo's symmetrical neurulation, points of dye were injected on either side of the embryo ($p_i = 300$, $p_c = 100$, $t_i = 0.5s$). The egg was then resealed and placed in the set-up. Pictures were taken every 5 minutes, and the distance between the points was determined.

3.3. Results and Discussion

Initial tests were done with Fast Green FCF, a common food dye with a large hydrophilic anion (Horobin & Kiernan, 2002). It was found that while the set-up was able to create a small grid of microinjected points, the points of dye began to fade after approximately 5 minutes (Figure 3.1).

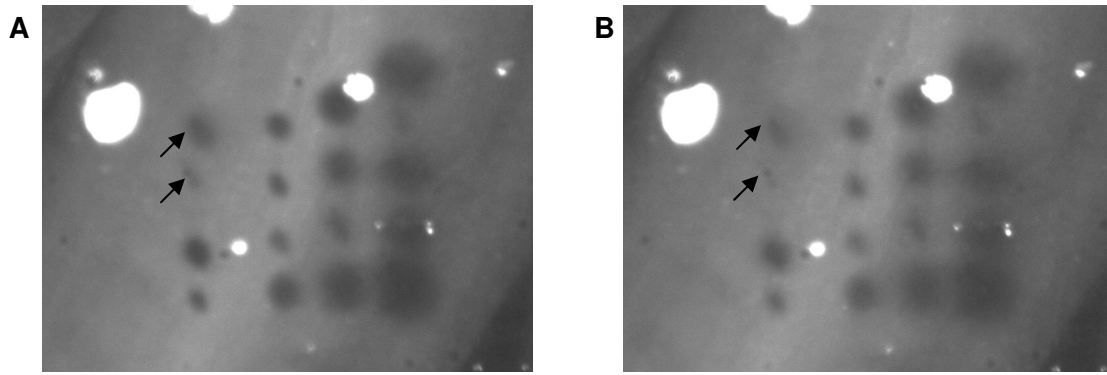


Figure 3.1: A chick embryo with a microinjected grid of Fast Green FCF compared at two time points, showing dissipation of the dye over time. A 0.5% (w/v) solution was microinjected in a grid on a 3-day old embryo. A) Grid at $t = 0$. B) Grid at $t = 5$ minutes. It can be seen that the points are dissipating with time. Arrows indicate the points where this is most apparent. While all the injections were done with the same microcapillary, the points increase in diameter from left to right because the tip becomes damaged with increased injections, resulting in increased volumes being injected, though the pressure and injection times remain the same.

The hydrophilicity of Fast Green FCF was most likely the cause of the dissipation, as the dye may be passed on from one cell to its neighbours. So while this dye had been previously used as a marker and a tracer (Horobin & Kiernan, 2002), it is clearly not suited for longer use, or for the purposes of the present study. The decision was made, therefore, to explore other vital dyes.

3.3.1. Testing Other Dyes

The purposes of the experiment required that the dye be non-toxic, non-fluorescent and hydrophobic. As well, due to the capabilities of the camera system, the dye should also provide enough contrast against the embryo to be visible.

A list of non-fluorescent dyes was compiled from Juarranz *et al.* (1986), who used the conjugated bond number (CBN) of the dye structure to predict fluorescence (Appendix 2). It was found that 70% of dyes with CBN greater than 30 were non-fluorescent. Therefore, dyes whose CBN was 29 or less were removed from

consideration. The study also examined the hydrophobic/hydrophilic characteristic of the dyes, using the water-octanol partition coefficient (log P). A positive log P value indicated that a dye was hydrophobic, and the list was further narrowed. Finally, Conn's Biological Stains (Horobin & Kiernan, 2002), a handbook for stains that have been used in biological and medical work, was used to research the remaining dyes, and to determine whether there were dyes that fit the requirements, but were not included in the previous study. Some of the remaining dyes were removed from consideration because their colour would not have provided enough contrast (metanil yellow, primuline, alizarin complexone). Others were rejected because their hydrophobicity required that working solutions be made with ethanol or DMSO, which are toxic to chick embryos. The final candidates were Janus Green B, Oil Red O, Pyronine Y, New Methylene Blue, and Neutral Red. Pyronine Y and New Methylene Blue were eventually rejected, as neither were available from suppliers. Neutral Red was added as a candidate, though it was originally removed from consideration based on the Juarranz *et al.* (1986) study. It is listed as hydrophilic in the original study, but Conn's (2002) notes that it is only hydrophilic in acidic aqueous solutions, while the lipophilic base toluylene red is present under basic conditions.

Similar to Fast Green FCF, tests were done to determine which of the three remaining candidates were best suited for the purposes of the present study (Figure 3.2). It was found that Neutral Red faded after approximately 30 minutes, and Janus Green B faded after approximately 110 minutes. Oil Red O remained visible for the entire run of the test, and was therefore chosen for the cell tracking tests.

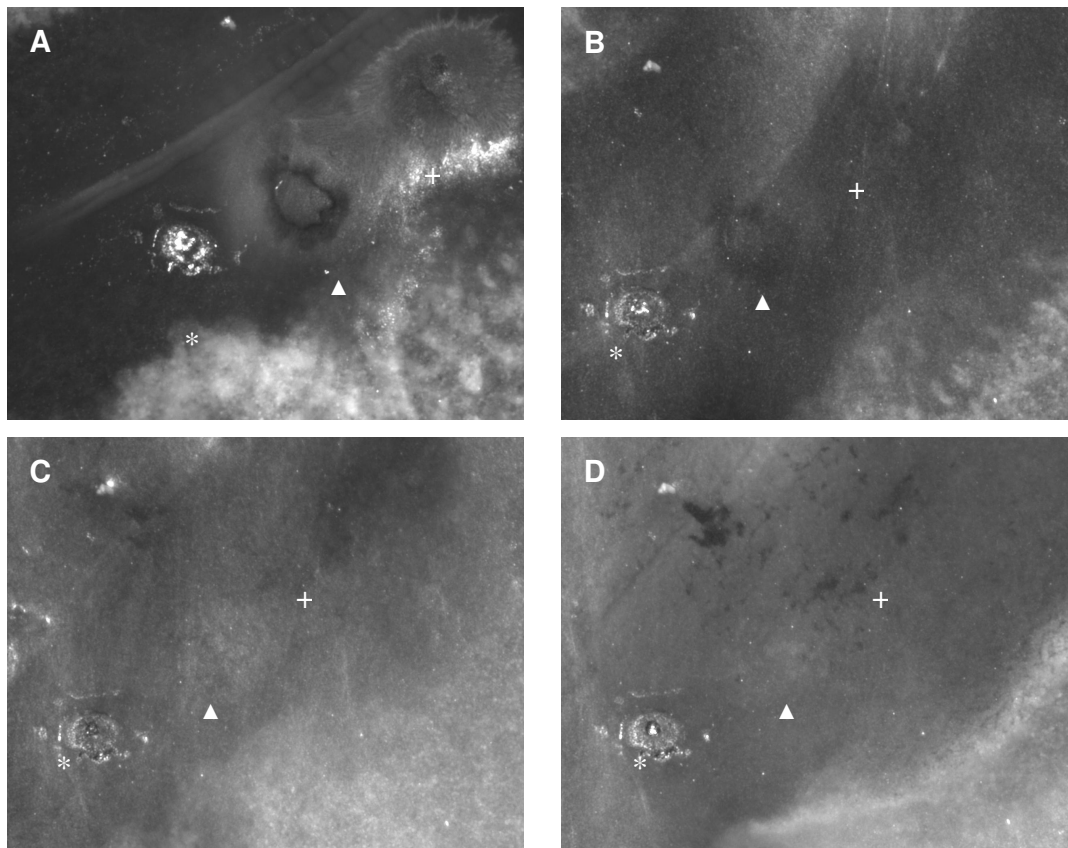


Figure 3.2: Comparing Oil Red O, Janus Green B and Neutral Red microinjected into a 3-day old chick embryo to determine which would be able to remain visible for the longest amount of time. A) The three dyes at $t = 0$. Oil Red O is denoted by the asterisk, Janus Green B by the triangle and Neutral Red by the plus sign. B) Picture taken at $t = 30$ minutes. The spot of Neutral Red has already dissipated, and Janus Green B has faded a bit. C) Picture at $t = 110$ minutes. Both Neutral Red and Janus Green B have faded, leaving only Oil Red O. D) Picture at $t = 360$ minutes. Oil Red O is still visible. As the present study requires that the dye used for cell tracking be visible after 6 hours, Oil Red O was chosen.

Oil Red O is a superlipophilic dye that has mostly been used as a stain for lipids, for example, to identify fat in foods, and to study aortic fatty streaks (Horobin & Kiernan, 2002). Almost no studies have used Oil Red O as a tracer or a marker, so it remains to be seen whether it will suit the purposes of the present study.

3.3.1. Approximating Microinjection Volume

Table 3 shows the data obtained from the microinjection volume tests. One can see that, as expected, the number of injections required to inject the $2 \mu\text{l}$ of solution from

the microcapillary decreases, and the volume per injection increases. Unfortunately, only 2 injections times were tested, as that was how long that microcapillary lasted before breaking. As previous studies had found that volumes had high reproducibility within a microcapillary, but volumes also varied between capillaries (Minaschek *et al.*, 1989), only 1 capillary was tested.

Table 3: Estimating Volume Expelled from Micropipette per Injection, with $p_i = 900$ psi and $p_c = 300$ psi. The count refers to the number of injections required to expel 2ul of a 0.1% (w/v) solution of Fast Green FCF from a microcapillary. Only 2 time points were recorded as the capillary broke after this point, and volume injected has been shown to vary between capillaries.

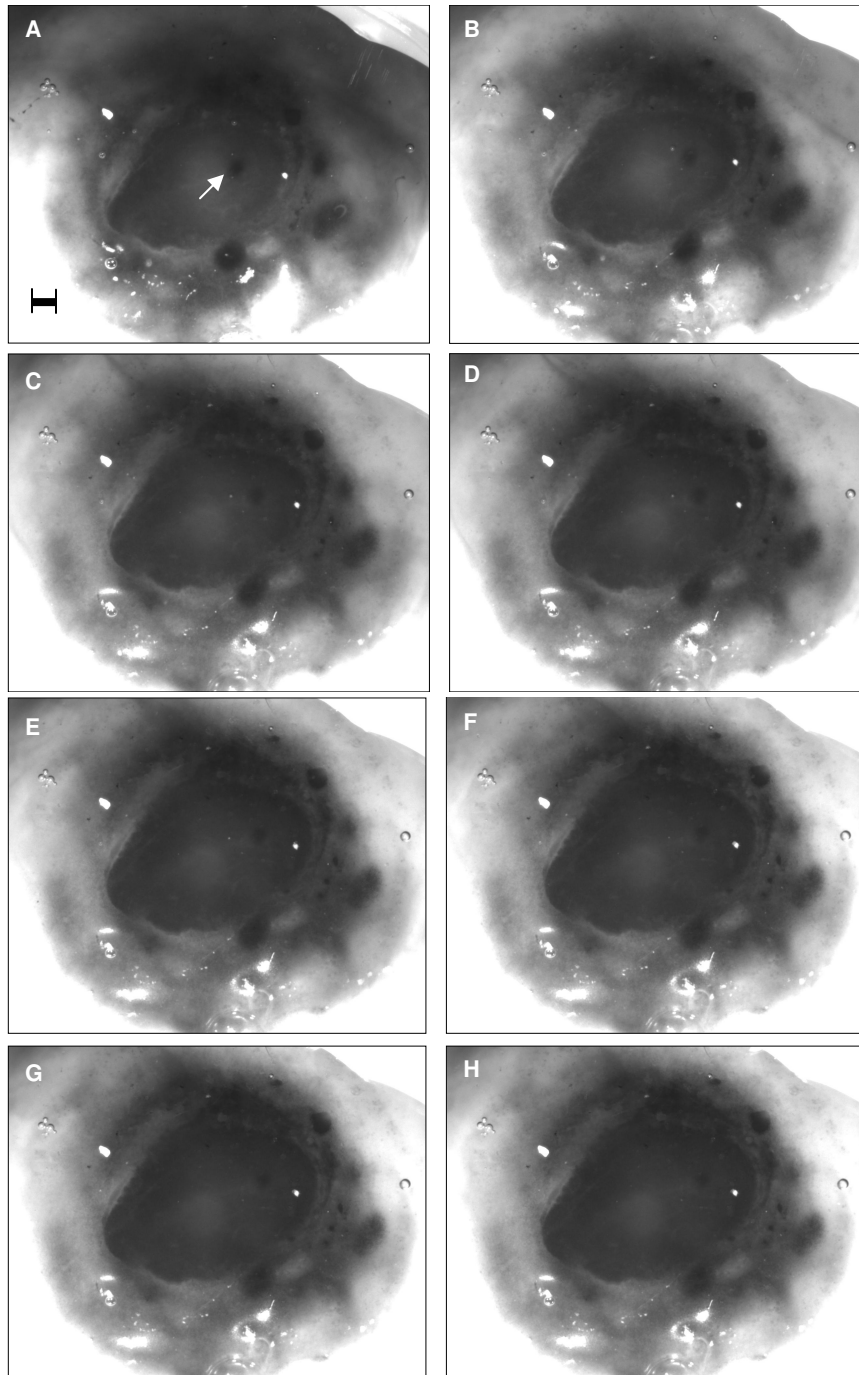
Injection time (s)	Count 1	Count 2	Count 3	Average	Standard Deviation	Volume per Injection (nl)
0.1	350	399	302	350	48.5	5.8
0.2	112	127	150	130	19.1	15.6

One major drawback in using this technique to determine volume per injection is the fact that the diameter of the tip may change with consecutive injections (Minaschek *et al.*, 1989). This is because the tip is so narrow that the solution can dry and clog the tip very easily. This may explain why, for example, for injection time of 0.2s, the injection counts for tests 1, 2 and 3 get larger, implying that there is less volume per injection. This may be due to the slow buildup of residue on the inside of the tip, much like the slow clogging of an artery.

3.3.3. Cell Tracking

Due to time restrictions, the cell tracking tests were not completed as scheduled. Some tests were run, but the results were unable to be used for tracking. The results of a sample microinjection test are depicted in Figure 3.3. While a point of dye can be seen on the neural plate at $t = 0$, the point dissipates during the test without moving, thus the distance could not be calculated. It was found that one major drawback of the set-up and

the placement of the micromanipulator was that it was very difficult to tell when the tip of the microinjector was actually touching the surface. As well, the microinjection had to be done in a timely manner, as the embryo is exposed to the air during this time. With more time and practice, however, the cell tracking envisioned for the present study could be done.



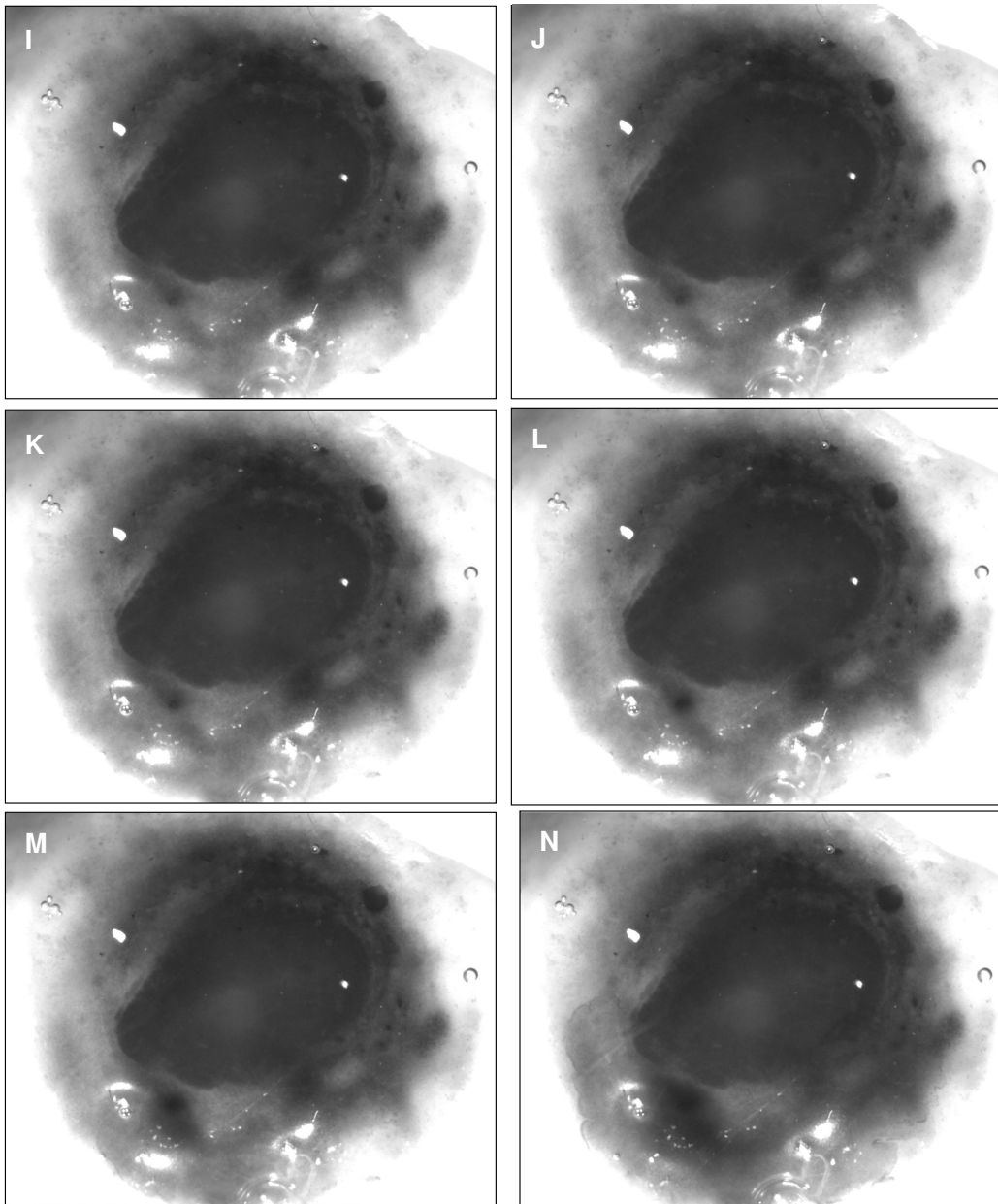


Figure 3.3: A sample microinjection done with Neutral Red shows that precise microinjection is difficult when the micromanipulator is driven by hand, and that Neutral Red dissipates too quickly to be suitable as a tracking dye. Panels A – N show pictures taken every 5 minutes, starting at $t = 0$ minutes. The white arrow indicates the one point that was placed on the neural plate. As can be seen the point dissipates during the run of the test. As well, ink from below the embryo leaked out after 70 minutes, so the test was ended. The scale bar represents $160\mu\text{m}$.

3.4. Conclusions

The aim of the present study was to track the movement of cells in the chick embryo during neurulation, time restrictions prevented this aim from being reached.

However, it was determined that Oil Red O would be suitable for the purposes of cell tracking, as it is a non-fluorescent hydrophobic dye that provides adequate contrast when microinjected into the chick embryo.

4. Conclusions and Future Directions

4.1. Conclusions

The aims of the present study were to 1) create a method where the embryo could develop *in ovo*, but was still available for manipulations and visualization during its development, and 2) examine the movement of cells in the early chick embryo during neurulation using that method.

The first goal was accomplished. While a protocol was developed in which a chick embryo could be visualized *in ovo* as it undergoes neurulation, but many compromises had to be made along the way. While we had initially wished to keep embryos available for manipulation throughout development, it transpired that the prototypes were unable to keep the embryo from drying out, and thus a “closed” system needed to be developed. The final set-up incorporates elements from the first two prototypes, and takes advantage of the Teflon windows developed by Kulesa and Fraser (2004). In this set-up, the embryo was able to develop, though at a decreased rate.

The second goal, however, was only half-accomplished. While Oil Red O was determined to be suitable for the purposes of cell tracking, time restrictions prevented us from actually conducting the cell-tracking tests. Future work would definitely include taking this next step.

This is the first study which has attempted to develop a chick embryo inside the egg while having the embryo available for visualization and manipulation. It was found that a localized air pocket was not enough to act as a virtual seal on the windowed egg.

4.2. Future Directions

The obvious next step would be to actually conduct the cell-tracking tests. The micromanipulator would be used to inject a series of points along the neural ridges of the embryo, and these points would be tracked as the embryo undergoes neurulation.

4.2.1. Future experiments regarding cell movement

Once cell movements with the set-up have been determined, the next step is to determine what occurs when this process is perturbed, for example, with drugs. Women who take antiepileptic drugs, such as valproic acid, have been shown to have an increased risk of having spina bifida-affected pregnancy (CDC, 1982). However, the mechanisms of valproic acid are not yet fully understood, and it is unknown how valproic acid affects cell movement, though an *in ovo* model has been developed (Whitsel *et al.*, 2002). It would be interesting, therefore, to take advantage of the symmetry of the chick embryo, and inject one side of the embryo with drugs, while using the other side as an internal control, and track how the cell movements differ.

Similarly, there are aspects of neurulation in chick that are still unknown. For example, there are proposed roles for microtubules and microfilaments in neurulation, though they have only been studied with regards to cell shape during neurulation (e.g. Smith & Schoenwolf, 1990). Experiments could be conducted in which the normal functioning of microtubules and microfilaments are disturbed, for example, by drugs such as colchicine and cytochalasin B, and the role these structures play in neurulation could be explored.

4.2.2. Future experiments regarding visualization

While the set-up developed is able to provide the conditions required for the experiments, it is by no means an ideal set-up. Improvements could be made in terms of the time it takes the chamber to heat up to temperature, as well as for the control of relative humidity within the chamber. As well, the injection of points of dye would be made more easily repeatable if the micromanipulator was computer-controlled, rather than hand-controlled.

Changes in the camera system and its capabilities could also improve the quality of the images taken and the types of experiments that could be conducted. The ability to take coloured pictures, for example, could allow for a greater variety of dyes to be used. Fluorescence capabilities would allow the use of DiI and DiO, two dyes that are now very commonly used.

The prototypes developed in the present study were unable to allow the egg to develop unsealed, but further experiments could be conducted. For example, if the camera system were moved to a heated and humidified room, it is possible that the embryo could develop without having to be resealed.

An interesting next step to take in terms of the set-up would be to expand it to allow for confocal microscopy. The current set-ups only allow for 2-D tracking of cells, and once a cell moves below the surface of the embryo, it can no longer be visualized. Confocal microscopy is essentially fluorescence microscopy with optical sectioning using a laser. Teddy *et al.* (2005) developed a method in which up to four fluorescent protein constructs could be microinjected into the neural tube lumen. The neural crest cells could then be tracked using a confocal microscope, without any negative effect to the

development of the embryo. This technique could be adapted for experiments with embryos at an earlier stage.

Literature Cited

- Acuna J, Yoon P, Erickson D, editors. The prevention of neural tube defects with folic acid. [report] Atlanta (GA): Centers for Disease Control and Prevention, 1999. [cited date] Available from: http://www.cdc.gov/bcbddd/folicacid/health_materials.htm.
- Afman, LA, Blom, HJ, Van der Put, NMJ, & Van Straaten, HWM. (2003) Homocysteine interference in neurulation: a chick embryo model. *Birth Defects Research (Part A)*, 67, 421-428.
- Ansorge, W. (1982) Improved system for capillary microinjection into living cells. *Experimental Cell Research*, 140, 31-37.
- Antin, PB, Fallon, JF, & Schoenwolf, GC. (2004) The chick embryo rules (still)! *Developmental Dynamics*, 229, 413.
- Bohren, CF & Albrecht, BA. (1998) Atmospheric Thermodynamics. New York: Oxford University Press.
- Botto, LD, Moore, CA, Khoury, MJ & Erickson, JD. (1999) Neural tube defects. *New England Journal of Medicine*, 341, 1509-1519.
- Campbell, LR, Dayton, DH, & Sohal, GS. (1986) Neural tube defects: a review of human and animal studies on the etiology of neural tube defects. *Teratology*, 34, 171-187.
- Celis, JE. (1984) Microinjection of somatic cells with micropipettes: comparison with other transfer techniques. *The Biochemical Journal*, 223, 281-291.
- Center for Disease Control and Prevention. (1982) Valproic acid and spina bifida: a preliminary report--France. *Morbidity and Mortality Weekly Report*, 31, 565-566.
- Center for Disease Control and Prevention. (1992a) Spina bifida incidence at birth – United States, 1983-1990. *Morbidity and Mortality Weekly Report*, 41, 497-500.
- Center for Disease Control and Prevention. (1992b) Recommendations for the use of folic acid to reduce the number of cases of spina bifida and other neural tube defects. *Morbidity and Mortality Weekly Report*, 41 (RR-14), 001-007.
- Chalfie, M, Tu, Y, Euskirchen, G, Ward, WW & Prasher, DC. (1994) Green fluorescent protein as a marker for gene expression. *Science*, 263, 802-805.
- Detrait, ER, George, TM, Etchevers, HC, Gilbert, JR, Vekemans, M & Speer, MC. (2005) Human neural tube defects: developmental biology, epidemiology, and genetics. *Neurotoxicology and Teratology*, 27, 515-524.

- Farley, TL. (2006) A reproductive history of mothers with spina bifida offspring – a new look at old issues. *Cerebrospinal Fluid Research*, 3, 10.
- Fineman, RM, Schoenwolf, GC, Huff, M, & Davis, PL. (1986) Causes of windowing-induced dysmorphogenesis (neural tube defects and early amnion deficit spectrum) in chicken embryos. *American Journal of Medical Genetics*, 25, 489-505.
- Fineman, RM & Schoenwolf, GC. (1987) Animal model: dysmorphogenesis and death in a chicken embryo model. *American Journal of Medical Genetics*, 27, 543-552.
- Fisher, M, & Schoenwolf, GC. (1983) The use of early chick embryos in experimental embryology and teratology: improvements in standard practice. *Teratology*, 27, 65-72.
- Frey, L & Hauser, WA. (2003) Epidemiology of neural tube defects. *Epilepsia*, 44 (Suppl. 3), 4-13.
- George, TM, & McLone, DG. (1995) Mechanisms of mutant genes in spina bifida: a review of implications from animal models. *Pediatric Neurosurgery*, 23, 236-245.
- Gräßman, A. (1970) Mikrochirurgische zellkerntransplantation bei säygetuerzellen. *Experimental Cell Research*, 60, 373-382.
- Holmes, LB, Driscoll, SG & Atkins, L. (1976) Etiologic heterogeneity of neural-tube defects. *New England Journal of Medicine*, 294, 365-369.
- Honig, MG, & Hume, RI. (1986) Fluorescent carbocyanine dyes allow living neurons of identified origin to be studied in long term cultures. *Journal of Cell Biology*, 103, 171-187.
- Horobin, RW & Kiernan, JA (Eds). (2002) Conn's Biological Stains: A Handbook of Dyes, Stains and Fluorochromes for Use in Biology and Medicine, 10th Ed. Oxford, BIOS Scientific Publishers Ltd..
- International Federation for Spina Bifida and Hydrocephalus. "Spina Bifida". [online] http://www.ifglobal.org/spina_bifida.asp?lang=1&main=6. Retrieved October 23, 2007.
- Juarranz, A, Horobin, RW & Proctor, GB. (1986) Prediction of in situ fluorescence of histochemical reagents using a structure-staining correlation procedure. *Histochemistry*, 84, 426-431.
- Kibar, Z, Capra, V & Gros, P. (2007) Toward understanding the genetic basis of neural tube defects. *Clinical Genetics*, 71, 295-310.

- Kulesa, PM. (2004) Developmental imaging: insights into the avian embryo. *Birth Defects Research (Part C)*, 72, 260-266.
- Kulesa, PM, Bronner-Fraser, M, & Fraser, SE. (2000) In ovo time-lapse analysis after dorsal neural tube ablation shows rerouting of chick hindbrain neural crest. *Development*, 127, 2843-2852.
- Kulesa, PM & Fraser, SE. (2000) In ovo time-lapse analysis of chick hindbrain neural crest cell migration shows cell interactions during migration to the branchial arches. *Development*, 127, 1161-1172.
- Kulesa, PM & Fraser, SE. (2004) A practical guide: in ovo imaging of avian embryogenesis. In *Imaging in Neuroscience and Development: a Laboratory Manual*. Edited by Yuste, R & Konnerth, A. New York; Oxford: Cold Springs Harbor Laboratory Press; Lavis Marketing.
- Lourens, S. (2002) Heating of hatching eggs before storage improves hatchability. *World Poultry*, 18, 24-25.
- Lowery, LA & Sive, H. (2004) Strategies of vertebrate neurulation and a re-evaluation of teleost neural tube formation. *Mechanisms of Development*, 121, 1189-1197.
- Mann, RA, & Persaud, TVN. (1978) Teratogenic effect of windowing eggs at early stages of avian development. *Experimentelle Pathologie*, 15, 324-334.
- McCaman, RE, McKenna, DG & Ono, JK. (1977) A pressure system for intracellular and extracellular ejection of picoliter volumes. *Brain Research*, 136, 141-147.
- Meijerhof, R. (2002) Incubation by embryo temperature. *World Poultry*, 18, 36-37.
- Meuli, M, Meuli-Simmen, C, Hutchins, GM, Yingling, CD, McBiles Hoffman, K, Harrison, MR & Adzick, NS. (1995) *In utero* surgery rescues neurological function at birth in sheep with spina bifida. *Nature Medicine*, 1, 342-347.
- Minaschek, G, Bereiter-Hahn, J & Bertholdt, G. (1989) Quantitation of the volume of liquid injected into cells by means of pressure. *Experimental Cell Research*, 183, 434-442.
- Mitchell, LE. (2005) Epidemiology of neural tube defects. *American Journal of Medical Genetics Part C*, 135C, 88-94.
- Northrup, H & Volcik, KA. (2000) Spina bifida and other neural tube defects. *Current Problems in Pediatrics*, 30, 317-332.

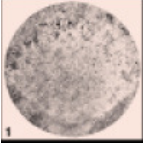
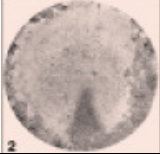
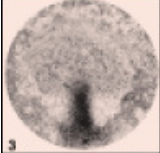
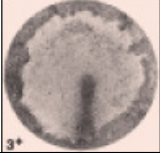



- Ruffins, S, Artinger, KB & Bronner-Fraser, M. (1998) Early migrating neural crest cells can form ventral neural tube derivatives when challenged by transplantation. *Developmental Biology*, 203, 295-304.
- Sang, H. (1994) Transgenic chickens – methods and potential applications. *Trends in Biotechnology*, 12, 415-420.
- Sang, H. (2004) Prospects for transgenesis in the chick. *Mechanisms of Development*, 121, 1179-1186.
- Schoenwolf, GC. (1991) Cell movements driving neurulation in avian embryos. *Development*, Supplement 2, 157-168.
- Schoenwolf, GC & Delongo, J. (1980) Ultrastructure of secondary neurulation in the chick embryo. *American Journal of Anatomy*, 158, 43-63.
- Schoenwolf, GC & Franks, MV. (1984) Quantitative analyses of changes in cell shapes during bending of the avian neural plate. *Developmental Biology*, 105, 257-272.
- Schoenwolf, GC & Smith, JL. (1990) Mechanisms of neurulation: traditional viewpoint and recent advances. *Development*, 109, 243-270.
- Schoenwolf, GC & Smith, JL. (2000) Mechanisms of neurulation. From *Methods in Molecular Biology*, Vol. 136: *Developmental Biology Protocols*, Vol II. Edited by Tuan, RS & Lo, CW. Humana Press Inc., Totowa, NJ.
- Scholz, O, Thiel, A, Hillen, W & Niederweis, M. (2000) Quantitative analysis of gene expression with an improved green fluorescent protein. *FEBS Journal*, 267, 1565-1570.
- Selleck, MAJ. (1996) Culture and microsurgical manipulation of the early avian embryo. In *Methods in Cell Biology*, Vol. 51: *Methods in Avian Embryology*. Edited by Bronner-Fraser, M. San Diego, Academic Press, Inc.
- Serbedzija, GN, Bronner-Fraser, M, & Fraser, SE. (1989) A vital dye analysis of the timing and pathways of avian trunk neural crest cell migration. *Development*, 106, 809-816.
- Smith, JL & Schoenwolf, GC. (1988) Role of cell-cycle in regulating neuroepithelial cell shape during bending of the chick neural plate. *Cell Tissue Research*, 252, 491-500.
- Snyder, GK & Birchard, GF. (1992) Water loss and survival in embryos of the domestic chicken. *Journal of Experimental Zoology*, 219, 115-117.


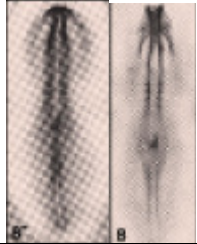





- Stern, CD & Bachvarova, R. (1997) Early chick embryo *in vitro*. *International Journal of Developmental Biology*, 41, 379-387.
- Stern, CD & Fraser, SE. (2001) Tracing the lineage of tracing cell lineages. *Nature Cell Biology*, 3, E216-E218.
- Stern, CD & Holland, PWH. (1993) *Essential Developmental Biology: A Practical Approach*. New York, Oxford University Press.
- Sutton, LN. (2007) Fetal surgery for neural tube defects. *Best Practice and Research: Clinical Obstetrics and Gynecology*, in press, doi:10.1016/j.bpobgyn.2007.07.004
- Teddy, JM, Lansford, R & Kulesa, PM. (2005) Four-colour, 4-D time-lapse confocal imaging of chick embryos. *BioTechniques*, 39, 703-709.
- Trinkhaus, JP & Gross, MC. (1961) The use of tritiated thymidine for marking migratory cells. *Experimental Cell Research*, 24, 52-57.
- Van Allen, MI, Kalousek, DK, Chernoff, GF, Juriloff, D, Harris, M, McGillivray, BC, Yong, S-L, Langlois, S, Macleod, PM, Chitayat, D, Friedman, JM, Wilson, RD, McFadden, D, Pantzar, J, Ritchie, S & Hall, JG. (1993) Evidence for multi-site closure of the neural tube in humans. *American Journal of Medical Genetics*, 47, 723-743.
- Van Dongen, PAM. (1984) Pressure injections of fluid in the nanoliter range via micropipettes. *Journal of Neuroscience Research*, 10, 281-291.
- Van Straaten, HWM, Janssen, HCJP, Peeters, MCE, Copp, AJ, & Hekking, JWM. (1996) Neural tube closure in the chick embryo is multiphasic. *Developmental Dynamics*, 207, 309-318.
- Vande Velde, S, Van Biervliet, S, Van Renterghem, K, Van Laecke, E, Hoebeke, P & Van Winckel, M. (2007) Achieving fecal continence in patients with spina bifida: a descriptive cohort study. *The Journal of Urology*, 178, 2640-2644.
- Waddington, CH. (1932) Experiments on the development of chick and duck embryos, cultivated *in vitro*. *Philosophical Transactions of the Royal Society of London, Series B*, 221, 179-230.
- Waller, DK, Shaw, GM, Rasmussen, SA, Hobbs, CA, Canfield, MA, Siega-Riz, AM, Gallaway, MS, & Correa, A. (2007) Prepregnancy obesity as a risk factor for structural birth defects. *Archives of Pediatric and Adolescent Medicine*, 161, 745-750.
- Walsh, DS & Adzick, NS. (2003) Foetal surgery in spina bifida. *Seminars in Neonatology*, 8, 197-205.






- Watkins, ML, Rasmussen, SA, Hoenin, MA, Botto, LD & Moore, CA. (2003) Maternal obesity and risk for birth defects. *Pediatrics*, *111*, 1152-1158.
- Whitsel, AI, Johnson, CB, & Forehand, CJ. (2002) An in ovo chicken model to study the systemic and localized teratogenic effects of valproic acid. *Teratology*, *66*, 153-163.
- Wojnarowicz, C & Olkowski, AA. (2007) Spina bifida in broiler chicken embryos. *The Veterinary Record*, *160*, 303-304.
- Wolpert, L. (2004) Much more from the chicken's egg than breakfast – a wonderful model system. *Mechanisms of Development*, *121*, 1015-1017.
- Yang, HJ, Wang, KC, Chi, JG, Lee, MS, Lee, YJ, Kim, SK, Lee, CS & Cho, BK. (2006) Cytokinetics of secondary neurulation in chick embryos: Hamburger and Hamilton stages 16-45. *Child's Nervous System*, *22*, 567-571.

Appendix I

Hamburger-Hamilton Stages (Pictures and text adapted from Stern & Holland, 1993)

Stage	Picture	Age	Brief Description
1			
2		~6-7 h (brief stage)	Primitive streak is short conical thickening; 0.3-0.5 mm long.
3	 	12-13 h	Primitive streak extends to centre of embryo; streak broad throughout. No groove.
4		18-19 h	Primitive streak grooved; ~1.88 mm long. Hensen's node present. <i>Area pellucida</i> pear-shaped
5		19-22 h	Notochord (head-process) visible as a rod of mesoderm extending from Hensen's node. No head fold
6		23-25 h (brief stage)	A fold of the blastoderm anterior to the notochord marks anterior end of embryo proper. No somites.

7			23-26 h	1 somite. Neural folds visible in head region
8			26-29 h	4 somites. Neural folds meet at level of midbrain. Blood islands present posteriorly.
9			29-33 h	7 somites. Primary optic vesicle present. Paired primordial of heart begin to fuse.
10			33-38 h	10 somites. First somite becoming dispersed. First indication of cranial flexure. 3 brain vesicles clearly visible. Optic vesicles not constricted at base. Heart bent slightly to right.
11			40-45 h	13 somites. Slight cranial flexure. 5 distinct neuromeres in hindbrain. Anterior neuropore closing. Optic vesicles constricted at bases. Heart bent to right.
12			45-49 h	16 somites. Head turning onto left side. Anterior neuropore closed. Primary optic vesicles and optic stalk well established. Auditory pit deep, but open. Heart slightly S-shaped. Head fold of amnion covers entire forebrain.
13			48-52 h	19 somites. Head turning onto left side. Telencephalon enlarged. Atrio-ventricular canal indicated by constriction. Head fold of amnion extends to anterior hindbrain.

14		50-53 h	22 somites. Forebrain and hindbrain form about a right angle. Visceral (branchial) arches 1 & 2, and clefts 1&2 distinct. Primary optic vesicle invaginating; lens placode formed. Opening of the auditory pit constricted. Rathke's pouch can be recognized. Ventricular loop of heart now ventral to atrio-ventricular canal. Amnion extends to somites 7-10.
15		50-55 h	24-27 somites. Lateral body folds extend to anterior end of wing level (somites 15-17). Prospective limb areas not yet demarcated. Amnion extends to somites 7-14. Axes of forebrain & hindbrain nearly parallel. Trunk rotation extends to somites 11-13. Visceral arch 3 & cleft 3 distinct. Cleft 3 shorter than cleft 2 & usually oval shape. Optic cup completely formed; double contour distinct in region of iris
16		51-56 h	26-28 somites. Lateral body folds extend to somites 17-20, between wings and legs. Wing lifted off blastoderm, represented by thickened ridge. Primordium of leg still flat. Amnion extends to somites 10-18. Rotation of trunk extends to somites 14-15. Tail bud a short, straight cone, delimited from blastoderm. Pineal gland (epiphysis) indistinct or not yet formed.
17		52-64 h	29-32 somites. Lateral body folds extend around entire circumference of body. Both leg & wing buds lifted off blastoderm approximately equal size. Trunk rotation to somites 17-18. tail bud bent ventrally, unsegmented. Pineal gland distinct. Indication of nasal pits
18		3 days	30-36 somites, extending beyond leg bud. Leg buds slightly larger than wing buds. L/W of wing ≤ 6.0 (L = anterior-posterior length measured along body wall; W = distance from body wall to apex). Axis of medulla at cervical flexure about 90° to posterior trunk. Trunk flexure shifted to lumbar region. Rotation extends to posterior of body. Leg buds no longer in horizontal plane. Tail bud turned to right, ~90° to axis of posterior trunk. Allantois short, thick-walled, not yet vesicular

Appendix II

List of dyes considered for cell tracking tests (adapted from Juarranz *et al.*, 1986)

Name	Colour Index #	CBN	log <i>P</i> (hydrophobicity)
<i>Acid Dyes</i>			
Amido black 10B	20470	34	-4.7
Biebrich scarlet	26905	30	-3.2
Brilliant yellow G	24890	35	-3.0
Chlorazol black E	30235	49	-3.3
Durazol blue BS	34200	56	-1.8
Durazol blue 8GS	74180	48	-9.8
Durazol blue 4RS	27925	44	-6.4
Durazol brilliant red BS	35780	62	-12.4
Durazol helio BS	27905	37	-0.5
Durazol red brown	34020	49	-1.4
Durazol red 6B	29065	44	-9.1
Durazol paper blue	74200	48	-14.6
Naphthol black B	27260	40	-10.1
Sirius red F3B	35780	62	-17.1
Sirius rose BB	25380	45	-13.8
Trypan blue	23850	45	-11.4
<i>Basic Dyes</i>			
Alcian blue 2GX		48	-2.0
Alcian blue 8GX	74240	48	-9.7
Astra blue 6GLL		57	-10.4
Brilliant green BP	42040	23	-2.3
Cuprolinic blue		44	-17.9
Janus green B	11050	34	4.0
Janus red B	26115	29	2.2
<i>Non-ionic Dyes</i>			
Dispersol blue BG	63305	22	0.0
Neozapon orange G	18745	25	0.4
Neozapon red BE	12716	50	4.4
Neozapon yellow	13900	23	-2.4
Oil red O	26125	30	9.0
Sudan III	26100	30	6.4
Sudan IV	26105	30	7.7
Sudan black B	26150	36	7.2

Appendix III

Table 4: Temperature and relative humidity test of Prototype 2. Lid closed, vent closed. Raw data.

Time (minutes)	Temperature (°C)	% RH
0	21	83.6
5	23	95
10	26	101
15	29	103.5
20	30	104.3
25	33	104.1
30	34	103.7
35	35	103.7
40	36	102.6
45	37	102
50	37	102.1
55	38	101.5
60	38	101.5
65	38	101.3
70	39	101.1
75	39	101.3
80	39	101.5
85	39	100.2
90	39	99.6
95	39	99.5
100	39	98.6
105	39	99.9
110	38	98.6
115	36	98.1
120	36	99.6
125	38	100.4
130	38	100.3
135	39	99.3
140	39	99.5
145	39	99.2
150	40	97.6
155	39	97.2
160	38	95.2
165	37	95.3
170	37	97.5
175	37	98.5
180	38	99.7
185	39	100.3
190	39	99.8
195	38	97.2
200	38	97.4
205	38	98.3
210	38	98.1
215	38	97.6
220	38	98.0

Table 5: Temperature and relative humidity tests for Prototype 2. Lid closed, vent open. Raw data

Time (minutes)	Temperature (°C)	% RH
0	21	83.6
5	23	95
10	26	101
15	29	103.5
20	30	104.3
25	33	104.1
30	34	103.7
35	35	103.7
40	36	102.6
45	37	102
50	37	102.1
55	38	101.5
60	38	101.5
65	38	101.3
70	39	101.1
75	39	101.3
80	39	101.5
85	39	100.2
90	39	99.6
95	39	99.5
100	39	98.6
105	39	99.9
110	38	98.6
115	36	98.1
120	36	99.6
125	38	100.4
130	38	100.3
135	39	99.3
140	39	99.5
145	39	99.2
150	40	97.6
155	39	97.2
160	38	95.2
165	37	95.3
170	37	97.5
175	37	98.5
180	38	99.7
185	39	100.3
190	39	99.8
195	38	97.2
200	38	97.4
205	38	98.3
210	38	98.1
215	38	97.6
220	38	98.0

Table 6: Temperature and relative humidity tests of Prototype 2. Lid closed, vent half-open. Raw data.

Time (minutes)	Temperature (°C)	% RH
0	31	69.1
5	31	73.7
10	31	80.6
15	32	83.4
20	33	84.1
25	33	85.6
30	34	83.0
35	34	82.5
40	34	81.7
45	34	83.4
50	34	83.1
55	34	81.0
60	35	81.1
65	35	84.0
70	35	83.5
75	35	83.5
80	35	84.4
85	36	85.0
90	35	83.3
95	36	78.1
100	37	89.0
105	38	100.1
110	38	83.5
115	39	81.9
120	37	85.1
125	37	84.3
130	37	81.1
135	42	79.7
140	39	79.5
145	38	92.3
150	37	81.3
155	37	100.6
160	38	84.1
165	38	77.6
170	37	85.0
175	37	80.7
180	39	84.5
185	37	87.7
190	39	82.1
195	36	103.6
200	39	77.7
205	37	94.2
210	37	94.1
215	38	89.7

Table 7: Temperature and relative humidity tests for Prototype 2. Lid open 1 cm, vent closed. Raw data.

Time (minutes)	Temperature (°C)	% RH	Time (minutes)	Temperature (°C)	% RH
0	30	91.5	240	34	80.6
5	32	81.8	245	35	98.2
10	30	76.1	250	36	103.5
15	29	94.7	255	35	98.5
20	32	77.5	260	36	91.0
25	31	87.4	265	37	84.5
30	29	85.1	270	36	92.2
35	32	78.7	275	38	97.2
40	33	87.1	280	38	61.2
45	32	72.5	285	35	80.7
50	33	85.5	290	36	87.7
55	33	80.2	295	38	91.3
60	32	77.5	300	35	89.2
65	32	86.7	305	35	95.4
70	30	92.1	310	36	96.0
75	32	73.1	315	36	83.5
80	32	79.7	320	37	102.0
85	32	85.4	325	36	77.1
90	34	89.1	330	36	77.4
95	32	80.5	335	36	90.5
100	32	71.1	340	37	96.2
105	32	86.7	345	35	98.0
110	32	81.7	350	36	92.1
115	32	84.0	355	35	83.0
120	32	94.0	360	36	96.2
125	33	97.1	365	37	85.7
130	33	82.1	370	37	100.5
135	33	79.9	375	37	91.7
140	33	87.4	380	36	79.5
145	32	96.5	385	36	75.4
150	33	77.5	390	36	87.7
155	33	77.1	395	37	86.5
160	33	70.4	400	36	86.4
165	33	85.5	405	36	98.3
170	33	85.4	410	36	71.5
175	35	74.1	415	36	86.7
180	34	74.1	420	38	92.1
185	34	62.1	425	36	86.3
190	35	64.7	430	37	84.7
195	34	87.4	435	36	82.7
200	36	92.5	440	37	84.1
205	35	72.7	445	36	90.1
210	35	85.5	450	35	84.1
215	35	87.0	455	35	71.4
220	36	93.1	460	36	76.0
225	35	87.4	465	36	91.0
230	35	92.5	470	37	87.1
235	35	75.1	475	36	75.4

Time (minutes)	Temperature (°C)	% RH	Time (minutes)	Temperature (°C)	% RH
480	36	79.1	615	38	26.7
485	37	80.4	620	39	33.7
490	35	91.5	625	39	22.4
495	36	84.2	630	39	25.0
500	37	84.3	635	38	20.3
505	36	81.2	640	38	24.2
510	36	83.5	645	37	17.5
515	36	90.1	650	38	29.0
520	37	85.1	655	37	18.1
525	37	91.4	660	38	22.5
530	36	76.1	665	39	22.5
535	37	73.3	670	38	22.1
540	38	64.5	675	37	37.7
545	37	64.7	680	34	48.2
550	39	36.6	685	35	47.6
555	40	49.5	690	36	31.1
560	38	32.4	695	36	27.0
565	41	34.4	700	35	29.7
570	41	24.5	705	33	35.5
575	39	17.1	710	39	28.5
580	41	14.7	715	36	25.1
585	39	19.7	720	36	19.7
590	39	15.6	725	35	22.0
595	37	21.6	730	38	8.2
600	34	32.1	735	38	7.8
605	35	54.5	740	37	7.6
610	38	27.1	745	39	7.6
			750	39	7.5

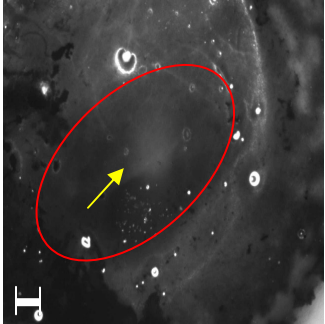
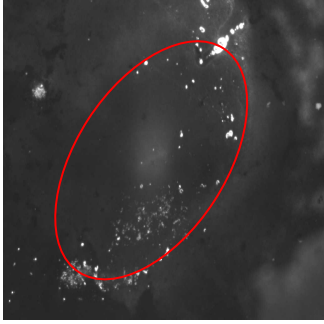
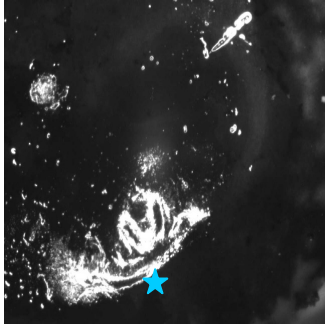


Table 8: Temperature and relative humidity for Prototype 3. Raw data.

Time (minutes)	Temperature (°C)	% RH	Time (minutes)	Temperature (°C)	% RH
0	32	16.6	160	38	17.5
5	33	18.6	165	38	17.7
10	35	20.5	170	38	13.3
15	36	17.1	175	38	16.1
20	37	17.7	180	38	18.7
25	38	16.7	185	38	21.5
30	38	21.0	190	38	15.7
35	39	22.0	195	38	27.1
40	39	19.7	200	38	15.5
45	39	17.1	205	38	16.5
50	39	19.7	210	38	15.1
55	39	18.1	215	38	13.7
60	40	16.7	220	38	16.3
65	39	15.7	225	38	19.5
70	39	16.3	230	38	21.5
75	38	16.7	235	38	17.6
80	37	18.1	240	38	17.1
85	38	20.5	245	39	17.5
90	38	19.3	250	38	16.7
95	38	10.1	255	38	17.3
100	38	15.6	260	38	14.3
105	38	16.7	265	38	16.1
110	38	15.5	270	38	14.5
115	38	19.7	275	38	13.4
120	38	20.0	280	38	14.2
125	39	16.5	285	38	15.5
130	38	15.5	290	38	17.1
135	38	15.4	295	38	14.8
140	38	15.0	300	38	16.7
145	38	17.6	305	38	20.2
150	38	17.5	310	38	17.7
155	38	15.1	315	38	13.5

Appendix IV

Raw data from developing chick embryos in Prototype 1. In tests with fewer than 5 pictures, all pictures are shown. For tests with greater than 5 pictures, 5 representative pictures were chosen to illustrate the test. Some tests did not have pictures, as they were simply to test whether changes made to the apparatus resulted in any improvement. All scale bars represent 100 μm (unless otherwise indicated), and are consistent within a test.

Test 1:

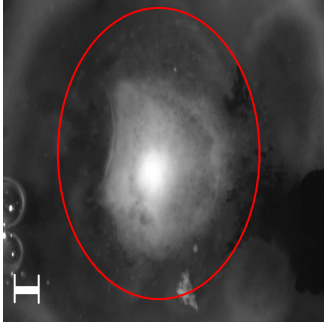

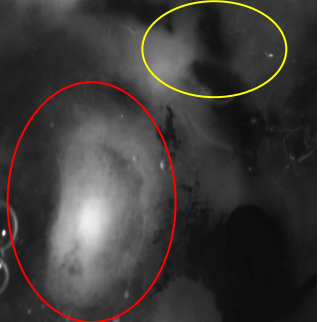
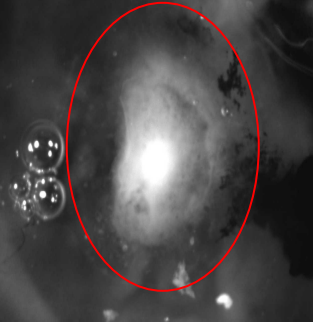
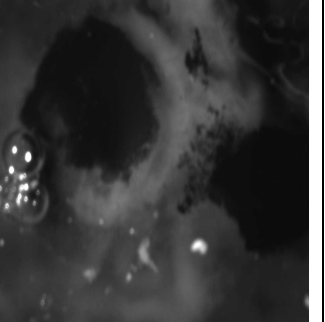
Time	0 h	1 h	1 h, 5 min	1 h, 10 min	1 h, 15 min
Picture					
Comment	The red oval outlines where the embryo is. The spot of light in the middle (shown by the yellow arrow) obscures much of the embryo.	The red oval again outlines the embryo, which has grown a bit since the beginning. The little dots of white are remnants of shell that fell into the egg during windowing.	The embryo begins to dry up, shown by light blue star.	The of the embryo continues to dry up, as evidenced by the growing amount of "skin" on the surface.	The surface of the embryo is now covered with the "skin"

Appendix V

Raw data from developing chick embryos in Prototype 2. All scale bars represent 100 μm , and are consistent within a test.

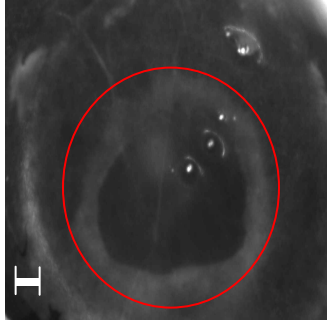
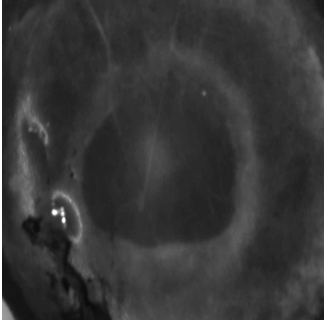
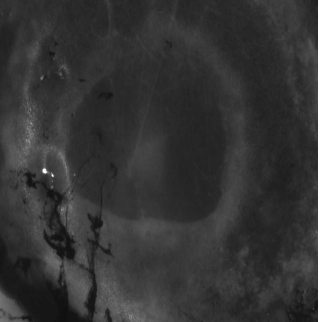
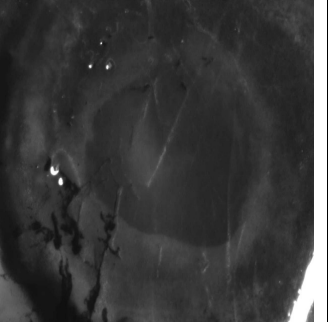
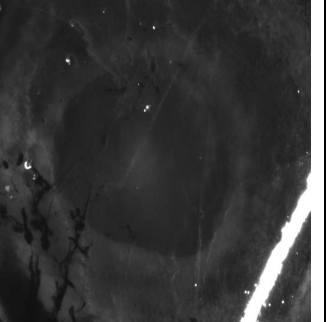
Test 1:

Using the initial version of Prototype 2, where the egg rests on a copper scourer sitting inside the container.

Time	0	10 min	25 min	30 min	40 min
Picture					
Comment	The embryo is outlined by the red oval. The bright spot in the middle of the picture is caused by the ring light reflecting off the surface of the embryo.	Again, the embryo is outlined by the red oval. Though it has shifted downwards a bit, there doesn't seem to be any change.	The embryo (red oval) continues its shift downwards. A small point of drying out has begun on the top corner (yellow circle), so some Chick Ringer's solution was added.	Embryo recentered (red oval). Not much change from initial picture.	Ink begins to leak through the embryo, most likely through the point in where the ink was injected beneath the blastoderm. Since the ink obscures the embryo, the test ends here.

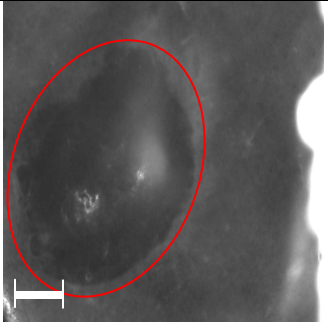
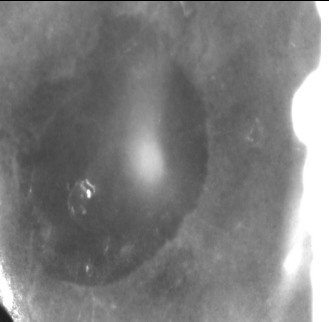
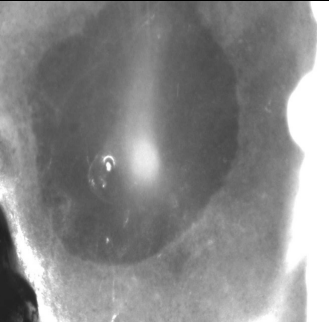
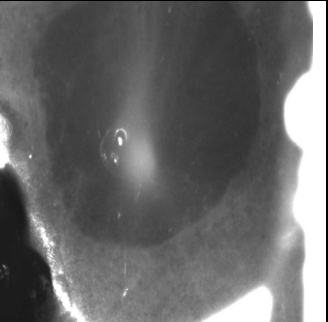
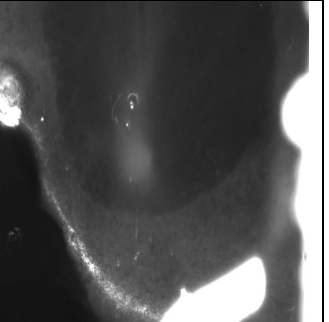
Test 2:

In this, and subsequent tests, pictures are taken every minute by the Tissue GUI program.

Time	0	30 minutes	90 minutes	150 minutes	240 minutes
Pictures					
Comment	The embryo is outlined by the red oval.	While there is some leaking of ink along the bottom of the embryo, it is not enough to obscure the main portion.	As the test continues, more ink begins to drift into the field of view. As well, a faint crackling can be seen forming on the surface, possibly due to drying out.	The crackling becomes much more obvious. The shape of the embryo itself seems to not have changed from the beginning.	The test was ended here because the surface of the embryo had taken on this odd cracked texture. As well, the essential shape of the embryo had not changed in 4 hours.

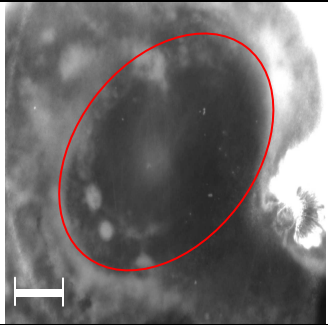
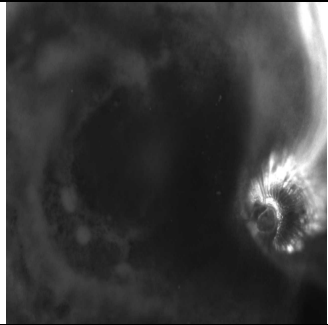
Test 3:

In this test, and subsequent tests, the copper scourer was replaced with the metal flange. The scale bar represents 200 μm .

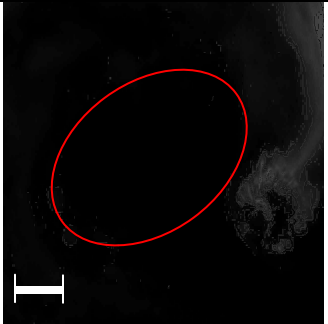
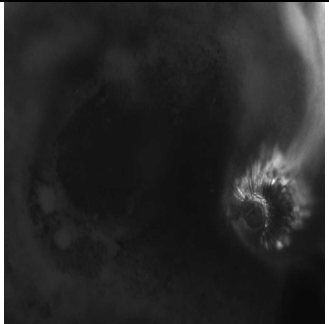
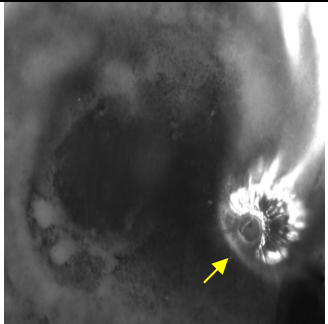
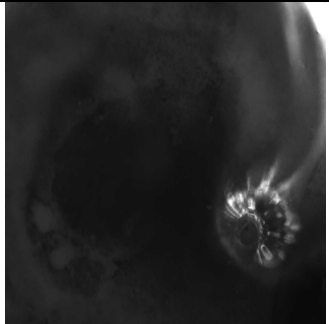
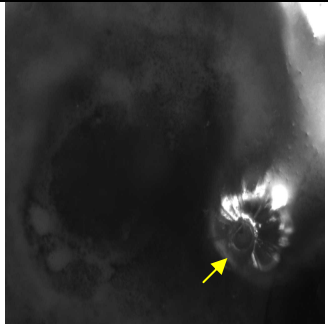
Time	0	15 minutes	30 minutes	55 minutes	76 minutes
Pictures					
Comment	The embryo is outlined by the red oval.		The embryo seems to be moving, and expanding, though all the features are obscured by the central glare.		The program crashes at this point, and the test ends. However, the embryo did not dry out.

The crashing of the program is later revealed to have been caused by the fact that the program was written to automatically adjust the lighting in the picture based on whether the picture seemed too bright or dark. The problem arose because the picture was too bright in some areas (where there was reflection), and too dark in others, so the program was attempting to simultaneously darken and lighten the picture.

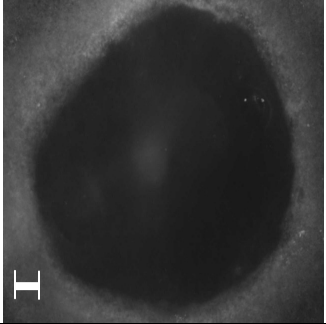
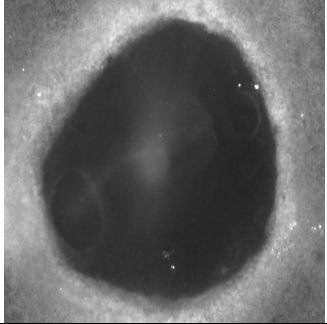
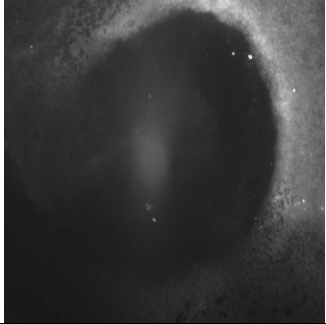
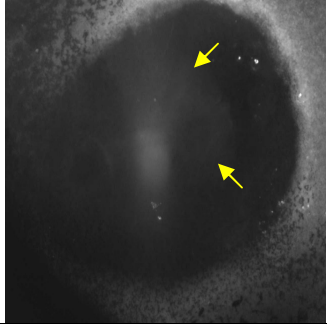
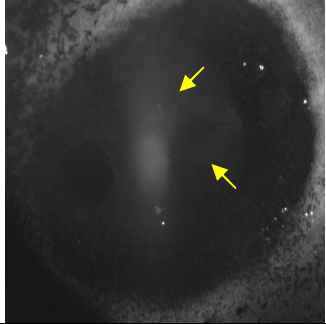
Test 4:

Time	0	10 minutes
Picture		
Comment	The embryo is outlined by the red oval. The scale bar represents 200µm.	The program crashes at this point (see above for reason).

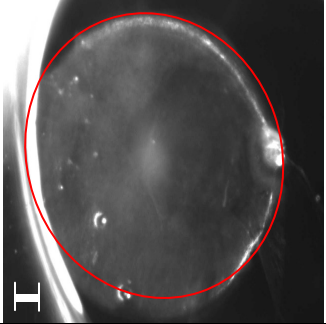
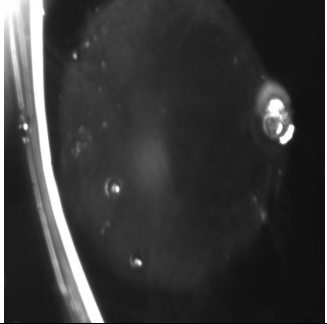
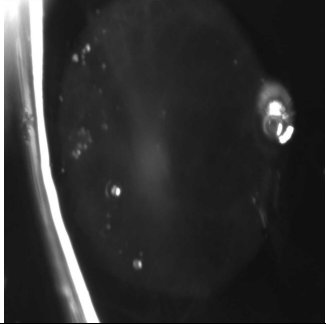
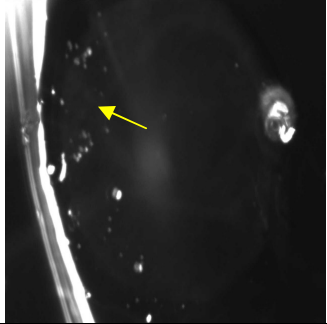
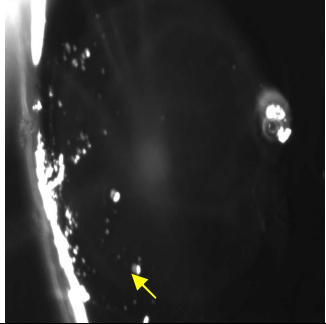
Test 5:

Time	0	15 minutes	30 minutes	45 minutes	56 minutes
Picture					
Comment	Because of the glare seen in previous pictures, the lighting was turned down in this test. The embryo (red oval) is very difficult to differentiate from the background. The scale bar represents 200 µm.	Evidence of the program's automatic adjustment of the light can be seen here, as the embryo is in more contrast to the background.	The embryo can be fairly clearly seen in this picture, though part of it is obscured by the growing spot of brightness (shown by the yellow arrow)	The automatic adjustment of lighting means that some pictures may be brighter, others darker.	The program crashes at this point. The embryo is beginning to dry out, shown by the wrinkling on the surface (yellow arrow)

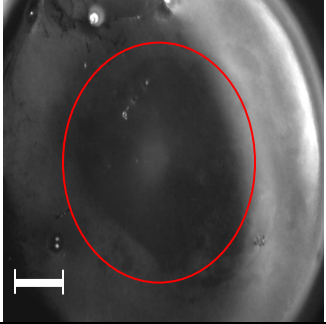
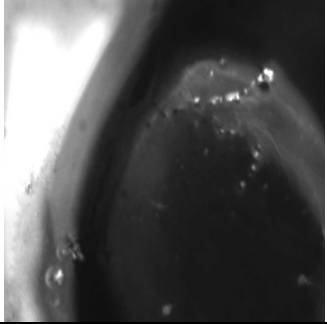
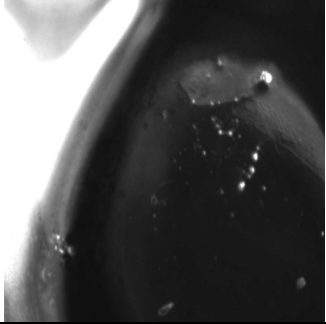
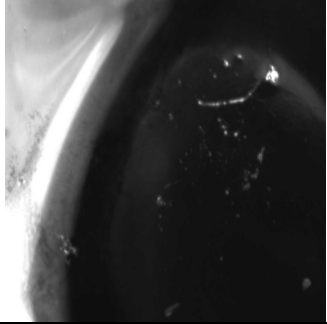
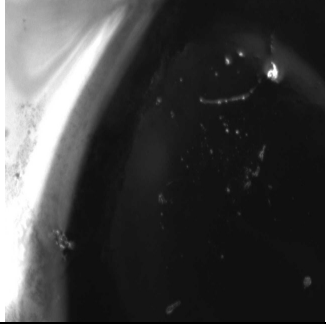
Test 6:

Time	0	100 minutes	215 minutes	330 minutes	449 minutes
Picture					
Comment	While the glare in the centre still obscures some of the embryo, the general shape of the embryo can be clearly seen here.	The embryo begins to expand; the lighting is adjusted to provide better contrast.	The embryo continues to elongate.	The beginnings of the neural ridges can be seen in this picture (yellow arrows)	After approximately 7.5 hours, the test is ended. The neural ridges are more obvious in this picture.

Test 7:

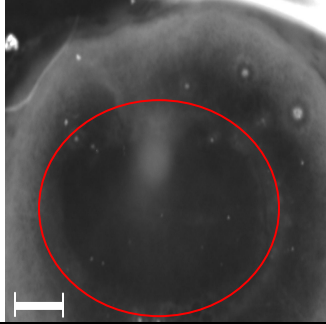
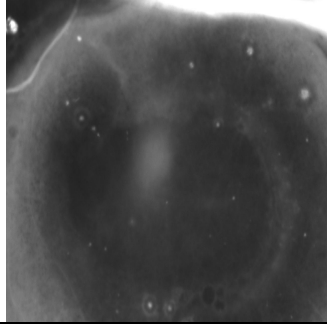
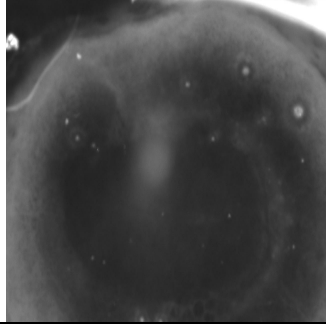
Time	0	75 minutes	150 minutes	225 minutes	292 minutes
Picture					
Comment	The embryo is rather difficult to see in this test. It is assumed that the circle of lightness (outlined by the red oval) is the embryo.	The bright central area is becoming dimmer.	Little change, though the area is getting darker.	The edge of the picture may be drying out (yellow arrow)	Test ended because embryo was no longer visible. Drying out is visible along the edge (yellow arrow). Because the embryo is not visible during this test, it is not considered a success.

Test 8:

Time	0	80 minutes	160 minutes	240 minutes	317 minutes
Picture					
Comment	The embryo is again difficult to see here. The red oval outlines what looks to be the embryo. The scale bar represents 200 μm .				With the exception of darkening of the central area, there does not seem to be much change in this test. The test is ended because the embryo can no longer be seen

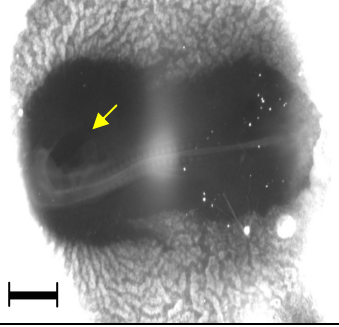
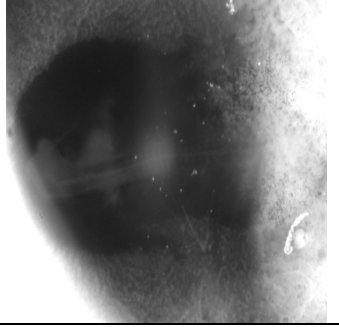
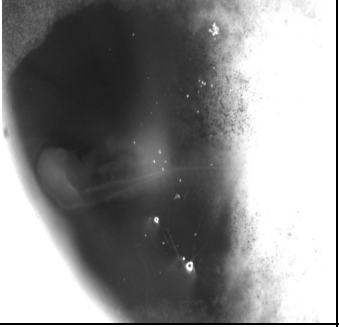
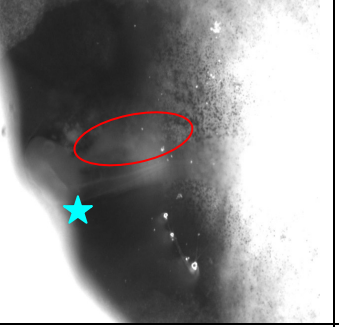

Test 9:

In this test, and subsequent tests, pictures are taken every 5 minutes by the Tissue GUI program. The albumen that was removed in the first step of windowing was then replaced above the embryo.

Time	0	45 minutes	85 minutes
Picture			
Comment	The embryo is outlined by the red oval. The scale bar represents 200 μm .		Test was ended by computer problems.

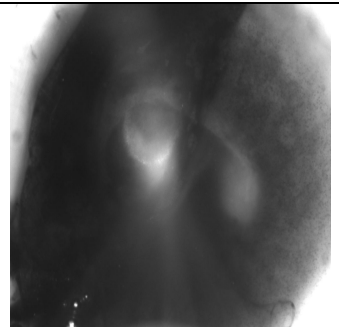
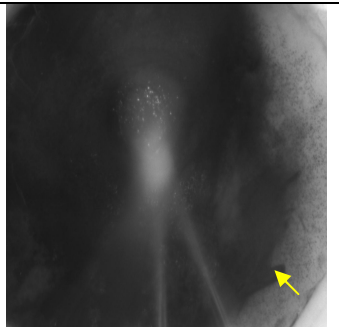
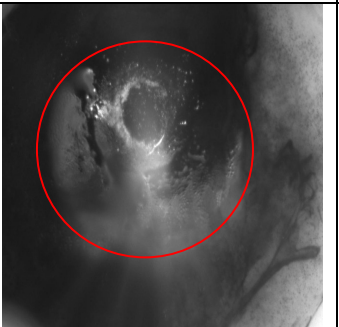
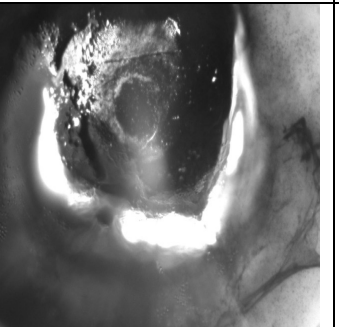
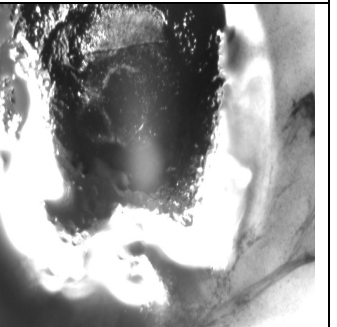
Test 10:

Testing prototype 2 with a 3-day old embryo, to ensure that the prototype would be able to keep an embryo alive, though at a later stage..

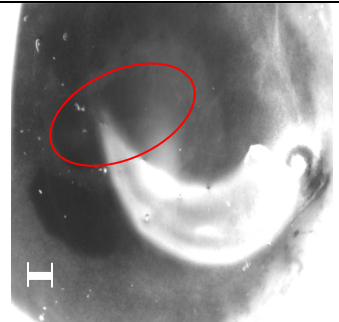
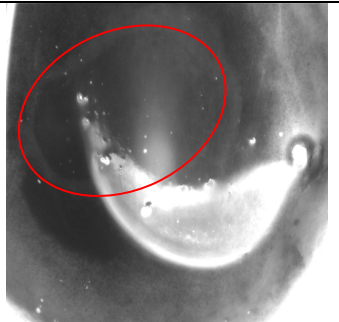
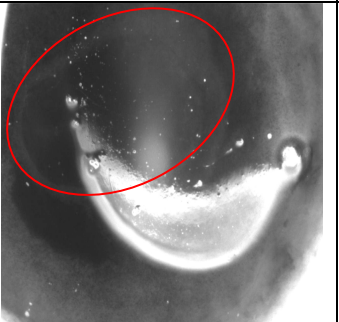
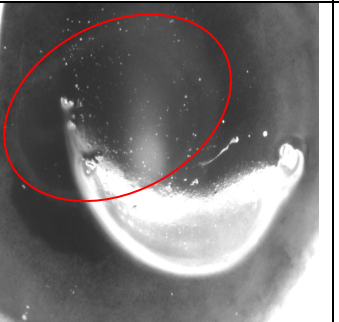
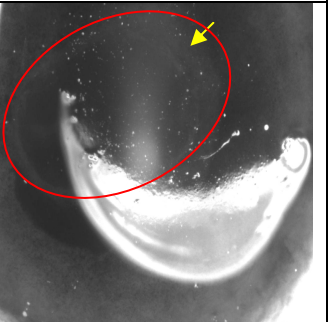
Time	0	40 minutes	80 minutes	120 minutes	150 minutes
Picture					
Comment	A 3-day old embryo. The heart (indicated by the yellow arrow) was watched to indicate life. The scale bar represents 250 μm .	The picture shows the heart mid-beat, so that it looks larger than originally.		There seems to be some perturbations along the inner edge of the embryo (red circle). As well, the cranial region seems to be losing its curved shape (light blue star).	The heart has stopped beating. This was taken as an indication that the embryo had died. The perturbation seems to have increased (red oval).

Test 11:

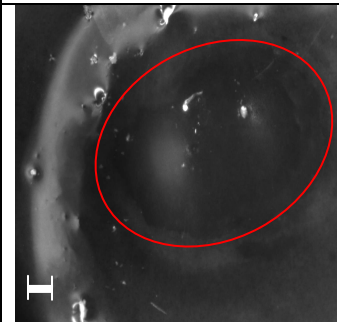
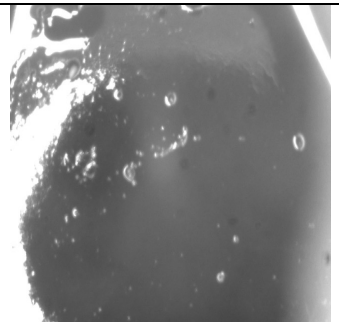
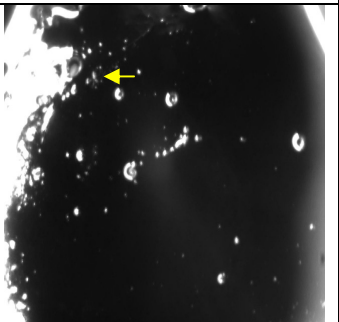
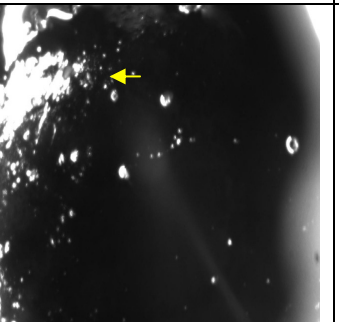
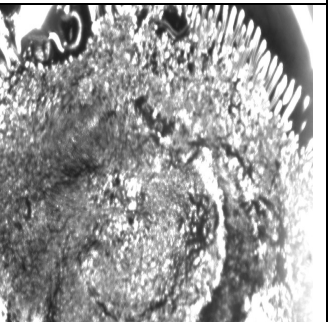
Placing a hygrometer in the apparatus showed a relative humidity of 80%. Therefore a ventilation panel was added to regulate humidity.

Time	0	150 minutes	300 minutes	450 minutes	650 minutes
Picture					
Comment	The majority of the embryo is obscured by the glare from the ring light.	The glare continues to obscure the embryo, though the embryo seems to have expanded (yellow arrow).	The embryo is starting to dry out, as evidenced by the growing spot of "skin" (red circle).	The embryo continues to dry out.	The test is ended. The embryo is now almost completely obscured by the dried out "skin" on top.

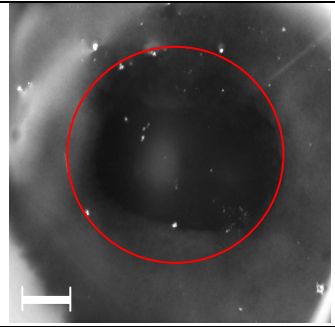
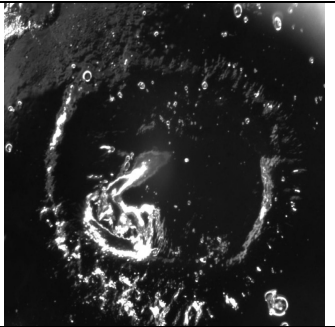
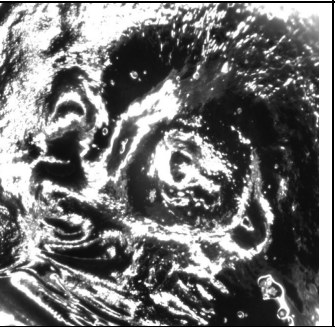
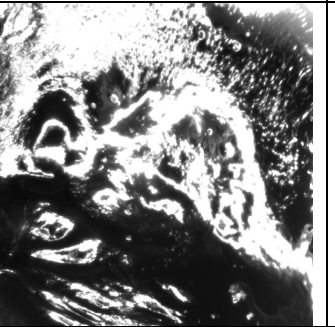
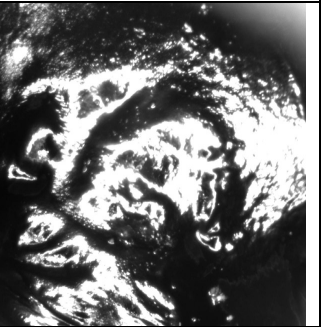
Test 12:

Time	0	50 minutes	100 minutes	150 minutes	220 minutes
Picture					
Comment	The embryo is outlined by the red oval. The scale bar represents 160 μm .	The embryo has expanded (red oval), and has taken on the characteristic peanut shape (see Appendix I)	The expansion continues (red oval), though more of the embryo is obscured by the glare of the light in the centre of the picture	The expansion seems to stop, or at least does not increase noticeably.	The test is ended here, because the embryo was drying out, as shown by the shininess of the surface (yellow arrow)

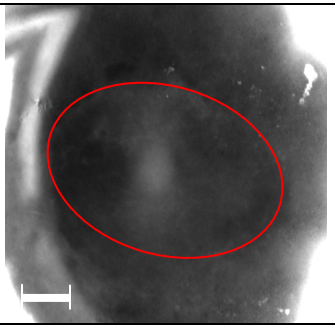
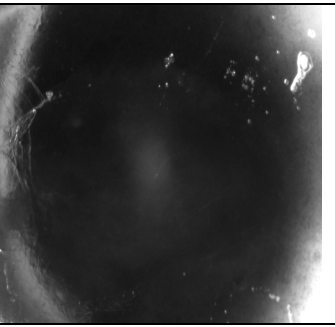
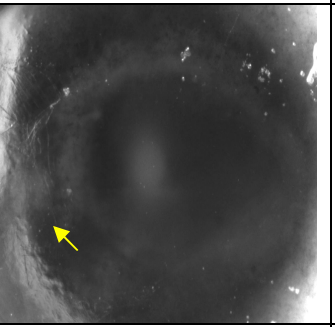
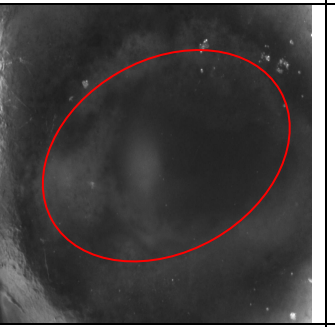
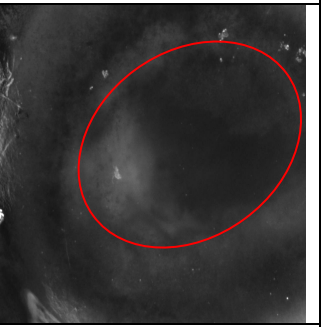
Test 13:

Time	0	150 minutes	300 minutes	450 minutes	600 minutes
Picture					
Comment	The embryo is outlined by the red oval.	The light box seemed to be malfunctioning, as the pictures tended to lighten and darken on their own.	Drying out is starting to occur (yellow arrow)	Drying out continues, most obviously where the yellow arrow.	The embryo is clearly dried out.

Test 14:

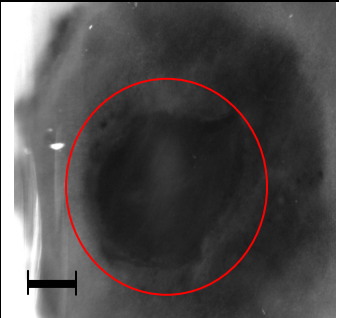

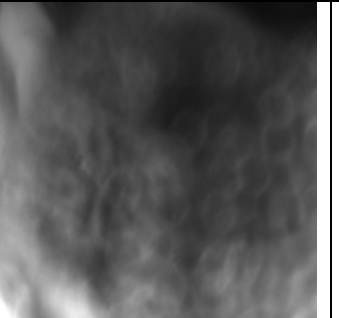
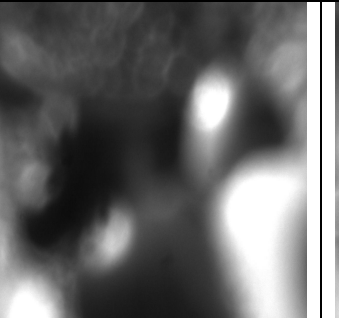

Time	0	150 minutes	300 minutes	450 minutes	600 minutes
Picture					
Comment	The embryo is outlined by the red oval. The scale bar represents 200 μm .	The embryo has already begun to dry out.			The embryo is dried out.

Test 15:

Time	0	160 minutes	320 minutes	500 minutes	650 minutes
Picture					
Comment	The embryo is outlined by the red oval. The central region of the embryo is still obscured by the glare. The scale bar represents 200 μm .	The image is much darker, and the embryo cannot be easily seen.	There is an odd distortion along the left side (yellow arrow), which may be indicative of the albumen on top drying out.	The embryo seems to be moving, and expanding a bit.	The embryo does not seem to grow much, only shift towards the right. As well, there seems to be some drying out along the left side of the field of view.

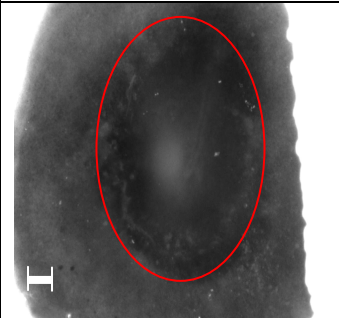
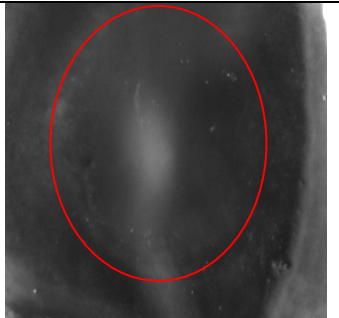
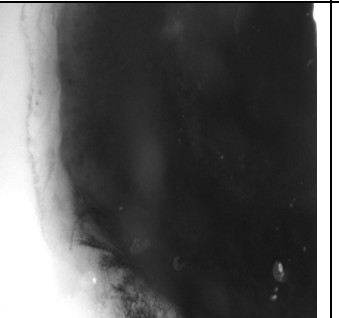
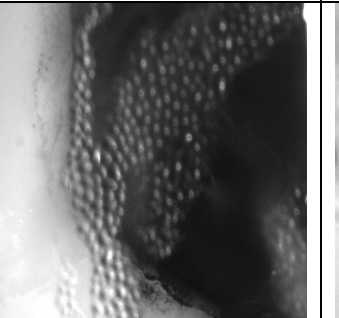
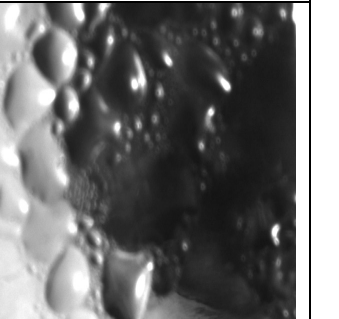
Test 16:

Given the previous tests either exhibited no growth or drying out of the embryo, it was decided that perhaps creating a closed system, by placing a cover slip on top of the domed lid, would provide the desired results. As well, a heated wire was placed around the lid in an attempt to prevent condensation from forming on the lid.

Time	0	20 minutes	40 minutes	65 minutes	90 minutes
Picture					
Comment	The embryo is outlined by the red oval. The scale bar represents 200 μm.	Condensation on the cover slip is beginning to distort the image of the embryo.	The condensation obscures the embryo.	Condensation increases.	Test is ended because it did not seem that the condensation would clear itself up.

Test 17:

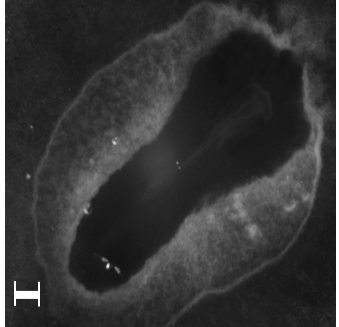
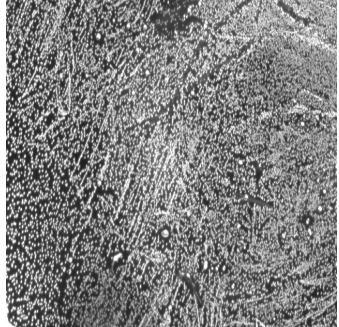
The cover slip was placed on top of the embryo, as being within the humid air may prevent condensation from forming. As well, RainX, a product designed to reduce fogging on car windshields, was applied to the side of the cover slip away from the embryo, to further prevent condensation.

Time	0	150 minutes	300 minutes	450 minutes	600 minutes
Picture					
Comment	The embryo is outlined by the red oval.	The embryo seems to have shifted, and image is less sharp.	Condensation is beginning to form on the underside of the cover slip.	Condensation continues, obscuring much of the embryo.	Test is ended. Condensation from the lid has started to drip onto the cover slip.

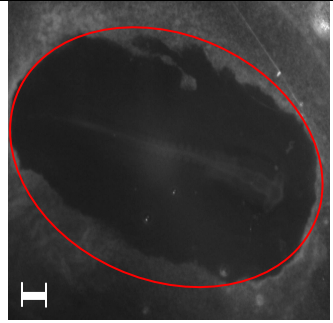
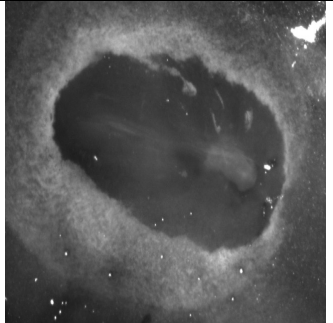
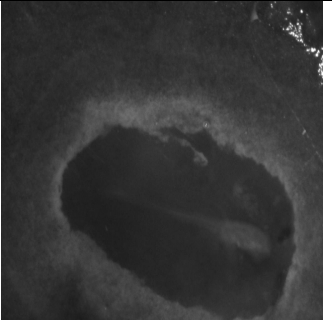

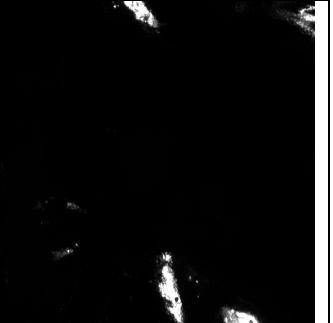
Appendix VI

Raw data from developing chick embryos in Prototype 3. Pictures were taken every 5 minutes with the Tissue GUI program. The first two tests were done with 2-day old embryos, which are more robust than 1-day old embryos, which are very fragile. In general, the test was allowed to run in its entirety, which is approximately 600 minutes or 10 hours. Exceptions will be noted with each test. Scale bars represent 100 μ m, unless otherwise noted, and the scale remains the same within a test.

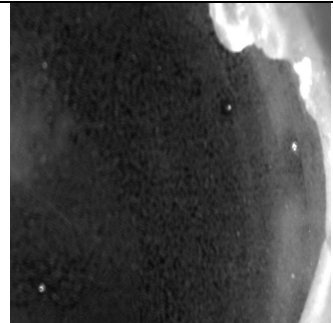
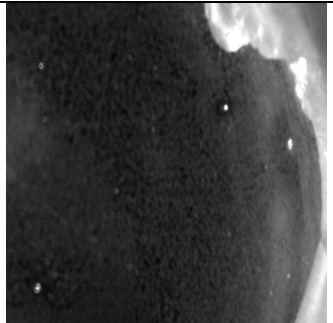
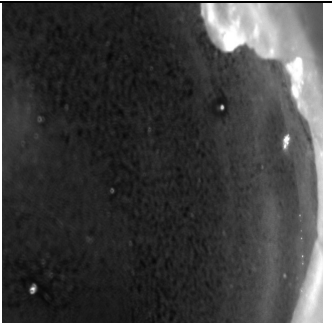
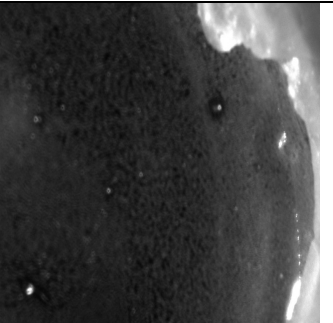
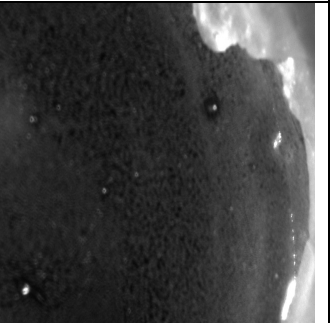
Test 1:

Time	Pre-window	0 h
Picture		
Comment	This is an image of the 2-day old embryo before the window was inserted.	In the time it took to seal the window into the egg, there was already condensation.

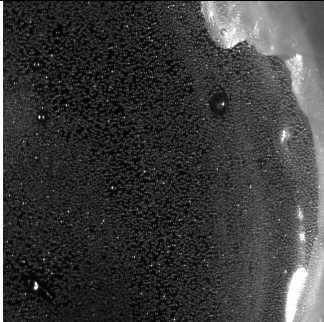
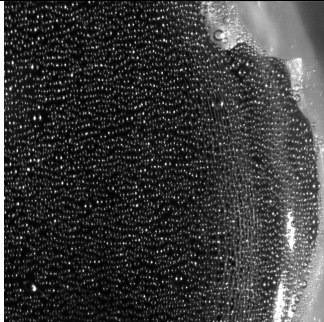
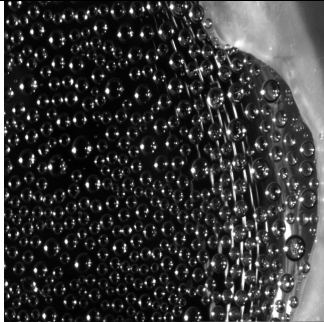
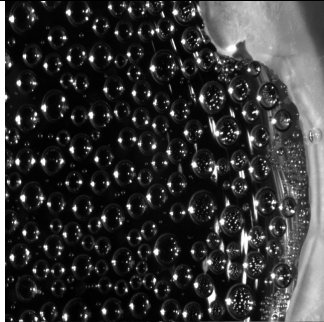
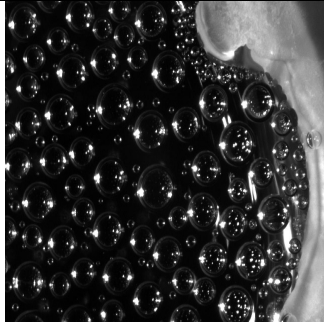
Test 2:
 Here, we tested whether the environmental chamber on its own was enough to provide the conditions required for an embryo to develop.

Time	0	105 minutes	195 minutes	240 minutes	600 minutes
Picture					
Comment	The 2-day old embryo can clearly be seen (red oval). The scale bar represents 150 μm .	As the initial images were too dark, the light was increased. The spine can clearly be seen.	The embryo was beginning to drift upwards, so was moved back down. The light is fading.	The light box fails at this point.	The test is run to completion, though nothing can actually be seen. Though, in actuality, the embryo had dried out, and the reflections off the surface are the bright spots in this picture.

Test 3:
 Since the environmental chamber was not sufficient, the Teflon window was used.

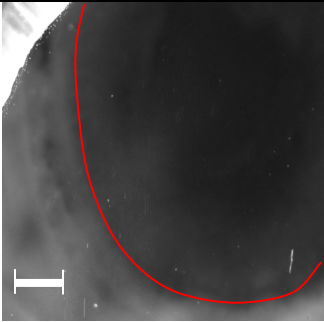
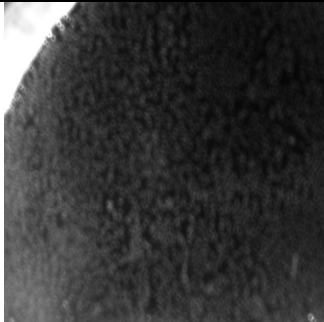
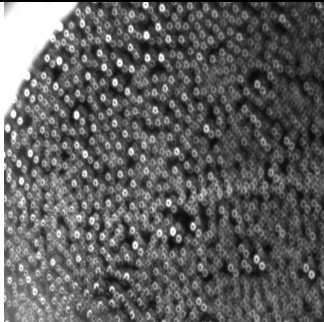
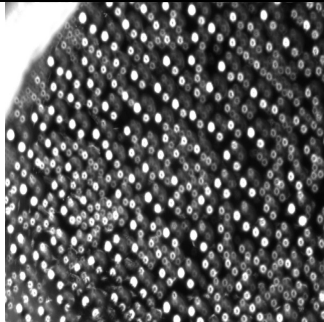
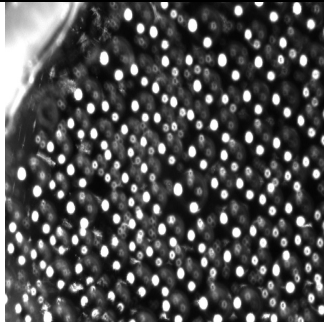
Time	0	15 minutes	30 minutes	45 minutes	65 minutes
Picture					
Comment	Before the test even begins, there is already condensation on the inside of the window.				The test was ended when it was realized that the apparatus had not yet reached optimal temperature (38°C), which may account for the condensation

Test 4:
 This test was done directly after the previous test, once the environmental chamber had reached 38°C, to see if the condensation, which usually forms before the egg is even placed in the apparatus, could clear up.

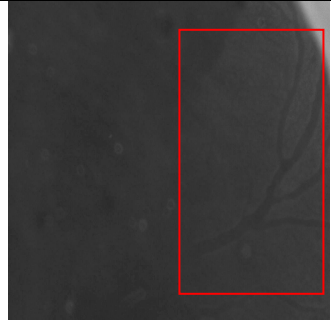
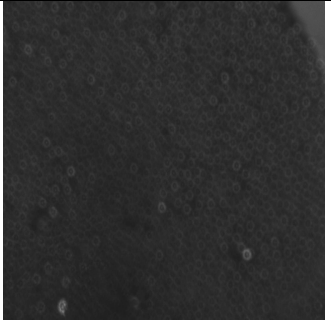
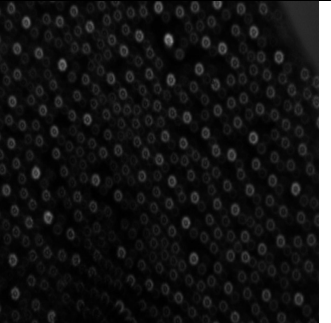
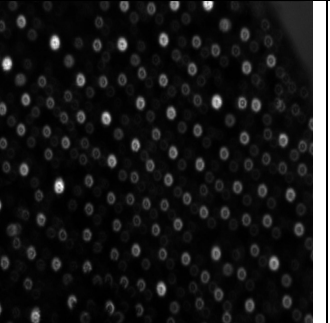
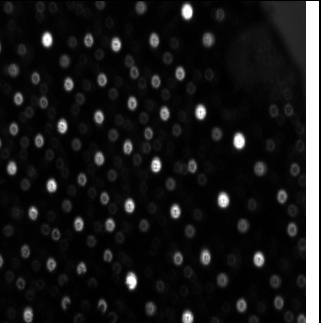
Time	0	150 minutes	300 minutes	450 minutes	600 minutes
Picture					
Comment	The condensation has already begun to form. The embryo cannot be seen.	As time goes on, the condensation only gets worse.			Test is run to completion, though condensation obscures everything.

84

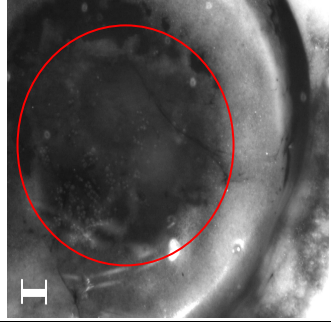
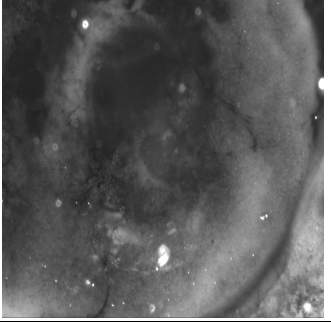
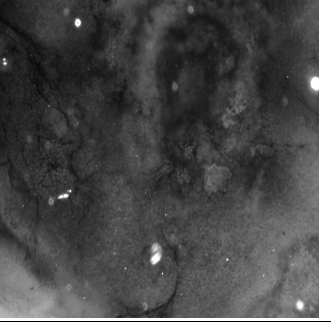
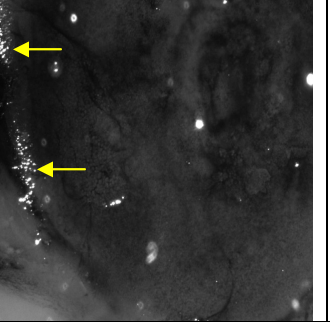
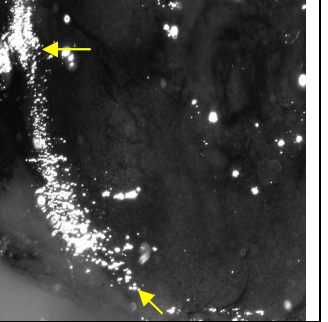
Test 5:

Time	0	150 minutes	300 minutes	450 minutes	600 minutes
Picture					
Comment	The outline of the embryo can be seen (red line) though details are fuzzy.	Condensation is beginning to form, though the outline of the embryo is still somewhat visible.	As condensation gets worse, even the outline of the embryo is now obscured.		Test is run to completion. Condensation obscures everything.

Test 6:
 This test was done with a 3-day old embryo. This was to test whether, similar to the situation with Prototype 2, a 3-day old embryo would be able to survive, while a 1-day old could not.

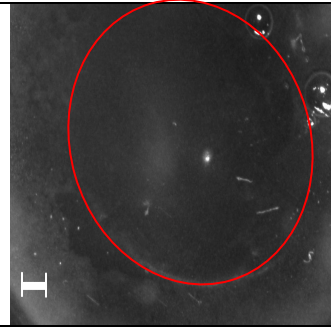
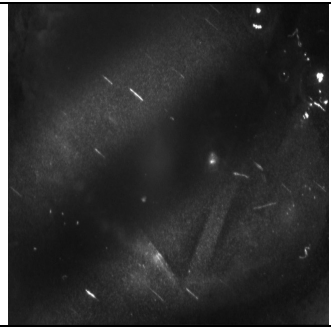
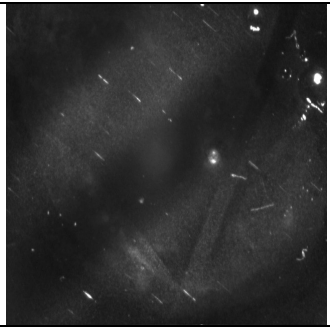
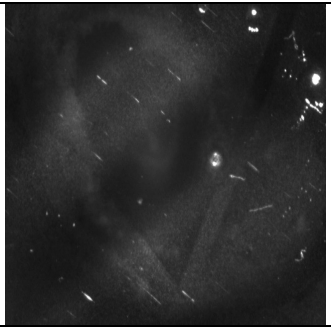
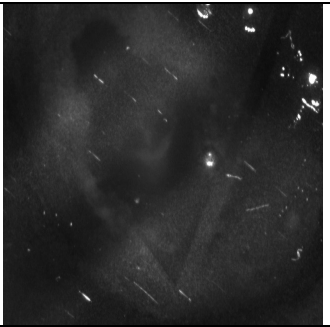
Time	0	95 minutes	190 minutes	285 minutes	380 minutes
Picture					
Comment	The 3-day old embryo is somewhat obscured, though the arteries can be faintly seen inside the red rectangle.	Condensation is beginning to form on the inside of the window.	The condensation continues to worsen.		The test was ended early, as it seemed obvious that the embryo would continue to be obscured by condensation.

Test 7:
 Upon suggestion from the researchers who developed the Teflon window, a cover slip with a drop of albumen was tried. Theoretically, the albumen prevents condensation from forming, as well as acting as a sealant for the cover slip to the egg.

Time	0	150 minutes	375 minutes	600 minutes	720 minutes
Picture					
Comment	The embryo can be seen (red circle), though details are rather murky, as the albumen may be causing distortion..	The embryo seems to be shifting towards the right. Again, details are rather murky.	Impossible to distinguish any features of the embryo. The wisps of black across the picture may just be ink.	The test is run to completion. A bit of drying out seems to be beginning (yellow arrows)	The test is allowed to run for another 2 hours. The embryo is showing signs of drying out (yellow arrows).

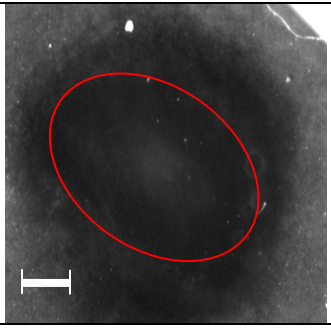
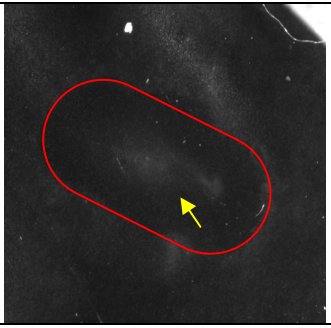
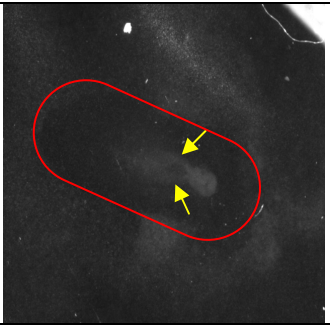
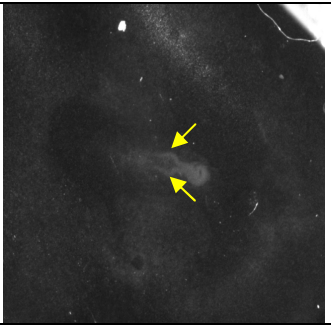
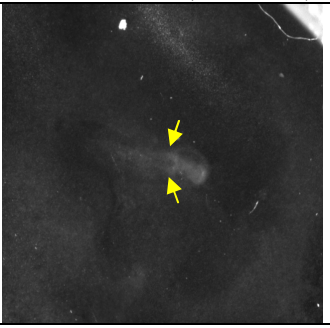
Test 8:

It was suggested that the condensation was caused by an air bubble trapped between the Teflon window and the embryo. Therefore, the simplest solution was to reverse the window, so that the Teflon side went downwards, with the acrylic ring facing upwards.

Time	0	150 minutes	300 minutes	450 minutes	600 minutes
Picture					
Comment	The embryo (outlined in red) seems to be somewhat obscured. This may be due to dirt or dust on the Teflon window.	There were some problems with the lighting, possibly because the lighting was originally an LED flashlight from above the chamber	Because of the lighting, the embryo was essentially impossible to see.		The test was run to the end. It is important to note that the reversal of the window did prevent condensation from forming.

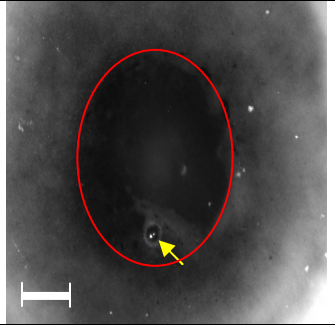
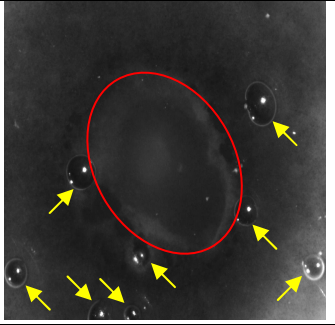
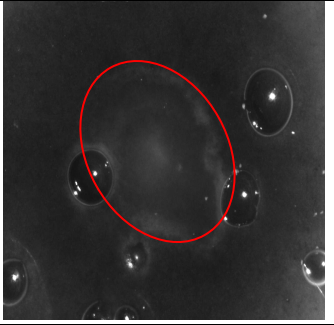
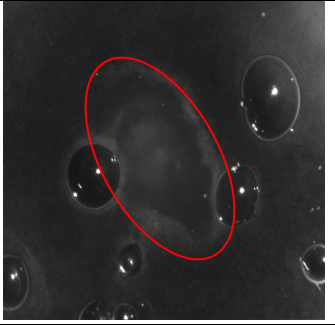
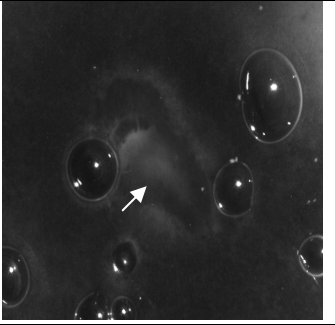
Test 9:

This test, and subsequent tests, was allowed to run for longer, to determine the full extent of the development possible with the apparatus.

Time	0	300 minutes	565 minutes	900 minutes	1200 minutes (20 hours)
Picture					
Comment	The embryo is outlined in red. Individual features cannot be seen at this time. The scale bar represents 200µm.	The embryo (in red) has begun to elongate and narrow. A very distinct neural groove forming (yellow arrow).	The two neural folds (yellow arrows) can be seen to be moving towards each other. The embryo is outlined in red.	The neural folds (yellow arrows) continue to fold and meet.	The test was ended at this time. The neural folds (yellow arrows) have still not completely fused yet.

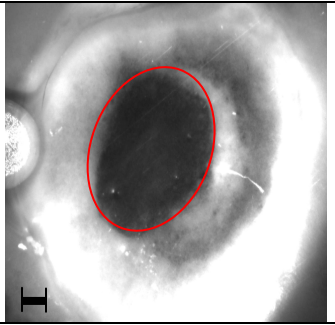
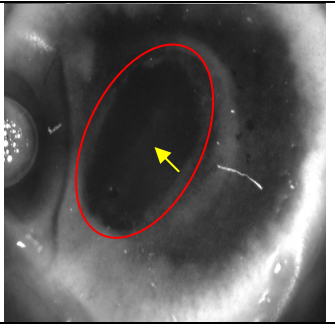
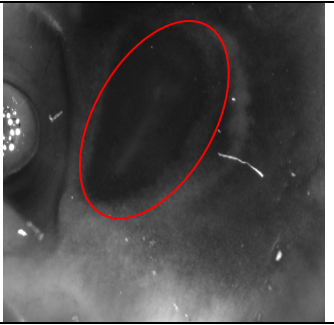
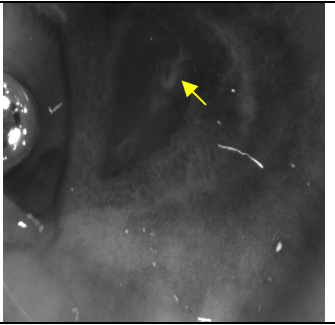
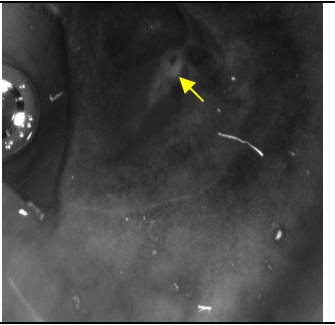
Test 10:

After the first successful run, the test was done again to ensure repeatability.

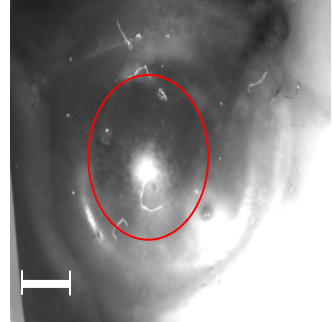
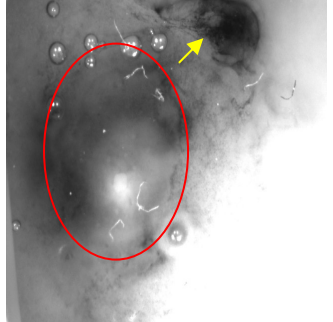
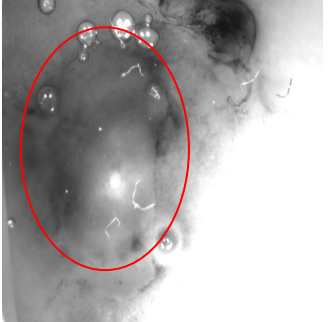
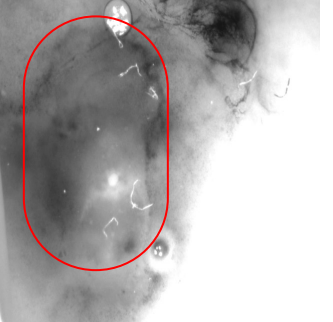
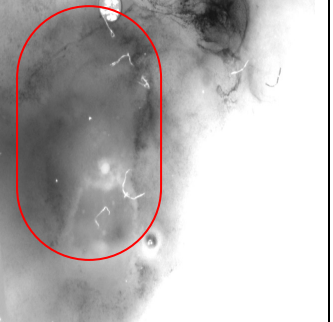
Time	0	300 minutes	600 minutes	900 minutes	1160 minutes
Picture					
Comment	An air bubble was trapped under the window (yellow arrow). The embryo is outlined in red. The scale bar represents 200 μm .	The ink solution spread out from under the embryo. The air bubble that was originally trapped may have caused more air bubbles to form (yellow arrows). The embryo (in red) has narrowed and elongated	The bubbles continue to get larger. The embryo (outlined in red) continued to narrow.	Again, the air bubbles continue to get larger. The embryo continues to narrow and lengthen.	The test was ended at this point. There seems to be some development of a neural groove in the centre of the embryo (white arrow).

Test 11:

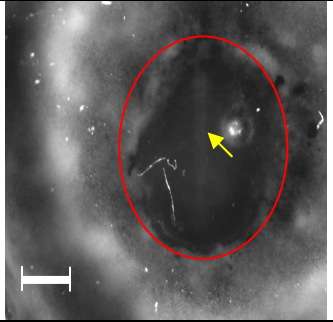
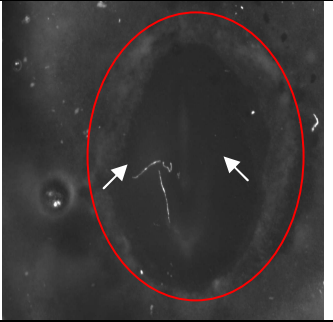
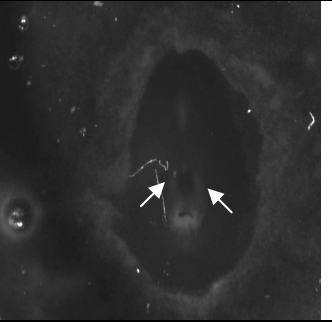
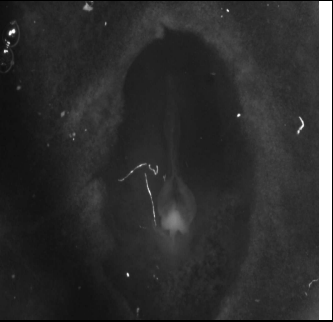
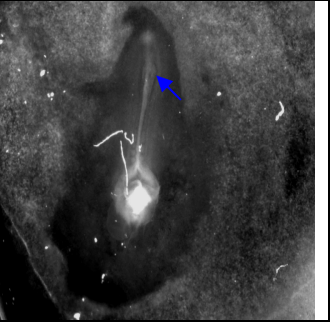
In an attempt to see the details of the embryo better, the lighting was turned higher for better contrast.

Test	0	300 minutes	700 minutes	1150 minutes	1440 minutes (24 hours)
Picture					
Comment	The embryo is outlined in red. There were some scratches on the window. The scale bar represents 160 μm .	The embryo (in red) has lengthened and narrowed. The neural groove can be seen in the centre (yellow arrow).	The embryo (in red) has shifted upwards. As well, it has continued to lengthen and narrow.	It appears that the neural groove is not forming normally, given the blob beginning to form (yellow arrow).	The test was ended after 24 hours. Development seemed abnormal. There seems to be bunching in the neural groove (yellow arrow).

Test 12:

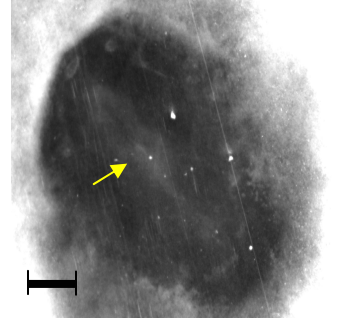
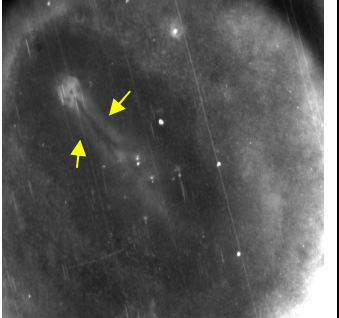
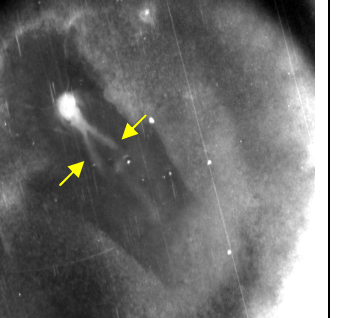
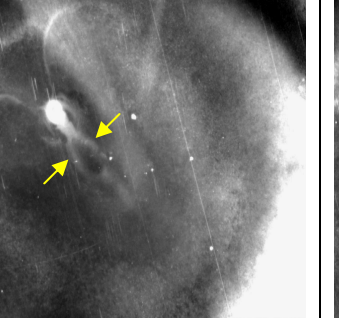
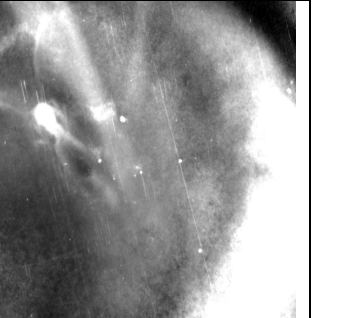
Time	0	300 minutes	600 minutes	900 minutes	1200 minutes
Picture					
Comment	The ink solution did not seem to completely spread beneath the embryo (in red). The scale bar represents 200µm.	An air bubble must have been trapped when the window was sealed in, as many air bubbles have formed. As well, the ink is beginning to leak above the embryo (yellow arrow).	Despite the lack of contrast, the borders of the embryo (in red) can still be estimated by where the ink is slightly darker.	Again, the borders of the embryo need to be estimated (in red), though it seems as if the borders have again narrowed and lengthened.	There does not seem to be much change between this and the previous picture, which may mean that the embryo has died.

Test 13:

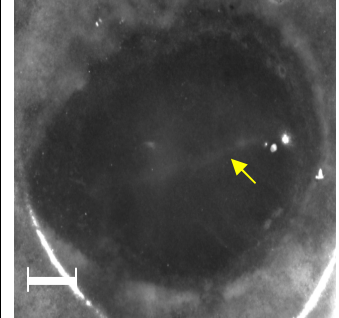
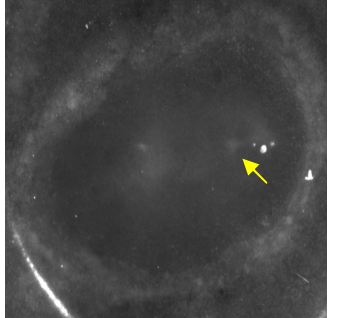
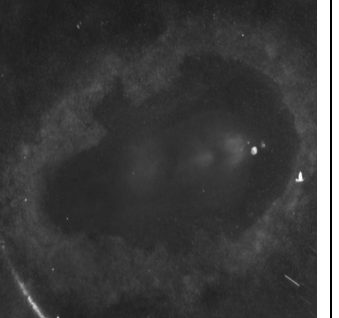
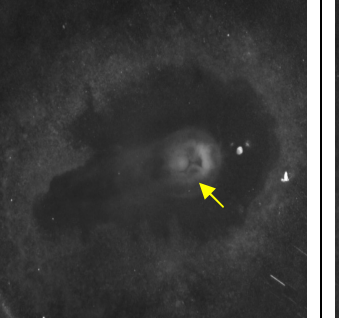
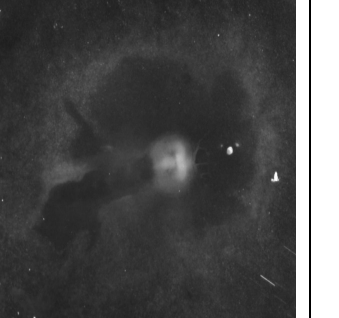
Time	0	200 minutes	500 minutes	835 minutes	1200 minutes
Picture					
Comment	The embryo (in red) has a distinct neural groove formed (yellow arrow). The scale bar represents 250µm.	The embryo (in red) has expanded, and the neural folds are faintly visible (white arrows).	The neural folds can be seen more clearly, rolling towards each other (white arrows).	The test is ended because the light box broke after this point.	A picture was taken manually at 1200 minutes. The neural folds can clearly be seen to have met and fused (blue arrow)

Therefore, it seems that the embryo is able to develop and undergo neurulation, though at a slower rate than expected according to Hamburger and Hamilton (see Appendix I).

Test 14:

Time	0	275 minutes	600 minutes	900 minutes	1200 minutes
Picture					
Comment	The embryo is somewhat distorted, because of imperfections in the Teflon window, but the neural groove can still be seen (yellow arrow).	The neural folds are beginning to roll together (yellow arrows).	The neural tube continues to form as the neural ridges (yellow arrows) meet and fuse.	There is not much change in this picture from the previous one, though it seems as if the fusion of the neural tube has continued (yellow arrows).	The test is ended here. The glare is most likely a result of the previously flat epiblast becoming a 3-D structure, and moving away from the Teflon window, distorting it.

Test 15:

Time	0	270 minutes	540 minutes	810 minutes	1080 minutes
Picture					
Comment	The embryo has a distinct neural groove (yellow arrow).	The embryo has elongated and narrowed slightly. The neural groove seems to have become blobby (yellow arrow).	Abnormal development may be occurring, since there seems to be no neural folds, and the neural groove is not straight.	There is definitely abnormal development, given the growing ball of tissue near the centre of the embryo (yellow arrow).	The test was ended at this point.

Test 16:

Time	0	230 minutes	460 minutes	690 minutes	925 minutes
Picture					
Comment	The details of the embryo are rather difficult to see in this image, though it becomes clearer later on.	The neural folds have begun to come together (yellow arrows).	The two neural ridges can clearly be seen (yellow arrows) coming closer together.	The neural ridges (yellow arrow) have met, and have begun to fuse.	This was a successful test. The formation of the spine can clearly be seen (yellow arrow).

Test 17:

Time	0	220 minutes	440 minutes	660 minutes	870 minutes
Picture					
Comment	The embryo (outlined in red) is partially obscured by air bubbles. The neural groove (yellow arrow) can faintly be seen)	The embryo (in red) seems to have expanded, though specific features still cannot be seen.	The neural ridges can be seen in this image (yellow arrow) though it seems to be developing abnormally	The neural folds (yellow arrows) seem to be moving closer together, the neural tube seems bunched, with an odd shape at the end of the tube (light blue star).	The test was ended at this point. There was definitely abnormal development, as the end of the neural tube did not seem to fuse (white arrow).

Test 18:

Time	0	515 minutes	700 minutes	1080 minutes	1440 minutes
Picture					
Comment	The embryo (in red) does not show any distinguishable features. The scale bar represents 200 μm.	Until this point, distinct features of the embryo could not be seen. Here, the neural groove (yellow arrow) is visible.	The black circle forming on the embryo (blue arrow) is the embryo moving away from the Teflon membrane.	The embryo seems to be developing normally, with the neural folds (yellow arrow) meeting and fusing.	The finished neural tube can clearly be seen (white arrow).

Test 19:

Time	0	335 minutes	720 minutes	1080 minutes	1440 minutes
Picture					
Comment	The embryo (outlined in red) is pear-shaped, and no features can be seen. The scale bar represents 150 μm.	The light was increased at this point so the embryo could be seen in more contrast. The neural folds can faintly be seen (yellow arrows).	The embryo has elongated, and the neural folds (yellow arrows) are beginning to meet and fuse.	The embryo is moving away from the Teflon window (light blue star). The neural folds are still coming together (yellow arrows).	The ending of the test shows the two neural ridges coming together (yellow arrows). Some fusion has occurred near the top (red asterisk).